OPTIMAL CONTROLLER DESIGN PROCEDURES FOR THE ATTENUATION OF SUBSYNCHRONOUS RESONANCE

A THESIS

Presented to

The Faculty of the Division of Graduate Studies

By

Ali Feliachi

In Partial Fulfillment

of the Requirements for the Degree

Doctor of Philosophy

in the School of Electrical Engineering

Georgia Institute of Technology

February, 1983

OPTIMAL CONTROLLER DESIGN PROCEDURES FOR THE ATTENUATION OF SUBSYNCHRONOUS RESONANCE

Approved by:

Athanasios P. Meliopoulos, Chairman

John F. Dorsey

Hans B. Puttgen

Date approved by Chairman: Feb 25, 1983

To My Parents

ACKNOWLEDGMENTS

It is a sincere pleasure to acknowledge the support and cooperation I received from my thesis advisor, Professor Athanasios P. Meliopoulos.

Dr. A. P. Meliopoulos suggested the research area of the thesis and provided invaluable advice and guidance throughout the course of the research. I am grateful for all the time and effort he devoted to me.

TABLE OF CONTENTS

TABLE OF CONTENTS (continued)

LIST OF TABLES

LIST OF ILLUSTRATIONS

LIST OF ILLUSTRATIONS (continued)

LIST OF ILLUSTRATIONS (continued)

SUMMARY

The thesis addresses the design problem of continuous and discrete optimal controllers to attenuate the subsynchronous resonance effects in electric power systems. A novel optimal control design methodology is developed for the computation of the control laws. It is embedded in the framework of a generalized dynamic simulation algorithm.

The applicability of the control design technique and the dynamic simulation procedure extends beyond the subsynchronous resonance control problem to the optimal control problem of general, nonlinear, large scale dynamic systems.

A general modeling procedure and a general dynamic simulation algorithm are developed by exploiting the structure of interconnected dynamic systems. The procedures have been applied to the electric power system, resulting in a digital dynamic simulation program. The developed program is modular. Each module represents a specific class of electric power apparatus modeled as a resistive companion network. The modeling and simulation algorithm embodies desirable features of a generalized simulation program: a) expandability, b) model accuracy, c) model optimization, d) sparsity, e) suitability to parallel processing and f) numerical stability.

The simulation algorithm is utilized as an analysis tool and also as the basis for a control design methodology. The design methodology is based on a gradient iterative technique. Sensitivity analysis,

performed within the framework of the simulation program, yields the gradient of a prespecified vector performance index with respect to the control parameters. At each iteration, the gradient is used to update the control parameters. The main properties of the approach are: a) a vector performance index rather than a scalar criterion is optimized allowing more flexibility in the assessment of the performance of the system; b) the procedure automatically handles important controller structures such as decentralized laws and combination of discrete and continuous strategies; c) physical limitations on the control gains are explicitly incorporated, thus resulting in realistic control laws; d) the resultant control scheme is feasible for implementation.

The basic thrust of the control design technique is the computation of a sensitivity matrix. The thesis presents two contributions: a) derivation of closed form expressions of the sensitivity matrix based on the system linearized model matrices; b) development of a unified approach for the computation of the linearized model of a large scale system from the linearized models of its individual elements.

The dynamic simulation and the control design methodologies are effectively applied to analyze and reduce the subsynchronous resonance effects in an actual electric power system.

CHAPTER I

INTRODUCTION

Economy of scale as well as environmental factors dictate the construction of large power plants at remote locations. A strong transmission network is required to transmit the electric power to consumption centers. Right-of-way requirements and cost minimization are important considerations in the design of the transmission circuits. Consequently, the established trend is toward remote power plant siting, larger plants, larger units, long and heavily loaded transmission lines and increased interconnection between power utilities. This trend, together with an increased emphasis on reliability and the corresponding increased stability requirements define certain technical issues in the operation of modern electric power systems. The need to transmit large amounts of electric power over long distances results in long ac transmission lines with high inductive reactances which limit the amount of power that can be transmitted and also affect the system transient stability. Installation of series capacitors lowers the effective inductive reactance of the transmission line but may create a resonant condition, referred to as subsynchronous resonance, at frequencies below the synchronous frequency of the system (60 or 50 Hz), [1]-[5]. The subsynchronous resonant oscillations can result in severe operational problem. In particular, two incidents of turbine generator shaft failure occured at the Mohave Generating Station in December of 1970 and

in October of 1971. These incidents led to an extensive study of the Subsynchronous Resonance phenomenon of the Mohave system [6]-[7] and the Navajo Generating plant [8]-[12].

Alternatives to series capacitors are additional/parallel transmission lines, higher voltages, and/or DC transmission lines. On an economical basis (i.e., accounting for capital and operating costs), series capacitor compensation is the optimium choice.

The objective of this study is the design of controllers to attenuate the subsynchronous resonance effects in electric power systems. The design of such controllers requires: a) a tool to analyze the subsynchronous resonance phenomenon; b) a methodology to design appropriate controllers.

This chapter reviews the concepts related to the objective of the study as found in the literature. Included are:

1. the definition of the subsynchronous resonance phenomenon and the related terminology;
2. techniques used to analyze transient phenomena in electric power systems and particularly the subsynchronous resonance phenomenon;
3. subsynchronous resonance countermeasures and controls.

Subsynchronous Resonance Phenomenon

Subsynchronous Resonance [4] is an electric power system condition where the electric network exchanges energy with a turbine generator at

one or more of the natural frequencies of the combined system below the synchronous frequency of the system.

Usually, the resonant frequencies are well separated from the synchronous frequency of the system. The losses in the system are sufficient to damp out relatively quickly any natural frequency oscillations set up by the transients in the system such as switching surges and fault initiation and clearing. However, in the case of subsynchronous resonance two factors tend to reduce the effective damping of the network. These are:

1. at the subsynchronous frequency, a synchronously rotating machine behaves like an induction generator;
2. the natural frequencies of the mechanical system, comprised of the shafts and masses of rotating synchronous machines, are excited by rapid changes in electrical output.

An explanation of subsynchronous resonance is offered with the aid of the simple radial system shown in Figure 1.

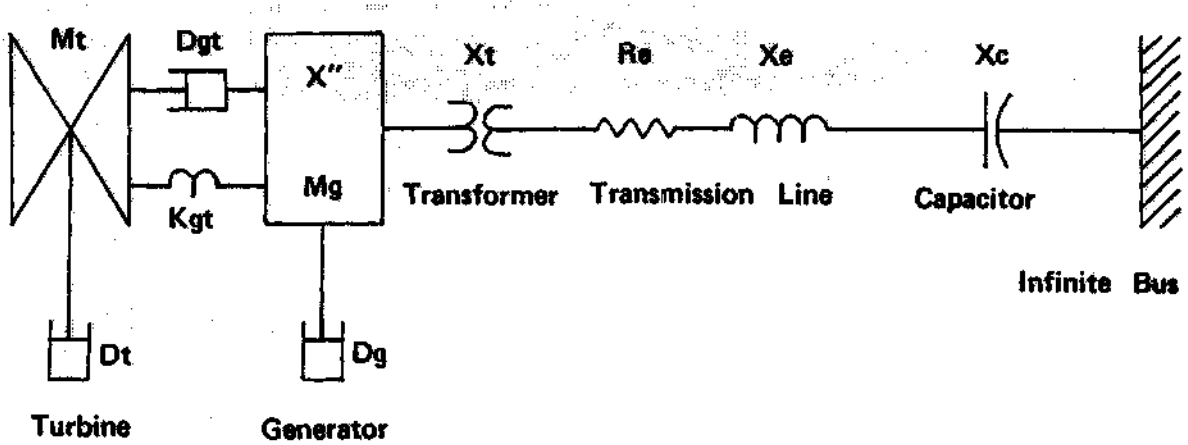

Figure 1. Simple Radial System

The electric system has a resonant frequency, fer:

$$fer = fo \sqrt{Xc/(X'' + Xe + Xt)}$$

where: fo : synchronous frequency

Xc : reactance of the series capacitor

X'' : generator subtransient reactance

Xe : reactance of the transmission line

Xt : reactance of the transformer

The above reactances are defined at the synchronous frequency, fo.

The excitation of the electric system by the resonant frequency will generate machine electric currents of frequency fr:

$$fr = fo \pm fer$$

A qualitative explanation is as follows: a balanced three phase set of armature currents at frequency (fer) produces a rotating magnetic field in the synchronous machine. The time distribution of the phase currents together with the space distribution of the armature windings cause rotation at an angular frequency of $2.\Pi.fer$. This field induces electric currents in the rotor winding of frequencies proportional to the relative speed between the armature field and the rotor. Positive (negative) sequence components of stator currents produce rotor currents at subsynchronous (supersynchronous) frequency fo - fer (fo + fer).

As the rotor magnetic field overtakes the more slowly rotating subsynchronous MMF in the armature, it produces a subsynchronous torque

having a frequency (fr) which is the difference between the electrical frequency corresponding to the synchronous frequency fo and the electrical subsynchronous frequency fer. The subsynchronous electrical frequency (fer) and the subsynchronous torque frequency (fr) are said to be complementary because they add to unity when expressed in per unit of the synchronous frequency fo.

There are two distinct subsynchronous resonance mechanisms: self-excitation and torsional natural frequencies.

Self Excitation

Synchronous machine generated voltages of subsynchronous frequency can sustain subsynchronous frequency currents to produce the effect called self excitation. There are two types of self excitation, one involving electrical dynamics (induction generator effect) and the other involving both electrical and mechanical turbine generator dynamics (torsional interaction).

Induction Generator Effect. The rotor circuits rotate faster than the rotating MMF caused by the subsynchronous armature currents. Therefore the rotor resistance to subsynchronous currents, viewed from the armature terminals, is negative. When this negative resistance exceeds the sum of the armature and network resistance at the resonant frequency self excitation results.

Thus, induction generator effects result from the apparent negative resistance characteristic of the generator at subsynchronous frequencies.

Torsional Interaction. Torsional interaction problems may occur when the electrical resonant frequency (fer) is near the complement of a torsional resonant frequency (fn) of the turbine generator shaft system.

Generator rotor oscillations at a torsional mode frequency (fn) induce armature voltage components of subsynchronous and supersynchronous frequency fen = fo ± fn. In the example of Figure 1 the natural frequency, fn, of the turbine/generator masses is given by:

$$fn = (1/2\Pi) \sqrt{Kgt/Mt}$$

where: Kgt : Generator-Turbine shaft stiffness

Mt : Turbine inertia.

When fn is close to fr the subsynchronous frequency voltage is phased to sustain the subsynchronous torques. If the component of subsynchronous torque in phase with rotor velocity deviation equals (exceeds) the inherent or mechanical damping torque of the rotating system, the system will sustain (amplify) subsynchronous torsional oscillations.

Torsional Natural (Mode) Frequencies

Transient torque analysis is the study of the response of turbine generator shaft systems to large amplitude disturbances such as faults in the transmission system.

Following a fault or disturbance, the turbine generator rotor masses will oscillate relative to one another at one or more of the turbine mechanical natural frequencies or torsional mode frequencies (fn) dependent on the nature of the disturbance.

If the complement of the electrical network resonant frequency (fo-fer) aligns closely with one or more of the natural frequencies (fn) of the mechanical system, excessive torques may be induced in the shafts following a system disturbance. This effect is referred to as shaft torque amplification.

Subsynchronous torsional resonance is responsible for shaft fatigue. The fatigue due to excessive torques and resulting sheer and longitudinal stresses of shaft material, is cumulative, i.e., each incident results in some loss of shaft life. Thus torsional resonant oscillations are intolerable and must be mitigated. A number of subsynchronous torsional oscillations mitigation techniques have been proposed. These techniques and the analysis procedures used to study them are reviewed next.

Subsynchronous Resonance Analysis Techniques

The analysis of the subsynchronous resonance phenomenon is a complex problem. It can be performed with a number of different techniques: a) eigenvalue analysis [13]-[15]; b) frequency scanning technique [16]; and c) transient torque analysis technique [17]-[19]. The applicability of eigenvalue analysis and frequency scanning techniques to this problem is limited because of the nonlinearities of the devices involved. They need to detect the possibility of subsynchronous resonance. Transient torque analysis technique is the primary method used.

The commonly used tools to analyze transient phenomena in electric

power systems are:

1. Transient Network Analyzers (TNA)
2. Analog and Hybrid Computers
3. Digital Computers

The TNA is a miniature power system model. System components are scaled down to low current and low voltage devices. Elements like transmission lines, transformers or source impedances are represented by inductors wound on magnetic cores. Ideal voltage sources behind appropriate reactances represent generators. Synchronous generators can be modelled with microalternators. While the TNA allows a real time simulation of transient phenomena, it is relatively inflexible and some models are very expensive. The setting up for a study is time consuming. The available equipment models limit the size of the system that can be simulated. In addition to these problems, there are certain technical limitations. For example, the power losses in the inductors tend to be disproportionately higher than the losses in the system component being modeled. Another technical limitation arises from the fact that the construction of models to simulate the finite length of the transmission line is very difficult. An approximation is utilized with the modeling of the transmission lines as cascaded lump parameters models.

Analog and Hybrid Computers are used for some specific simulation studies. The major advantage of an analog computer is the simultaneous integration of all the differential equations. However the set up time problem and the cost limit the applicability of these computers.

Digital Computers are attractive because of their computational capabilities, cost and flexibility. Computer programs are being developed as tools for all engineering and operational studies [20]-[21]. Today the average power utility owns computers big and fast enough to handle the majority of their computational problems. System planners are acquiring and operating their own minicomputer systems for load flow and transient stability simulations. It is in this present economic environment that digital simulation [22]-[24] is expanding and evolving rapidly in order to satisfy an increasing demand for more accurate modeling and greater user convenience.

While the digital computer is available to the system engineer, program development still requires a great deal of manpower. Also the operating cost in studies is very high. In the past, emphasis was placed on two aspects: model development and computer code development. Other aspects such as efficiency of the basic algorithms and maximum utilization of computer technology have not been adequately addressed.

New power components with complex functions and dynamic responses are being incorporated into the system. For example, transformer models with explicit representation of iron core nonlinear characteristics must be developed for the study of ferroresonance phenomena. Examining existing algorithms, it is obvious that the amount of effort required to develop and add new device models is prodigious. Attempts to further increase program efficiency are hamstrung by the inability of conventional algorithms to accomodate numerical techniques that the new models require. These limitations began to assume large proportions several years ago when it first became necessary to include devices

requiring sophisticated analysis procedures such as static VAR devices, pipe-type-cables, modern silicon-carbide surge arresters, or to analyze phenomena such as ferroresonance, subsynchronous resonance, etc. With regard to the mentioned problems, the following questions are raised:

1. Is there a general model form that includes all power system device models - those in current use as well as those to be developed?
2. Is there a general form that includes all possible integration formulae and other processes for calculating the response of a model?
3. Is it possible to devise a network simulation algorithm that can accomodate both the above mentioned general forms and hence avoid the growing pains of conventional algorithms?
4. Is it possible to develop generalized power system elements and simulation algorithms which will take maximum advantage of low cost computing systems?

These questions motivated the development of a dynamic simulation algorithm for general composite systems. This algorithm addresses the problem of computational efficiency by decomposing the computational task into a number of small computationally independent entities. Two main advantages result from this decomposition: a) each small independent computational task can be optimized depending on the specific system and b) parallel processing can be employed in a multiprocessor computer system.

This simulation algorithm is then applied to the interconnected

electric power system. Each device in the system is modeled as a generalized resistive companion network with minimum number of interface variables. These general modeling and simulation procedures yield a modular and expandable power system dynamic simulation program. The basic component of the computer program is a library of power system elements. The computer program constitutes the analysis tool for the study of the subsynchronous resonance phenomenon and the basis of the proposed control design approach.

Subsynchronous Resonance Control

The next main topic addressed in this review is the design procedures to mitigate the subsynchronous resonance effects.

Series capacitors, which are used to compensate the series inductance of a transmission line, are the main cause of subsynchronous resonance effects. The control of the electric current through the capacitors or the voltage across the capacitors can mitigate or eliminate the subsynchronous resonance damage to turbine generators [25]. A number of control schemes have been proposed [26]-[36] including: a) filtering and damping, b) dynamic stabilization and c) control via the generator exciter. Some of these controls is hoped to mitigate subsynchronous resonance. Since complete elimination of subsynchronous resonance has not been demonstrated yet, a number of protection schemes against subsynchronous resonance have been developed and implemented. The control and protection schemes are surveyed next.

Filtering and damping

Static Blocking Filters. This filter, made up of LC tank circuits in series with each phase of the generator step-up transformer, is tuned to contribute positive resistance at frequencies which coincide with the complement of the torsional natural frequencies. It isolates the machine from the system at the critical frequencies which otherwise may trigger subsynchronous torsional oscillations.

Line Filter. An appropriately sized reactor is connected in parallel with series capacitor to form the line filter. It blocks the electric currents and voltages of a given frequency. Thus it can be applied to mitigate subsynchronance torsional resonance when a single frequency is involved and the source of the problem is a single line.

Bypass Damping Filter. The bypass damping filter is an LC filter, appropriately tuned and connected in shunt across the series capacitor in each phase. It is designed and tuned to act as a low inductive/resistive bypass path for the flow of subsynchronous currents in the network and as a high impedance at the subsynchronous frequency.

Dynamic Filter. The dynamic filter is an active device placed in series with the generator to eliminate the subsynchronous voltage generated by rotor oscillations. It is extremely bulky and impractical.

Dynamic Stabilizer. This device consists of thyristor modulated shunt reactors which are connected to the isolated phase bus of the affected turbine generator unit. The design, size and control of the stabilizer are chosen to provide sufficient current in the generator armature at critical subsynchronous frequencies to cancel the current

from the transmission system interaction.

Excitation System Damper. The objective is to modulate the output of the excitation system in response to torsional oscillations of a turbine generator. The exciter induces subsynchronous resonance voltages in the armature circuit. The effective damping is increased by appropriate variations of the field voltage.

Protection Against Subsynchronous Resonance

Because subsynchronous resonance may cause costly damage to the system it is necessary to protect the system. A number of protection schemes has been developed and implemented. They are reviewed below.

Torsional Motion Relay. This device detects excessive mechanical stresses in the turbine generator shaft and operates to disconnect the machine from the transmission system. The input to the tripping relay is proportional to rotor speed.

Armature Current Subsynchronous Relay. This relay monitors the content of subsynchronous frequency currents in the armature current. It trips whenever these currents assume excessive values.

Torsional Monitor. The Torsional Monitor is a sophisticated device which monitors the shaft torsional vibrations resulting from electrical oscillations or disturbances on the transmission network. Specifically, this device senses rotor speed variations and converts the data by means of analog circuits into oscillating torques on each shaft which are continuously displayed. The torsional monitor is not a

protection device.

System Switching and Generator Tripping

System Switching. The basic idea of this protection scheme is to isolate the generator from the series capacitor. Whenever subsynchronous resonant oscillations are detected the machine is switched onto an uncompensated system.

Unit Tripping. A unit tripping scheme is applied to provide protection against subsynchronous resonance transient torque for predetermined system conditions and fault locations.

In summary, many countermeasures have been proposed to mitigate the effects of subsynchronous resonance. However, regarded singly, none of the proposed countermeasures can be considered as the solution to the problem. Moreover, many of the countermeasures are rather specialized: they are suitable only for certain system configurations and situations. Most of the employed schemes are heuristic. Some of them require trial and error tuning at prespecified frequencies after installation. Others may be impractical. For example, the physical size of a blocking filter makes it impractical. Many of the proposed schemes have been experimentally implemented and some experience has been accumulated. The consensus is that none of the proposed schemes is totally satisfactory for practical, economical and technical reasons. A combination of some of the countermeasures may be a solution to the problem. An acceptable combination of countermeasures may involve a number of decentralized control schemes of the mixed (continuous and

discrete) type. The electric power system is geographically dispersed. Thus, decentralized control schemes, which use local information only, are technically feasible to implement. However, these decentralized control schemes must be coordinated to be most effective. It seems tempting to cast the problem as an optimal control problem and then solve it using conventional optimal control theory techniques. But the electric power system has many characteristics that make a conventional, centralized optimal controller not feasible for implementation. Some of these electric power system characteristics are:

1. high dimensionality
2. nonlinearity
3. time dependence
4. geographic dispersion
5. stiffness

Added to these characteristics is the requirement of a decentralized controller structure. It is then desirable to formulate the problem as an optimal control problem with a specific controller structure (decentralized) and specific constraints on controller capability. This idea has motivated the research of this thesis.

A control design methodology has been developed to solve this optimal control problem. The proposed methodology is applied within the framework of the simulation algorithm mentioned earlier. The objective of the methodology is to optimize a vector performance index with a feasible controller. The design of an optimal controller is based on Sensitivity Analysis: the sensitivities of postulated performance

criteria are employed in a gradient algorithm to compute the optimal control variables. The applicability of the method extends beyond the subsynchronous resonance control problem to the optimal control problem of general, nonlinear, large scale dynamic systems.

Thesis Outline

The objective of this thesis is to provide a solution for the attenuation of the subsynchronous resonance effects given a controller structure. An optimal control design methodology is developed to accomodate any control structure. For the control of subsynchronous resonance a feasible combination of discrete and continuous controllers is designed.

Chapter II presents the general modeling and simulation procedures. These procedures are employed to develop a digital power system dynamic simulation program. This program constitutes the required analysis tool for this study.

Chapter III presents a review of the control problem. An approach for the solution of the control problem within the framework of the simulation algorithm is outlined. This novel approach, which is based on optimization, requires a sensitivity analysis of the system performance with respect to the control parameters. Chapters IV and V present the approach to this problem within the framework of the simulation algorithm. In particular, Chapter IV outlines the derivation of a linearized model of the overall system within the framework of the simulation algorithm. The linearized model is utilized to derive closed

form expressions of the sensitivities of the system performance with respect to the control variables. The sensitivities are utilized in an iterative gradient algorithm to compute the optimal values of the control variables.

The approach described in chapters II, III and IV is applied to control the subsynchronous resonance effects on an actual electric power system. The results constitute the topic of chapter V. Finally chapter VI concludes the thesis and summarizes the contributions.

CHAPTER II

MODELING AND DYNAMIC SIMULATION

Large scale systems comprise a large number of interconnected components. In particular the electric power system, as known today, is an interconnection through high voltage transmission circuits of many geographically distant generating units and load centers. Reliability as well as economic considerations led to a highly complex system. The difficulties related to the analysis, control and operation of this system have dramatically increased with its size. The "engineering way" of coping with this problem is to rely on a simplified model as long as some degree or criterion of accuracy is satisfied. In this context, "simplified model" implies either a model of simpler structure or a lower order model, which presumably captures the essentials of the system characteristics. Traditionally simplified models were selected based on experience and agreement with observed system component responses. Perturbation and Aggregation methods are employed to provide a theoretical basis for the selection of simplified models. Aggregation [37]-[38] methods are utilized to reduce the dimension of the system. An exact lower order model is obtained only when the system is reducible. If the system is in its minimal form, then approximate aggregation methods are used. Perturbation methods [39]-[42] can also be used to simplify the model. The idea here is to ignore some dynamic

interactions. The perturbation in itself can be either singular (strong coupling) or nonsingular (weak coupling). The transient stability problem in electric power systems has been investigated in this context. Several approaches have been proposed which are grouped under the name "Coherency Methods" [41]-[52]. It is assumed that the system can be decomposed into two areas. The Study Area, where the machines close to the fault respond as individual units and thus are modeled in great detail, and the External Area, which consists of machines more distant that can be aggregated depending on the coupling among themselves.

The accuracy of the analysis is directly related to the system model utilized. Different models are chosen for different studies. Presently, there is no universal model for the electric power system. Many times only a small portion of the system is modeled for a specific case study, ignoring the rest of the system. Moreover, using a description of the whole interconnected system leads to challenging and difficult computational tasks. The examination of the interconnected systems reveals that all the system information is contained in two sets of equations: a set of decoupled, independent, dynamical equations characterizing the individual components and a set of coupled equations characterizing the interconnections. Consequently, by decomposing a large scale composite system into a number of independent devices, the computational task can be decomposed into a number of small and independent computational tasks. Three main advantages result from this decomposition:

1. each component can be modeled in as much detail as is needed;

2. each computational task can be optimized to achieve maximum computational efficiency;
3. parallel processing can be employed, assuming a multiprocessor computer system is available.

In this chapter, the interconnection property of large scale composite systems is exploited to model the system and to develop a general dynamic simulation algorithm. The concepts and procedures are applied to the electric power system for which a dynamic simulation program is developed. The most important properties of these procedures that make them attractive are outlined.

System Description

Consider a composite system, S, which comprises a collection of p subsystems, Sk, k=1,2,...,p, as shown in Figure 2. Let s be the number of interconnections and D(I) be the set of devices that form interconnection I. The exploitation of the structure of the system S reveals that the system S can be described in terms of the dynamical equations of the p independent subsystems Sk and in terms of the properties of the s interconnections.

Each subsystem Sk is described with a set of independent dynamical equations of the generic form:

$$f_k(\dot{x}_k, x_k, u_k, t) = 0 \qquad (1)$$

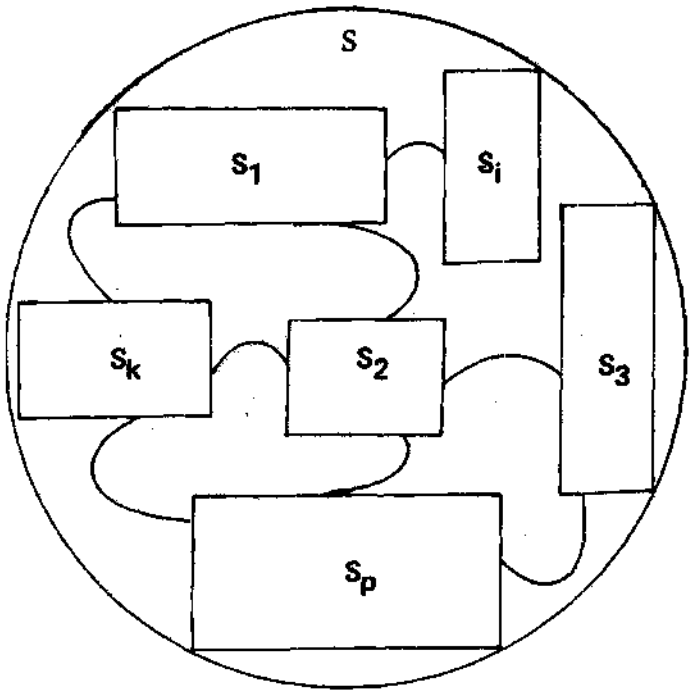

Figure 2. Composite System S

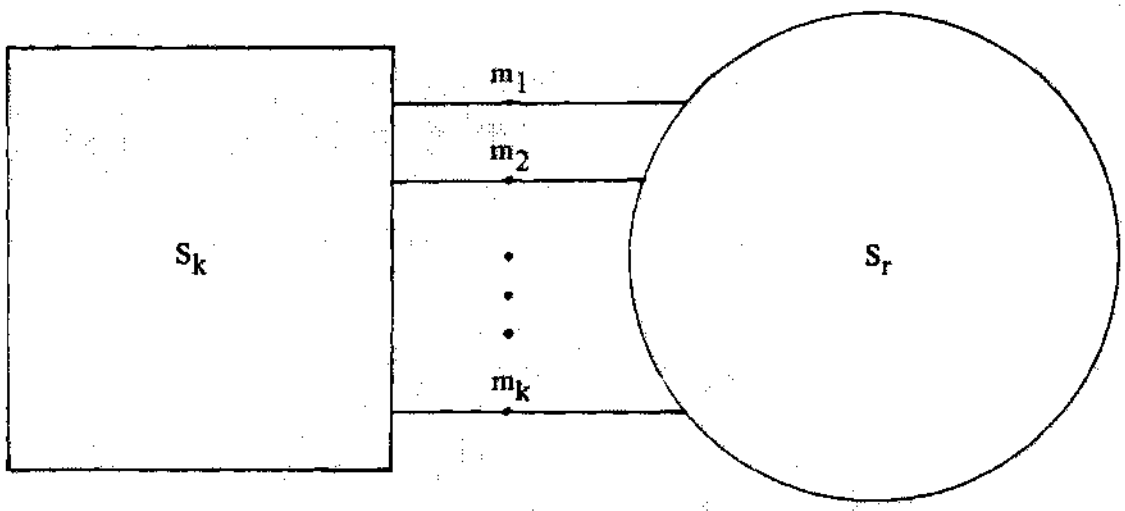

Figure 3. Subsystem S_k Connected to Rest of System S_r through m_k-ports

where : f_k : $n_k x 1$ function vector

x_k : $n_k x 1$ vector of description variables

u_k : $m_k x 1$ vector of interface through variables

t : time

. : denotes time derivative

Note that in the case of an electric power system the interface through variables will be the currents through the circuits that link the device Sk to the rest of the system.

Subsystem Sk is linked to the rest of the system, Sr, through m_k-ports as shown in Figure 3. This connection can be described with a set of algebraic equations (conservation laws, e.g., Kirchhoff's laws) of the form

$$l_j(x_1, x_2, \ldots, x_p, u_1, u_2, \ldots, u_p) = 0 \qquad (2)$$

where $j = 1, 2, \ldots, s$

The knowledge of equations (1) and (2) is sufficient to describe the interconnected system S. Consequently, each one of the susbsystems Sk can be modeled independently utilizing equation (1) only. Then the composite model for the system S is built up from the independent subsystem models and the interconnection equations (2). The modeling procedure for a single device Sk is discussed in the next section.

Device Modeling

The modeling problem for a device Sk connected to the rest of the

system Sr is defined as follows: given a device Sk, connected to the rest of the system Sr through m -ports, as in Figure 3, find its generalized model assuming that the dynamical equations of the device Sk are known. The basic ideas of the modeling procedure are illustrated next.

The dynamics of the device Sk are described with a set of nonlinear differential equations (1). The same component Sk can be described by an appropriate vector of algebraic difference equations resulting from sampling or numerical integration of the dynamical equations (1):

$$g(x(t),\ x(t-\alpha(h)),\ u(t),\ u(t-\beta(h)),\ t-\gamma(h)) = 0 \qquad (3)$$

where $\alpha(h)$, $\beta(h)$ and $\gamma(h)$ are positive functions of h, and h is the sampling rate or the integration time step. The subscript k is dropped for notational simplicity.

It will be assumed that the numerical integration of equation (1) has been performed with the absolutely stable trapezoidal rule. This does not limit the model in any way. The concepts can be developed with a number of other suitable numerical integration techniques.

It is important to partition the variables of the subsystem under consideration into two groups:

1. internal variables: x_B , these variables are proper to the device Sk only. They are not shared with any other element.
2. interface across variables: x_A , these variables are common to

the device Sk and all other devices connected to Sk (e.g., in a power system these variables correspond to the interface voltages).

Thus equation (3) can be partitioned as:

$$g(x_A(t),x_B(t),x_A(t-\alpha_A(h)),x_B(t-\alpha_B(h)),u(t),u(t-\beta(h)),t-\gamma(h)) = 0 \quad (4)$$

Upon elimination of the internal state variables $x_B(t)$, and solution for the variables $x_A(t)$, the above equation is transformed into:

$$x_A(t) = g'(x_A(t-\alpha_A(h)),x_B(t-\alpha_B(h)),u(t),u(t-\beta(h)),t-\gamma(h)) \quad (5)$$

The above concepts are now clarified by using the trapezoidal rule of integration explicitly.

Linearization of equation (1) yields:

$$Ax(t) + E\dot{x}(t) = Bu(t) \quad (6)$$

where A and E are nxn matrices and B is an nxm matrix.

The partition of equation (6) into m interface equations and (n-m) internal equations yields:

$$A1.x_A(t) + A2.\dot{x}_A(t) + A3.x_B(t) + A4.\dot{x}_B(t) = A5.u(t) \quad (6.1)$$

$$B1.x_A(t) + B2.\dot{x}_A(t) + B3.x_B(t) + B4.\dot{x}_B(t) = 0 \qquad (6.2)$$

where the matrices A's and B's have the following dimensions:

A1, A3, and A5 are mxm;

A2 and A4 are mx(n-m);

B1 and B3 are (n-m)xm;

B2 and B4 are (n-m)x(n-m).

Upon application of the trapezoidal rule of integration in the interval [t-h, t]:

$$[h'A1+A3]x_A(t)+[h'A1-A3]x_A(t-h)+[h'A2+A4]x_B(t)+[h'A2-A4]x_B(t-h)=$$

$$= [h'A5]u(t)+[h'A5]u(t-h) \qquad (7.1)$$

$$[h'B1+B3]x_A(t)+[h'B1-B3]x_A(t-h)+[h'B2+B4]x_B(t)+[h'B2-B4]x_B(t-h)= 0 \qquad (7.2)$$

where h'=h/2.

Solving (7.2) for $x_B(t)$ and substituting in (7.1):

$$\{[h'A1+A3]-[h'A2+A4][h'B2+B4]^{-1}[h'B1+B3]\}x_A(t) =$$

$$= \{[h'A1-A3]-[h'A2+A4][h'B2+B4]^{-1}[h'B1-B3]\}x_A(t-h) -$$

$$- \{[h'A2-A4]-[h'A2+A4][h'B2+B4]^{-1}[h'B2-B4]\}x_B(t-h) +$$

$$+ [h'A5]u(t) + [h'A5]u(t-h) \qquad (8)$$

In equation (8) the variables depending on time t-h are known and thus can be treated as constants. The application of this generic equation to power systems result in selecting the variables $x_A(t)$ and u(t) to be the voltages and the currents at the terminals of the device, (i.e., $x_A(t)=v(t)$, $u(t)=i(t)$). Thus equation (8) can be written as follows:

$$Yeq.v(t) = i(t) + I(t-h) \qquad (9)$$

where:

$$Yeq = [h'A5]\{[h'A1+A3]-[h'A2+A4][h'B2+B4]^{-1}[h'B1+B3]\}$$

$$I(t-h) = [h'A5]\{[h'A5]i(t-h) -$$

$$-([h'A1-A3]-[h'A2+A4][h'B2+B4]^{-1}[h'B1-B3])v(t-h) -$$

$$-([h'A2-A4]-[h'A2+A4][h'B2+B4]^{-1}[h'B2-B4])x_B(t-h)\}$$

Equation (9), which is a particular form of equation (5), can be interpreted as follows: in the time interval [t-h, t] the device Sk can be represented as a resistive network with conductance matrix Yeq and current sources I(t-h) as in Figure 4.

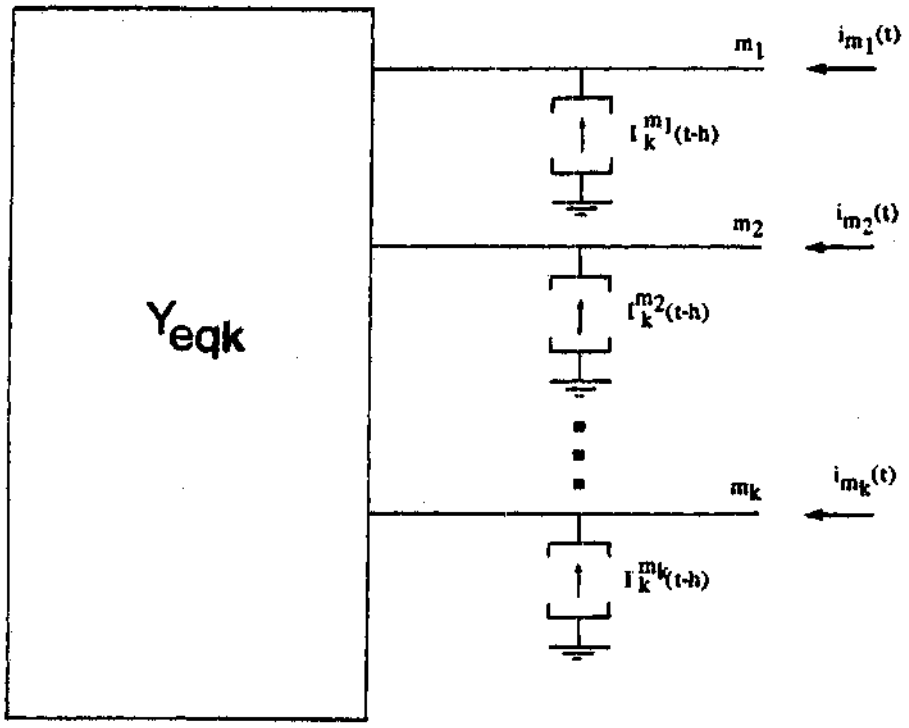

Figure 4. Generalized Model for Subsystem S_k

The equivalent conductance matrix Yeq has a minimal dimension. Its dimension is equal to the number m of interface variables independently of the model dimension of the device. Consequently, each device can be modeled as a generalized resistive network of dimension equal to the number of interconnections of the device to the rest of the system. As far as the overall system is concerned, the contribution of each component is contained in the information carried by the conductance matrix Yeq and the "past history" current sources I(t-h).

Numerical Stabilization. The above modeling procedure is obtained through numerical integration of the differential/algebraic equations which describe the element. It is well known that numerical computation of derivatives can generate numerical noise. The noise

consists of oscillations which, if not damped, persist and corrupt the solution. The calculations of the voltage drop across a lumped inductance is an example. It is possible that the interaction of this model with other system components lead to an amplification of the generated noise. Consider for example an inductor in series with a circuit breaker. The opening of the breaker results in a high voltage across the inductor. The numerical computation of this voltage will assume a large numerical error which will propagate through the system. In many cases noise amplification leads to numerical instability.

Lumped inductances appear in many power system component models: generators, transformers, loads, etc. To damp the numerical oscillations across lumped inductances parallel resistances are used as shown in Figure 5a.

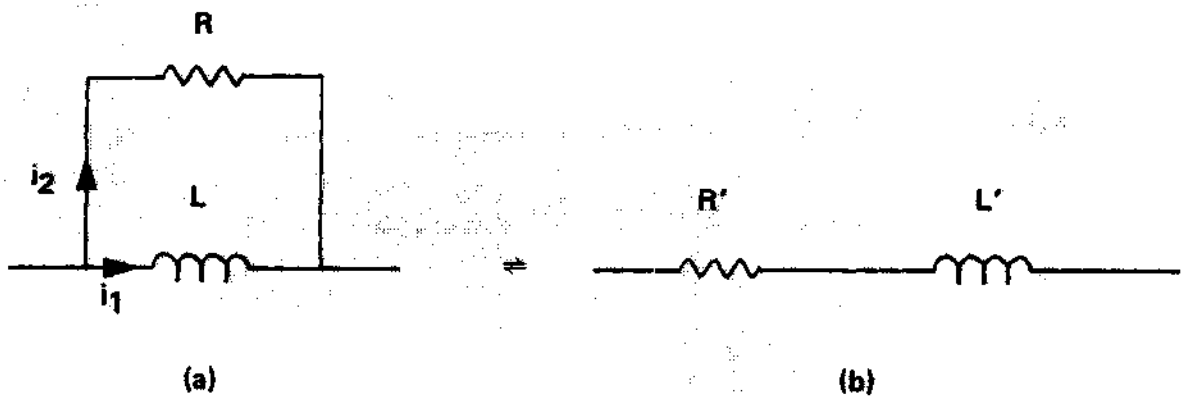

Figure 5. Lumped Inductance with Numerical Stabilizer

The objective is to obtain the same frequency response in some prespecified frequency range for the actual model and its damped

version. An addition of a resistance in parallel with an inductance is equivalent to replacing a constant lossless element by a lossy, frequency dependent model as shown if Figure 5b.

From the above figures, the following relationships are obtained:

$$R' = R.w^2.L^2/(R^2 + w^2.L^2) \qquad (10.1)$$

$$w.L' = R^2.w.L/(R^2 + w^2.L^2) \qquad (10.2)$$

It is then obvious that the frequency response of the new element will differ from that of a pure inductance. In fact:

$$\lim_{w \to \infty} L' = 0 \qquad (11.1)$$

$$\lim_{w \to 0} L' = L \qquad (11.2)$$

$$\lim_{R \to \infty} L' = L \qquad (11.3)$$

$$\lim_{R \to 0} L' = 0 \qquad (11.4)$$

Thus the error will increase with frequency and decrease with an increasing value of the parallel resistance R.

On one hand, it would therefore appear desirable to use as large a parallel resistor as possible to reduce the response error. On the other hand however the damping effect, measured by the ratio $D = R'/wL'$, decreases with an increase in the size of the resistor R. In fact:

$$D = R'/wL' = wL/R \tag{12.1}$$

$$\lim_{R \to \infty} D = 0 \tag{12.2}$$

From the physical analysis of the damping scheme, it is then clear that the choice of the value of the damping resistance R has to be based upon the following two conflicting criteria:

a) minimum introduced error in the frequency response

b) maximum effectiveness of the damping of the numerical oscillations.

In the next section, an error analysis is performed which provides a rational basis for the selection of the numerical stabilizers.

Error Analysis. The following error analysis is performed for the trapezoidal integration. Similar error analysis can be performed for other integration techniques. Consider Figure 5a; then

$$v = L.di_1/dt \tag{13.1}$$

$$v = R.i_2 \qquad (13.2)$$

Performing a numerical integration of the above equations through the trapezoidal rule, with time step h=2h', yields:

$$h'v(t) + h'v(t-h) = Li_1(t) - Li_1(t-h) \qquad (14.1)$$

$$v(t) - v(t-h) = Ri_2(t) - Ri_2(t-h) \qquad (14.2)$$

where $h' = h/2$. Let $G = 1/R$, then addition of equations (14.1) and (14.2) yields:

$$v(t) = [1/(G+h/2L)][i(t)-i(t-h)] - a.v(t-h) \qquad (15)$$

where $a = [1-(2LG/h)]/[1+(2LG/h)]$

A unit step current excitation yields:

$$v(1) = 1/[G+h/2L]$$

$$v(2) = -a.v(1)$$

$$\vdots$$

$$v(n) = (-a)^{n-1} v(1), \quad n = 2, 3, \ldots$$

Thus depending on the value of a, the behavior can be under or over damped. Of particular interest is the critically damped case in which setting of v(k) occurs in one time step. This requires a = 0 or Go = h/2L. This is not necessarily the best choice of G as the next section confirms.

The discrete model of an inductor, using trapezoidal integration with time step h, is identical in behavior to the continuous model of a line using a lossless stub line with travel time h/2 and characteristic impedance 2L/h. The input admittance of the lossless stub line is:

$$Y = G - j[h/2L\tan(wh/2))] \qquad (16)$$

But the exact input admittance is -j/wL. Thus, the error is:

$$error = G - j[(h/2L\tan(wh/2))-(1/wl)]$$

Normalizing the error yields:

$$ER = jGwL + [(wh/2\tan(wh/2))-1] \qquad (18)$$

Note that in the limit, ER=0 when w goes to 0.

Theoretically, the maximum reproduceable frequency is related to the sampling rate h by:

$$fm = 1/2h \tag{19}$$

However, at this frequency the error is:

$$ER = jG.\Pi.L/h - 1 \tag{20}$$

Even for G=0, the error is at least 100%. Therefore it is meaningless to use this sample rate h for signals with higher frequency content than fm.

It is practical to restrict the reproduceable maximum frequency fm to some practical frequency fp=k.fm where k, the frequency range coefficient, is less than 0.5, even when no shunt damping resistor is used.

From the error expression it is seen that for a fixed value of G, as the frequency decreases, both the error due to discretization and the error due to the parallel conductance decrease. The error can even be decreased by reducing the value of G. In fact:

$$|ER| = \{G^2w^2L^2 + [(wh/2\tan(wh/2))-1]^2\}^{\frac{1}{2}} \tag{21}$$

But the value of G determines the damping effect:

$$D = wLG \tag{22}$$

The error ER and the damping effect D are related by:

$$|ER| = \{D^2 + [(wh/2\tan(wh/2))-1]^2\}^{\frac{1}{2}} \quad (23)$$

It is clear that a decrease in the value of G will decrease the error while it will deteriorate the damping effect.

The error can be expressed in terms of the frequency range coefficient k and the damping coefficient b which is defined as b = G/Gc. Thus

$$D = b.k.\pi/2 \quad (24)$$

and

$$|ER| = \{D^2 + [(k\pi/2\tan(k\pi/2))-1]^2\}^{\frac{1}{2}} \quad (25)$$

The preceding analysis suggests that an acceptable value for G can be determined with the following steps:

1. specify a frequency range, i.e., determine k
2. specify a damping effect ratio D, i.e., determine b.

For example, selecting b=0.15, k=0.25, insures that the error introduced by either the discretization or the damping conductance does not exceed 6% for any frequency lower than 0.25fm the combined error is less than 8%. Much lower errors are, of course, incured at lower frequencies.

Illustrative Example. The modeling procedure is illustrated with

an example. The device to be modeled is the simplest generator model. In Park's variables the synchronous machine has the 0-d-q equivalent networks shown in Figure 6. The dynamics of the device are described with the following differential equations which are expressed on the generator 0-d-q coordinate system:

$$v_0 = (r_0+R_1\ )i_0 - R_1\ i_1 \tag{26.1}$$

$$v_d = (r+R_2\ +R_4\ )i_d - R_4\ i_f - R_4\ i_{dm} - R_2\ i_2 + wL_q i_q \tag{26.2}$$

$$v_q = (r+R_5\ +R_6\ )i_q - R_6\ i_{qm} - R_5\ i_4 - wL_d i_d + wL_{AD} i_f \tag{26.3}$$

$$\dot{\delta} = w - 1 \tag{26.4}$$

$$3\tau\ \dot{w} = 3Tm - (L_d-L_q)i_d i_q + L_{AD} i_q i_f - Dw \tag{26.5}$$

$$\dot{i}_1 = -\ [R_1\ /(L_0\quad\ )][i_1 - i_0] \tag{26.6}$$

$$\dot{i}_2 = -\ [R_2\ /l_d][i_2 - i_d] \tag{26.7}$$

$$\dot{i}_3 = -\ [R_3\ /l_f][i_3 - i_f] \tag{26.8}$$

$$\dot{i}_4 = -\ [R_5\ /l_q][i_4 - i_q] \tag{26.9}$$

$$v_f = (R_3\ +R_4\ +r_f)i_f - R_3\ i_3 - R_5\ i_d + R_5\ i_{dm} \tag{26.10}$$

$$\dot{i}_{dm} = -\ [R_5\ /L_{AD}][i_{dm} - i_d + i_f] \tag{26.11}$$

$$\dot{i}_{qm} = -\ [R_6\ /L_{AQ}][i_{qm} - i_q] \tag{26.12}$$

Upon integration of the above equations with the trapezoidal rule

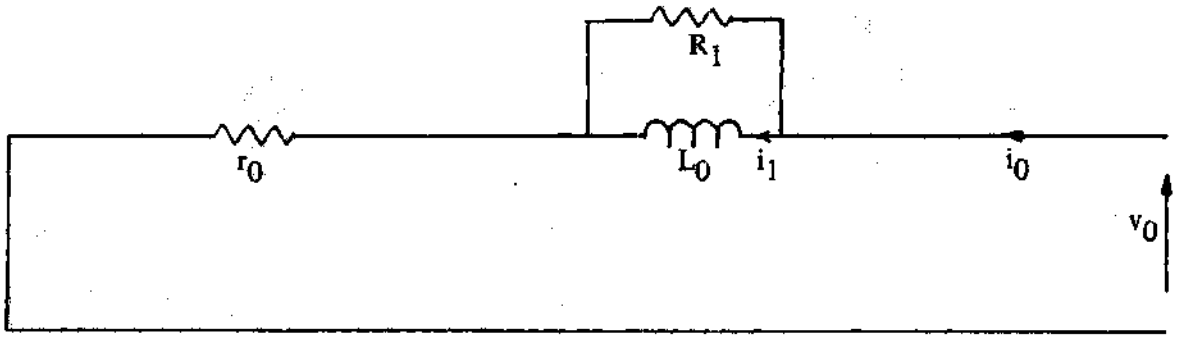

0-Axis Equivalent Circuit

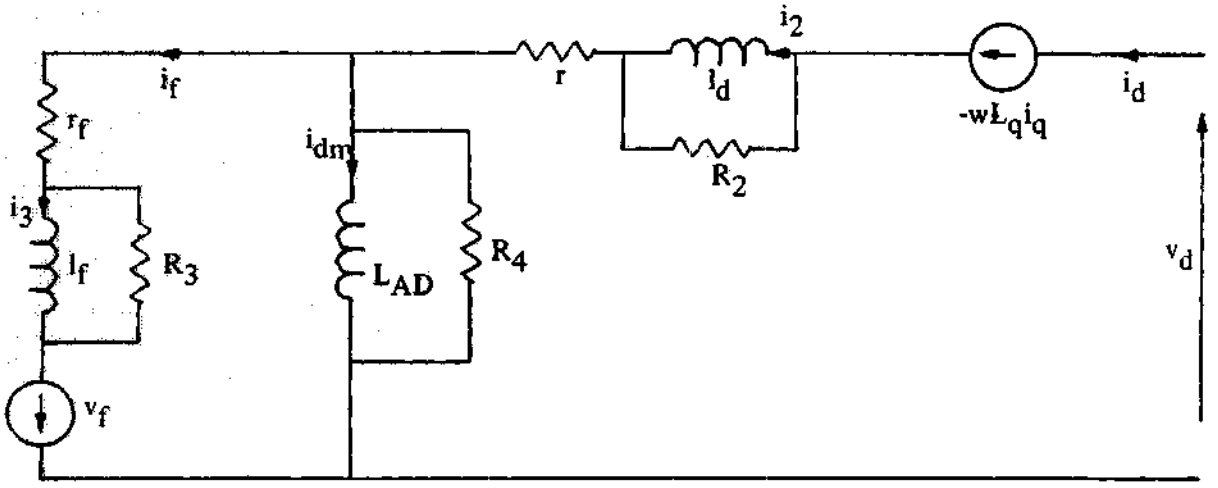

d-Axis Equivalent Circuit

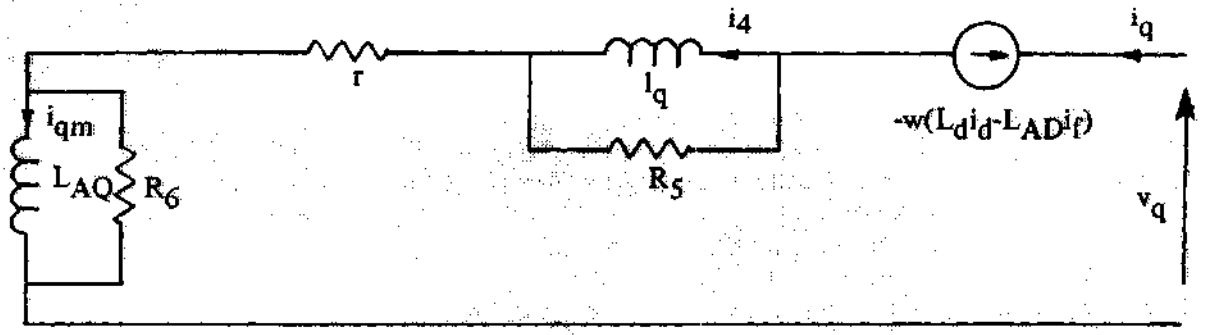

q-Axis Equivalent Circuit

Figure 6. Generator o-d-q Equivalent Circuits (with Numerical Stabilizer)

of integration, with time step h, it results:

$$C(t-h).v(t) = Z(t-h).i(t) - b(t-h) \qquad (27)$$

where: $i = [i_0\ i_d\ i_q]^T$

$$v = [v_0\ \ v_d\ \ v_q\ \ \delta\ \ w\ \ i_1\ \ i_2\ \ i_3\ \ i_4\ \ i_f\ \ i_{dm}\ \ i_{qm}]^T$$

$$Z(t) = \begin{bmatrix} r_0 + R_1 & 0 & 0 \\ 0 & r+R_2+R_4 & L_q w(t) \\ 0 & -L_d w(t) & r+R_5+R_6 \\ 0 & 0 & 0 \\ 0 & \frac{h}{6\tau}(L_d-L_q)i_q(t) & \frac{h}{6\tau}[(L_d-L_q)i_d(t)-L_{AD}i_f(t)] \\ -h'R_1/L_0 & 0 & 0 \\ 0 & -hR_2/2l_d & 0 \\ 0 & 0 & 0 \\ 0 & 0 & -hR_5/2l_q \\ 0 & -R_4 & 0 \\ 0 & -hR_4/2L_{AD} & 0 \\ 0 & 0 & -hR_6/2L_{AQ} \end{bmatrix}$$

$$C = \begin{bmatrix} I(3x3) & C12 \\ 0(9x3) & C22 \end{bmatrix}$$

where I(3x3) is a 3x3 identity matrix and 0(9x3) is a 9x3 zero matrix, and:

$$C12 = \begin{bmatrix} 0 & 0 & R_1 & 0 & 0 & 0 & 0 & 0 & 0 \\ 0 & -L_q i_q & 0 & R_2 & 0 & 0 & R_4 & R_4 & 0 \\ 0 & L_d i_d - L_{AD} i_f & 0 & 0 & 0 & R_5 & -L_{AD} w & 0 & R_6 \end{bmatrix}$$

$$C22 = - I - h' . C22'$$

where I is a 9x9 identity matrix,

$$h' = h/2$$

$$C22' = \begin{bmatrix} 0 & -1 & 0 & 0 & 0 & 0 & 0 & 0 & 0 \\ 0 & D/3\tau & 0 & 0 & 0 & 0 & 0 & i_q L_{AD}/3\tau & 0 \\ 0 & 0 & R_1/L_0 & 0 & 0 & 0 & 0 & 0 & 0 \\ 0 & 0 & 0 & R_2/l_d & 0 & 0 & 0 & 0 & 0 \\ 0 & 0 & 0 & 0 & R_3/l_f & 0 & -R_3/l_f & 0 & 0 \\ 0 & 0 & 0 & 0 & 0 & R_5/l_q & 0 & 0 & 0 \\ 0 & 0 & 0 & 0 & R_3/h' & 0 & R' & R_4/h' & 0 \\ 0 & 0 & 0 & 0 & 0 & 0 & R_4/L_{AD} & R_4/L_{AD} & 0 \\ 0 & 0 & 0 & 0 & 0 & 0 & 0 & 0 & R_6/L_{AQ} \end{bmatrix}$$

where $R' = (r_f + R_3 + R_4)/h' + 1$

$$
b(t)=\begin{bmatrix}
-(r_0 + R_1)i_0(t) + R_1\, i_1(t) + v_0(t) \\
-(r+R_2 + R_4)i_d(t) + R_4\,[i_f(t)+i_{dm}(t)] + R_2\, i_2(t) + v_d(t) \\
-(r+R_5 + R_6)i_q(t) + R_6\, i_{qm}(t) + R_5\, i_4(t) + v_q(t) \\
\delta(t) + h'w(t) - h \\
h'Tm + [1-(hD/6\tau)]w(t) \\
[h'R_1/(L_0)][i_0(t)-i_1(t)] + i_1(t) \\
[h'R_2/(l_d)][i_d(t)-i_2(t)] + i_2(t) \\
[h'R_3/(l_f)][i_f(t)-i_3(t)] + i_3(t) \\
[h'R_5/(l_q)][i_q(t)-i_4(t)] + i_4(t) \\
2v_f - (r_f+R_3+R_4)i_f(t) + R_3\, i_3(t) + R_4\,[i_d(t)-i_{dm}(t)] \\
[h'R_4/(L_{AD})][i_d(t)-i_f(t)-i_{dm}(t)] + i_{dm}(t) \\
[h'R_6/(L_{AQ})][i_q(t)-i_{qm}(t)] + i_{qm}(t)
\end{bmatrix}
$$

By decomposing the vector v(t) into interface across variables $x_A(t)$ and internal description variables $x_B(t)$ as:

$$x_A = [v_0 \;\; v_d \;\; v_q]^T$$

$$x_B = [\delta \;\; w \;\; i_1 \;\; i_2 \;\; i_3 \;\; i_4 \;\; i_f \;\; i_{dm} \;\; i_{qm}]^T$$

Then, equation (27) can be written as:

$$\begin{bmatrix} C11 & C12 \\ 0 & C22 \end{bmatrix} \begin{bmatrix} x_A(t) \\ x_B(t) \end{bmatrix} = \begin{bmatrix} Z11 & Z12 \\ Z21 & Z22 \end{bmatrix} \begin{bmatrix} i\ (t) \\ 0 \end{bmatrix} - \begin{bmatrix} b1(t-h) \\ b2(t-h) \end{bmatrix}$$

Upon elimination of $x_B(t)$:

$$x_A(t) = [Z11-C12.C22^{-1}.Z21]i\ (t) - [b1(t-h)-C12.C22^{-1}.b2(t-h)]$$

which is the generalized resistive model sought, with:

$$Yeq = [Z11 - C12.C22^{-1}.Z21]^{-1}$$

$$I(t-h) = - Yeq.[b1(t-h) - C12.C22^{-1}.b2(t-h)]$$

Interface Network Model

As described in the previous section, every component in the system is modeled as a generalized resistive network. The interface variables are the only links between the different devices. As long as these variables are expressed in the same coordinate system the individual devices can be interconnected together. The resulting system shall be called the Interface Network. This system itself will be described with an appropriate resistive model.

Thus, to build up the interface network the following steps are taken:

1. express all interface variables in the same coordinate system;
2. utilizing the connectivity equations, interconnect all the devices.

The second step is performed by utilizing nodal analysis. Assuming that the device Sk is connected to interconnection I, the companion resistive network describing the device is:

$$Y_{eqk} \cdot x_A^I(t) = i_k^I(t) + I_k(t-h) \tag{9}$$

where $x_A^I(t)$ = across variables at interconnection I

$i_k^I(t)$ = through variables at interconnection I, for device Sk.

If the device Sk is connected to more than one interconnections, equation (9) must be partitioned appropriately.

Now consider all the devices that form interconnection I. Let D(I) represent the set of these devices, and Mi be the number of devices in D(I). All devices in the set D(I) share the same interface variables. Thus:

$$\begin{aligned} Y_{eq1} x_A^I(t) &= i_1^I(t) + I_1(t-h) \\ Y_{eq2} x_A^I(t) &= i_2^I(t) + I_2(t-h) \\ &\cdot \\ &\cdot \\ &\cdot \\ Y_{eqM_i} x_A^I(t) &= i_{M_i}^I(t) + I_{M_i}(t-h) \end{aligned} \tag{29.1}$$

In addition, the nodal equations at interconnection I are:

$$\sum_{k\epsilon D(I)} i_k^I(t) = 0$$

Upon substitution of $i_k(t)$, $k \in D(I)$, from the equations (29.1):

$$\left(\sum_{k=1}^{M_i} Y_{eqk}\right) x_A^I(t) = \sum_{k=1}^{M_i} I_k(t-h)$$

or

$$Y_{eq}^I . x_A^I(t) = I^I(t-h) \qquad (29.2)$$

This procedure is repeated for each interconnection. Assuming a system with s interconnections, the following equations are obtained:

$$Y_{eq}^1 \; x_A^1(t) = I^1(t-h)$$

$$Y_{eq}^2 \; x_A^2(t) = I^2(t-h)$$

$$\vdots$$

$$Y_{eq}^s \; x_A^s(t) = I^s(t-h)$$

or, in compact matrix notation:

$$G(t-h).x(t) = b(t-h) \qquad (30)$$

where : G is the interface network conductance matrix

x is the vector of interface across variables

b is the vector of past history current sources

The conductance matrix G is made up from the matrices Yeqk's and has the following form:

$$G = \begin{bmatrix} G11 & & & & & & \\ & G22 & & & & & \\ & & \ddots & & & & \\ & & & Gii & Gij & & \\ & & & Gji & Gjj & & \\ & & & & & \ddots & \\ & & & & & & Gss \end{bmatrix}$$

In the matrix G above the matrices Gij are formed from elements of the matrices Yeqi's. All the diagonal submatrices Gii are nonzero. However the off-diagonal submatrix Gij is nonzero only if there is a device between interconnection I and interconnection J.

Equation (30) shall be called the interface network equation.

Standard sparsity coded techniques based on optimally ordered triangular factorization are employed for the solution of the interface network equation.

Dynamic Simulation Algorithm

The interface network is modeled with equation (30) as a resistive network. The conductance matrix G and the past history current sources b are obtained from the individual system component models. The system response is then computed with the repetitive solution of equation (30) and subsequent substitution into the individual device equations. At every time step equation (30) is formed from the resistive model of each device.

The general algorithm for the computation of the dynamic response of a system in the time interval [0 , T] involves the following steps:

Step 1: Define initial conditions (t=0)

Step 2: Update time; i.e., let t=t+h. If t>T Stop

Step 3: Compute the resistive model of each device Sk in the system, i.e., compute:

- $Y_{eqk}(t-h)$

- $I_k(t-h)$

Step 4: Form the interface resistive network:

$G(t-h).x(t) = b(t-h)$ and

Solve this equation for x(t)

Step 5: Go to Step 2.

It is important to note that step 3 involves a number of independent computational tasks.

Power System Dynamic Simulation Program

The described generalized modeling procedures have been utilized towards the development of a power system dynamic simulation program. This program is easy to use, modular and expandable. Moreover it impacts on a number of other important issues in a very favorable way. These are:

1. Model Accuracy
2. Model Optimization
3. Sparsity
4. Suitability to Parallel Processing

These issues are discussed in the next sections.

The basic component of the computer program is a library of computer subprograms, one for each power system element. Once the data for all elements are read the program requires a power flow solution to determine the steady state. The results of the load flow are used to determine the initial conditions. The iteration scheme for the computation of the dynamic response is very simple. In each iteration all elements are scanned to compute the equivalent conductance matrix and equivalent past history current sources. These quantities are transformed into a common frame of reference. The computation of these

quantities is very simple. Each element is identified with a code. The code dictates the call of a certain subprogram from the library.

The generalized power system simulation program has been validated with numerous test cases. One specific test is the Benchmark model for subsynchronous resonance [80]. For example, Figure 7a, which is taken from reference [80], compares to Figure 7b, which is obtained with the generalized power system dynamic simulation program.

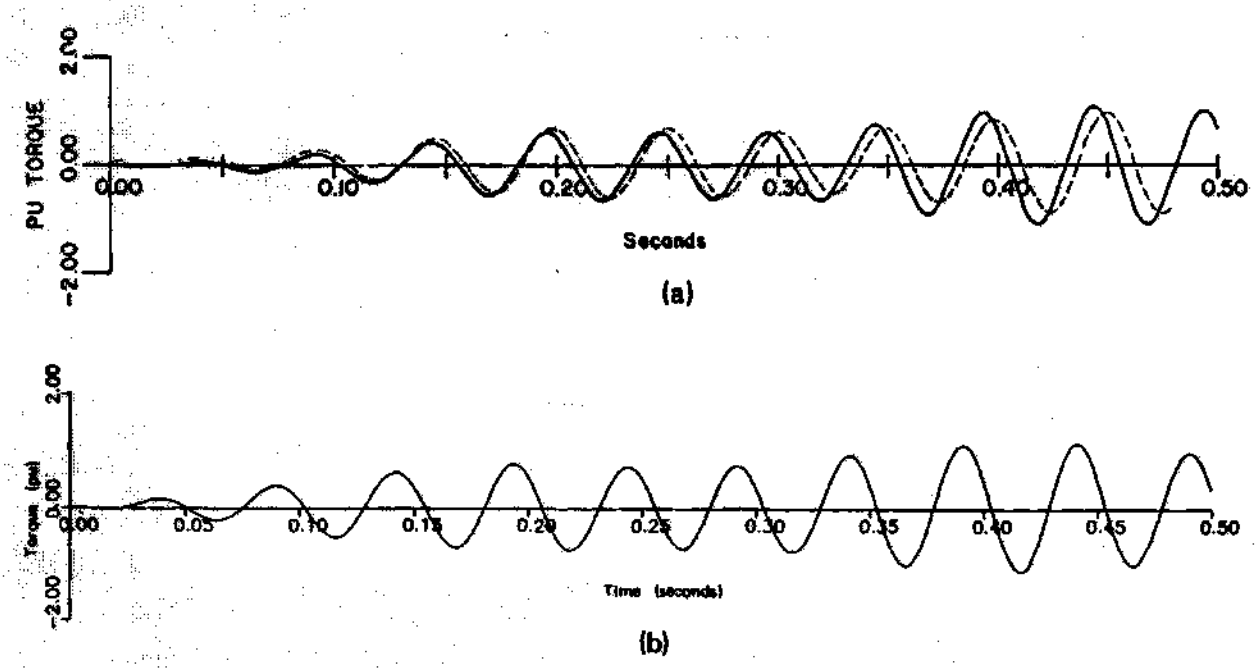

Figure 7. Torsional Oscillations on Generator—Exciter Shaft

a) Curve Taken from Reference [80]
b) Curve Obtained with the Generalized Power System Dynamic Simulation Program

Model Accuracy

The formation of the interface network is independent of the particular models employed for system component representation. For each device there are no restrictions on:

1. the dimension of the subsystem describing the device. While the set of dynamical equations describing each element has no influence on the structure of the interface network, it determines the accuracy of each mode
2. the numerical procedure utilized to obtain the discrete state equations. Here the objective is to formulate an appropriate resistive network for each device. Thus the numerical procedure (integration) utilized for one device is independent of the procedure utilized for another device. Hence different numerical integration rules can be applied to accomodate different devices.

Thus, model accuracy can be optimized by an adequate choice of the device dimension and an appropriate integration scheme.

Model Optimization

The computational procedure for the resistive model of each device can be optimized. For example, the conductance matrix of linear elements is constant. Hence it is computed only once, and stored, in the initialization stage. For nonlinear elements the conductance matrix and the past history current sources need to be updated at each iteration. The device equations are studied and an analysis is performed to determine the minimum number of computations required for the update of the resistive model. Thus, the computational algorithm associated with a particular device can be optimized. Many times this optimization can be effected by inspection. This is so because the

computational procedure for a given device is rather simple. In general, optimization of the computational procedure may involve one or more of the following:

1. storage of time independent/linear intermediate results
2. optimal ordering of dynamical equations
3. specialized sparsity techniques
4. etc.

Sparsity

The described computational procedure is extremely suitable to exploitation of the sparsity properties of the equations involved. Sparsity exploitation can occur at the device level as well as at the interface network level. At the device level, specialized sparsity techniques are applied. At the interface network level, the sparsity properties of the admittance matrix of equation (30) is exploited. Note that the submatrices which make up the conductance matrix G are in general 3x3 matrices. The location of these submatrices is dependent upon the ordering of the interconnections. The interconnections can be optimally ordered such as to minimize the computational effort for the solution of the interface equation. To this purpose standard optimal ordering algorithms [53] can be utilized.

Parallel Processing

The simulation algorithm described above is naturally suitable for parallel processing. It has very important features required for a good

parallel processing methodology. First of all, the computational task "Step 3" of the algorithm can be performed in parallel for each device. Secondly, the amount of data shared between a given device and the interface network is minimum: for linear elements only the interface variables need to be shared, for nonlinear elements the interface variables and the resistive model parameters need to be shared. The internal state variables and other parameters of any of the devices need not be shared. The third feature is that the algorithm is simple and uniform. In fact "Step 4" of the algorithm is independent of the particular models employed for system component representation. All components are described with a conductance matrix and a past history vector (a resistive network). It is obvious that the simulation program can be easily implemented in a multiprocessor system. An example of such an implementation is shown in Figure 8. It is simple enough to provide simple answers to problems such as hardware, b) optimization of communication links, c) implementation with the off-the-shelf components, etc. For example, maximization of hardware utilization can be achieved by assigning the same amount of computations to each processor.

Summary

The basic approach and the concepts utilized to develop a general modeling procedure and a general dynamic simulation algorithm for large scale composite systems were presented. These procedures result from the exploitation of the structure of the interconnected dynamic systems.

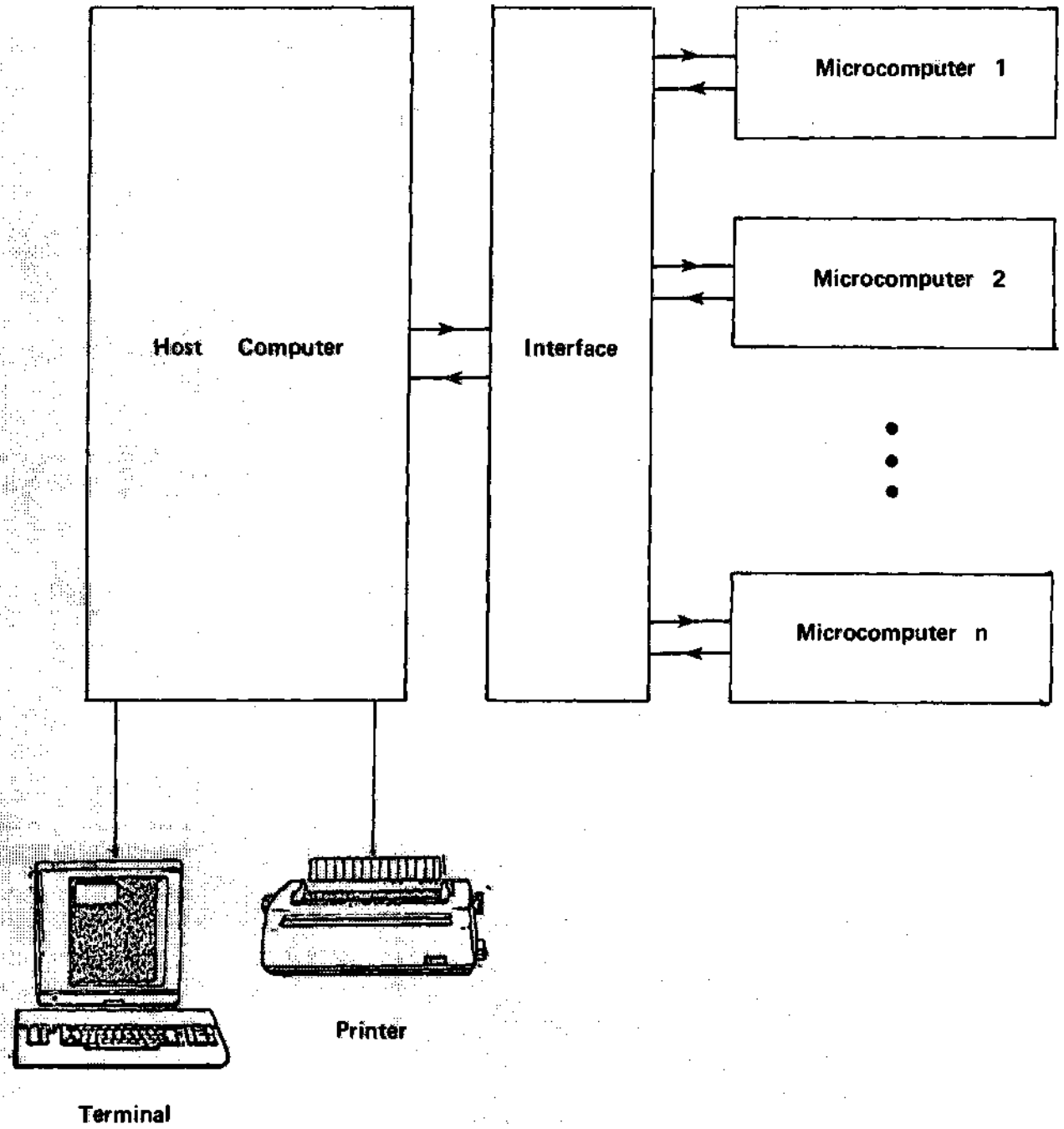

Figure 8. Special Purpose All Digital Machine for Power System Dynamic Simulation

The methodology has been applied to the electric power system. The result is a digital, dynamic simulation program. This program is modular. Each module represents a power apparatus modeled as a resistive companion network. The interface network, obtained by interconnecting the individual elements together, has an equivalent resistive network model. The attractive properties of the digital, modular, dynamic simulation program were discussed. These properties are:

1. expandability
2. model accuracy
3. model optimization
4. sparsity
5. numerical stability
6. suitability to parallel processing.

The simulation program forms the basis for the formulation of the optimal control problem of composite dynamical systems. It is used to investigate the mitigation of subsynchronous resonant oscillations in electric power systems. These topics are presented in the next chapters.

CHAPTER III

THE CONTROL PROBLEM

A control scheme is defined as any system that regulates, tracks or in general controls the flow of some quantities in some desired fashion. The objective of Optimal Control Theory is to determine a control law that will cause a process to satisfy the physical constraints and at the same time optimize the performance of the system measured with a performance index [54]-[55].

The first step towards the solution of the control problem is the development of a mathematical model of the physical system. This step includes the description of the dynamics of the system to be controlled (state equations) and the description of system constraints and possible alternatives (control and state constraints). The second step describes the task to be accomplished and a statement of the criterion for judging the performance. These two steps, or the problem formulation, take into account the designer's objectives, e.g., accuracy, simplicity, cost, reliability, size, etc.

Dynamic Programming [56] and the Minimum Principle [57] have been applied to solve the control problem. When the system is linear, the optimal control law is defined with a matrix differential or algebraic equation, for the finite time and the infinite time problems respectively. In this case the control law is a linear combination of

the state variables (feedback law). For a nonlinear system this approach leads to a nonlinear partial differential equation known as the Hamilton-Jacobi-Bellman equation. One way to solve the latter equation is to guess a form for the solution and then check whether it satisfies the given equation and its boundaries. It is important to note that the control law is not unique. But in general, the optimal strategy is in the form of feedback of the state variables of the system.

For a large scale system, the above accurate mathematical solution might not be feasible. The electric power system in particular is nonlinear, time varying, stiff, and geographically dispersed. The design of control schemes should address issues such as feasibility, computational effort, cost and reliability of hardware such as communication links. Specifically, economic and reliability reasons favor decentralized control schemes. Also, for many problems, some combination of continuous and discrete control laws are required. These goals of structuring a distributed information and decision framework, combining discrete and continuous control schemes, do not mesh well with the available centralized methodologies and procedures of the classical and modern control theories [58]-[62]. For example, many times conventional procedures applied to large scale, stiff, dynamic systems result in centralized control schemes which are not acceptable due to high gains, nonmeasurable state variables, etc. Moreover, the control strategy depends on the choice of the performance index. However, in many cases, the performance index cannot be selected in a generally acceptable way. Such selection is usually based on trial and error methods.

This Chapter presents a novel approach for the design of controllers applicable to general large scale, nonlinear, stiff, dynamic systems. The approach is based on sensitivity analysis of a vector performance index. It results in an optimal control law since it optimizes over the different components of the vector performance index. Physical constraints on controller structures are explicitly incorporated ensuring design feasibility. In fact the controller structure as well as the controller structure constraints are determined by the designer.

Control Design Procedure

This section presents a novel control design procedure. The method is based on a gradient iterative technique performed within the framework of the dynamic simulation algorithm presented in chapter II. Computationally, the method is based on Sensitivity Analysis of some prespecified vector performance index with respect to some control parameters. At each iteration, the simulation algorithm provides the sensitivity matrix. An important characteristic of this approach is that the structure of the controller is defined by the designer. Consequently, the control scheme is an optimal (optimization of a performance index) and feasible (control structure and constraints predetermined) strategy. Indeed, the designer knows what controller has access to what information.

Mathematically, the problem is formulated as follows. The objective is to minimize the different components of a p-vector

performance index,or cost, C, according to some weights wi, i=1,2,...p. The vector performance index C is defined with:

$$C = [\ J_1,\ J_2,\ \ \ldots\ \ ,J_p\ ]^T \tag{31}$$

Each performance index J_i is described with an equation of the form:

$$J_i = -\tfrac{1}{2} \int_0^T g_i(x,u,t)\ dt \tag{32}$$

where x is the state vector and u is the control vector.

As mentioned earlier the control scheme has a prespecified structure. So, assuming a control structure u = u(k,x), centralized or decentralized, continuous or discrete, with a number of adjustable parameters k (gains or logical variables), each performance index can be expressed as:

$$J_i = -\tfrac{1}{2} \int_0^T g\ (x,k,t)\ dt \tag{33}$$

where k is a qx1 control parameter vector.

The control problem can then be stated as follows: given the control structure u(k,x), the mathematical model of the plant f(x,x,k,t)=0, and a vector performance index C, compute the optimal values of the control parameter vector k.

Note that the performance indices J_i's that form the vector C may not be optimized simultaneously by the same value of the vector k. Then, the problem of optimizing the different entries of C

simultaneously is not well defined. One way to solve the problem is to optimize the following weighted index:

$$J = C^T.W.C \tag{34}$$

where W is a pxp weight matrix of full rank p.

The vector performance index C is nonlinear. For this reason the defined control problem is solved iteratively via a gradient technique performed within the framework of the simulation procedure. Specifically, the time period of interest [0,T] is divided into a number n of shorter time intervals [ih,(i+1)h]. Then, at each iteration the vector performance index is linearized around an operating point. The time step, h, is chosen small enough so that the linearization technique is sufficiently accurate.

Upon linearization of the vector performance index C, around an operating point k_i :

$$C(k) = C(k_i) + \Sigma(k_i).(k-k_i) + h.o.t. \tag{35}$$

The above expression requires the computation of a qxp sensitivity matrix Σ defined by:

$$\Sigma = \partial C^T / \partial k \tag{36}$$

The matrix Σ represents the sensitivity of the prespecified vector performance index C with respect to the control parameter vector k. The computation of the matrix Σ is the central point of the

procedure.

Upon linearization of the performance index C the quantity J to be minimized takes the form:

$$J = \sum_{i=1}^{n} \Delta J_i \qquad (37)$$

with

$$\Delta J_i = (z_i + \Sigma_i^T . k_i)^T . W . (z_i + \Sigma_i . k)^T$$

where $z_i = C(k_i) - \Sigma_i^T k_i$

This procedure transforms the problem into a linear quadratic problem.

The necessary conditions for the minimization of the scalar ΔJ, with respect to the vector k, are:

$$d\Delta J/dk = 0$$

Applications of these conditions yield:

$$d\Delta J_i/dk = 2 \Sigma_i W(z_i + \Sigma_i^T k) = 0$$

$$(\Sigma_i W \Sigma_i^T)k = - \Sigma Wz$$

The qxq matrix $\Sigma_i . W . \Sigma_i^T$ has a rank r=minimum(p,q). Since W is

a matrix with full rank p, the matrix $\Sigma_i.W.\Sigma_i^T$ is invertible only if p>q. Otherwise, generalized inverse [63]-[64] is used. In any case, the optimal value of k is given by:

$$k = -(\Sigma_i.W.\Sigma_i^T)^{\#1}\Sigma_i.W.z_i \tag{38}$$

where #1 denotes generalized inverse.

The two cases are summarized below:

Case 1. p>q : regular inverse is used

Case 2. p<q : generalized inverse is used.

This step determines a gradient direction. The control parameter vector k, at iteration (i+1), is updated via:

$$k_{i+1} = k_i - \alpha^*.d_i \tag{39}$$

where $d_i = (\Sigma_i.W.\Sigma_i^T)^{\#1}\Sigma_i.W.[C(k_i) - \Sigma_i^T k_i]$

α^* is an optimum scalar

The optimal value of the scalar α^* is obtained utilizing a quadratic fit, as in Figure 9. This requires the computation of the performance index at two different values of α, namely α_1 and α_2. The optimal value of α is given by:

$$\alpha^* = \frac{(\alpha_1^2 - \alpha_2^2)J_o + \alpha_2^2 J_1 - \alpha_1^2 J_2}{(\alpha_1 - \alpha_2)J_o + \alpha_2 J_1 - \alpha_1 J_2}$$

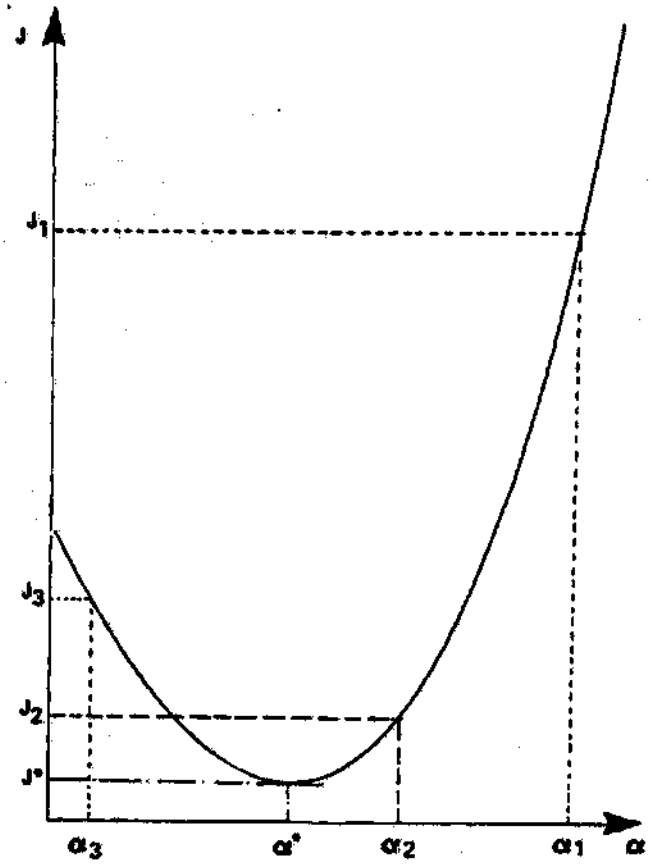

Figure 9. Quadratic Fit

The control procedure, developed above, is iterative. It is repeated until the gradient vector d indicates that further improvements cannot be effected. The major difficulty in computing the gradient direction d is the computation of the sensitivity matrix Σ. This computation is obtained as a by-product of the simulation algorithm and will be discussed in chapter IV. At each iteration, a linearized model for the composite system is obtained. This model is utilized to compute the sensitivity matrix Σ. A flow chart in Figure 10 illustrates the control design procedure.

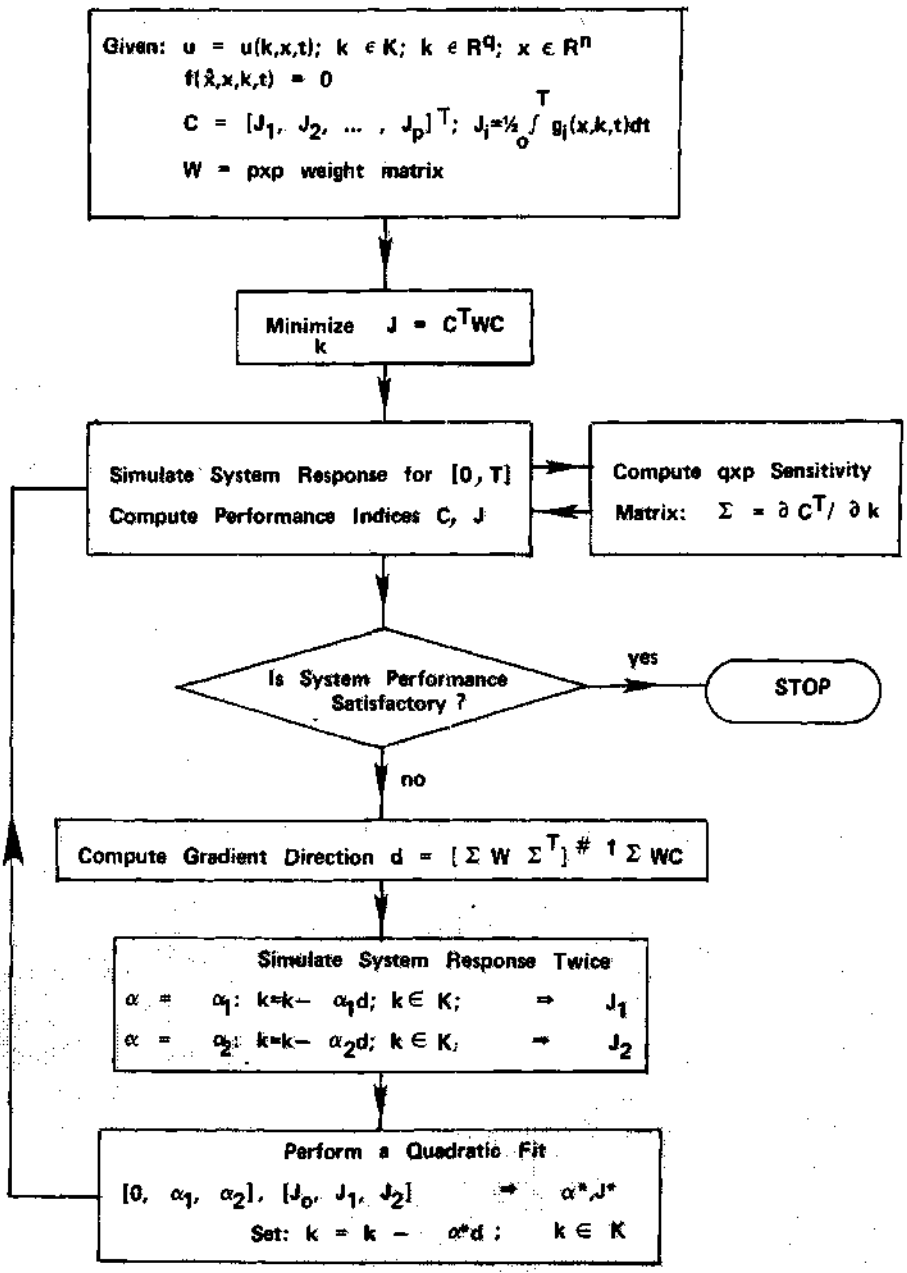

Figure 10. Flow Chart of the Control Design Algorithm

Summary

In this chapter, a novel control design methodology was developed. The main properties of this approach are:

1. a vector performance index is optimized, rather than a scalar criterion, hence the designer has a clear picture of the controllers impact on different measures of system performance at each iteration;
2. the presented control design approach makes it simple to handle important controller structures such as decentralized controllers, combination of discrete and continuous controllers. Also it is very easy to incorporate explicitly the physical limitations on the control gains, etc.

In summary, the proposed procedure provides a solution to the control problem by optimizing the components of a vector performance index. The main contributions of this optimal control design technique are: a) the direct computation of the sensitivities of the system performance index with respect to the control parameters, and b) the development of a unified approach for the computation of the linearized model of a large scale system from the linearized models of its individual devices. These contibutions are further discussed in chapters IV and V.

CHAPTER IV

SENSITIVITY ANALYSIS

The control design methodology, developed in chapter III, requires the computation of the sensitivity matrix Σ :

$$\Sigma = dC^T/dk = [dJ1/dk \; dJ2/dk \; \ldots \; dJp/dk] \tag{40}$$

The objective of this chapter is to develop closed form expressions of the matrix Σ in terms of the linearized model of the system elements. The closed form expressions are obtained utilizing the theory of Calculus of Matrices [65]-[67]. Results from the theory of Calculus of Matrices are reviewed in The appendix.

Derivations of closed form expressions for the sensitivities require a linearized system model. The first section of this chapter deals with the computations of the linearized model while the sensitivity matrix expressions are developed in the second section.

Linearized Model

A linearized model for the composite system is built up from the linearized models of the individual system components. This section deals specifically with the electric power system.

Component Linearized Models

The electric power system elements can be grouped into two classes: linear components and nonlinear components. The linear components are represented with a state model with constant matrices. These matrices need to be computed only once. However, the state model describing the nonlinear components change with the operating point. In the subsequent analysis it will be assumed that the nonlinear state models are linearized around the operating point.

Since the different system components are considered as independent entities, their models are in general described in different coordinate systems chosen uniquely to accomodate the particular device. In order to build up the composite system linearized model it is necessary to express all the models in the same coordinate system. This step of translating all the device models to a reference framework will in some cases require a coordinate transformation. The transformation is usually nonlinear and time varying. When such a transformation is needed, the coordinate translation is performed before the linearization procedure. As an example, in an electric power system, the generator is described in a time varying coordinate system based on the machine 0-d-q axes. However all the other power devices are described in a fixed coordinate system. The fixed coordinate system can be chosen as the reference framework. Consequently, the generator equations are translated to the fixed reference coordinate system through a time varying, nonlinear transformation. Hence, assuming that the generator has the following model:

$$\dot{x} = Ax + Bu \tag{41}$$

and if T1 and T2 represent the appropriate coordinate transformations:

$$x1 = T1.x \tag{42.1}$$

$$u1 = T2.u \tag{42.2}$$

Then

$$\dot{x}1 = (T1.A.T1^{-1} + T1.\dot{T}1\ )x1 + T1.B.T2^{-1}.u1 \tag{43}$$

The linearization procedure is illustrated with two typical examples: a) a linear device - transmission line; b) a nonlinear device - generator.

Transmission Line. The equivalent 0-d-q networks of a simple model transmission line are shown in Figure 11. The transmission line is described with a set of 9 linear differential equations:

$$\dot{x} = Ax + Bu \tag{44}$$

where $x = [io\ id\ iq\ io'\ id'\ iq'\ vom\ vdm\ vqm]^T$

$u = [vo\ vd\ vq\ vo'\ vd'\ vq']^T$

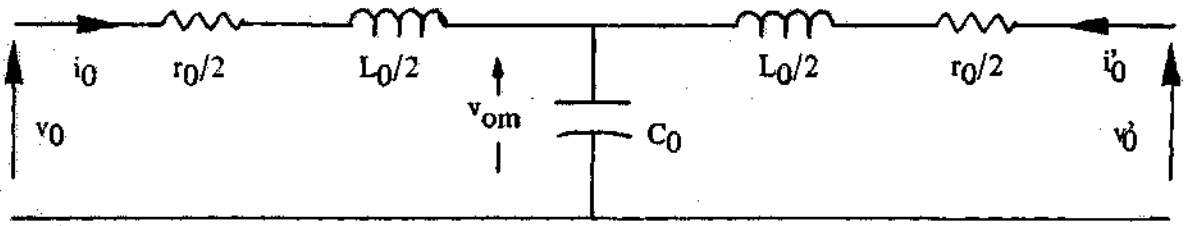

0-Axis Equivalent Circuit

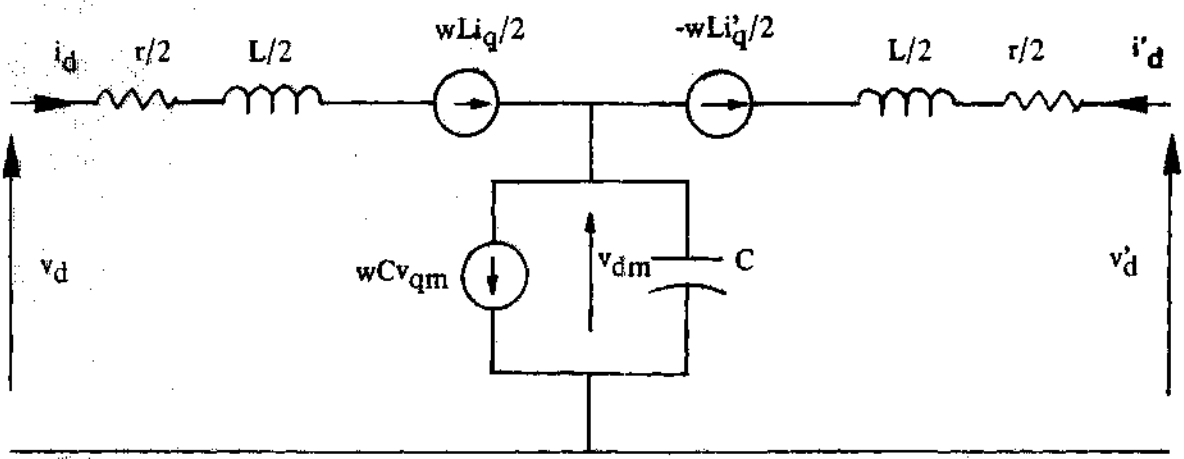

d-Axis Equivalent Circuit

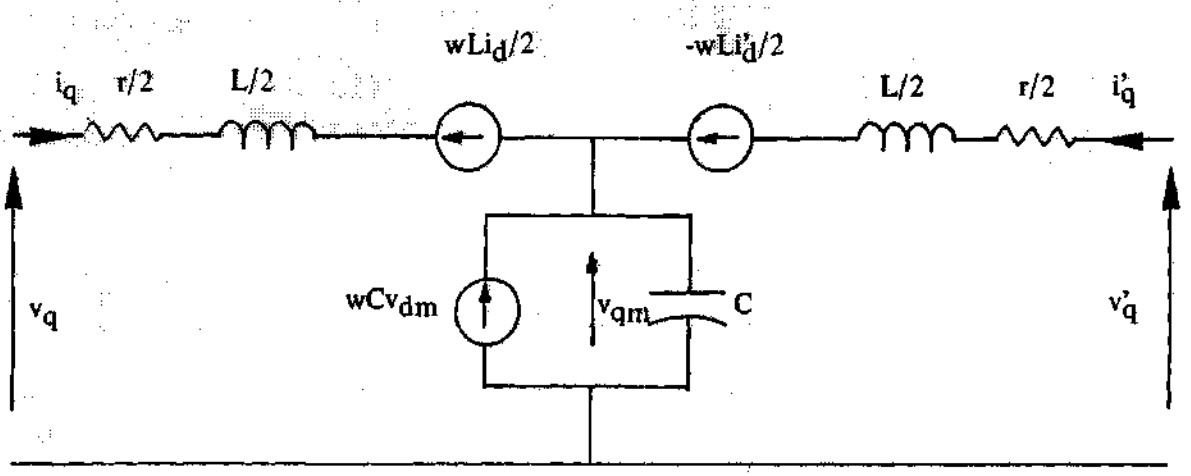

q-Axis Equivalent Circuit

Figure 11. Transmission Line 0-d-q Equivalent Circuits

$$A = \begin{bmatrix}
\frac{ro}{Lo} & 0 & 0 & 0 & 0 & 0 & \frac{2}{Lo} & 0 & 0 \\
0 & \frac{r}{L} & -1 & 0 & 0 & 0 & 0 & \frac{2}{L} & 0 \\
0 & 1 & \frac{r}{L} & 0 & 0 & 0 & 0 & 0 & \frac{2}{L} \\
0 & 0 & 0 & \frac{ro}{Lo} & 0 & 0 & \frac{2}{Lo} & 0 & 0 \\
0 & 0 & 0 & 0 & \frac{r}{L} & -1 & 0 & \frac{2}{L} & 0 \\
0 & 0 & 0 & 0 & 1 & \frac{r}{L} & 0 & 0 & \frac{2}{L} \\
1/Co & 0 & 0 & 1/Co & 0 & 0 & 0 & 0 & 0 \\
0 & 1/C & 0 & 0 & 1/C & 0 & 0 & 0 & 0 \\
0 & 0 & 1/C & 0 & 0 & 1/C & 0 & 0 & 0
\end{bmatrix}$$

$$B = \begin{bmatrix}
2/Lo & 0 & 0 & 0 & 0 & 0 \\
0 & 2/L & 0 & 0 & 0 & 0 \\
0 & 0 & 2/L & 0 & 0 & 0 \\
0 & 0 & 0 & 2/Lo & 0 & 0 \\
0 & 0 & 0 & 0 & 2/L & 0 \\
0 & 0 & 0 & 0 & 0 & 2/L \\
0 & 0 & 0 & 0 & 0 & 0 \\
0 & 0 & 0 & 0 & 0 & 0 \\
0 & 0 & 0 & 0 & 0 & 0
\end{bmatrix}$$

Generator. In this section, the linearized model of the generator shown in Figure 12 is developed. On the generator coordinate framework, the model is described [68] with:

$$E\dot{x} = Ax + Bu \tag{45}$$

where $x = [i_0\ i_d\ i_q\ \delta\ w\ i_f]^T$

$u = [v_0\ v_d\ v_q]^T$

$$E = \begin{bmatrix} Lo & 0 & 0 & 0 & 0 & 0 \\ 0 & L_d & 0 & 0 & 0 & 0 \\ 0 & 0 & L_q & 0 & 0 & 0 \\ 0 & 0 & 0 & 1 & 0 & 0 \\ 0 & 0 & 0 & 0 & 1 & 0 \\ 0 & 0 & 0 & 0 & 0 & L_f \end{bmatrix}$$

$$A = \begin{bmatrix} -ro & 0 & 0 & 0 & 0 & 0 \\ 0 & -r & -wL_q & 0 & -L_q i_q & 0 \\ 0 & wL_d & -r & 0 & L_d i_d - L_{AD} i_f & -wL_{AD} \\ 0 & 0 & 0 & 0 & 1 & 0 \\ 0 & -ai_q & bi_f - ai_d & 0 & -c & bi_q \\ 0 & 0 & 0 & 0 & 0 & -r_f \end{bmatrix}$$

where: $a = (L_d - L_q)/3\tau$

$b = L_{AD}/3\tau$

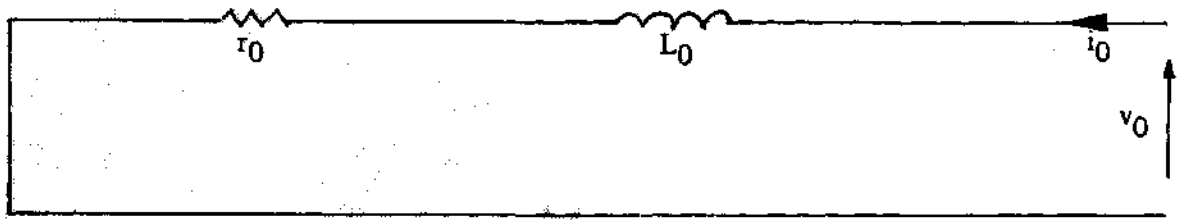

0-Axis Equivalent Circuit

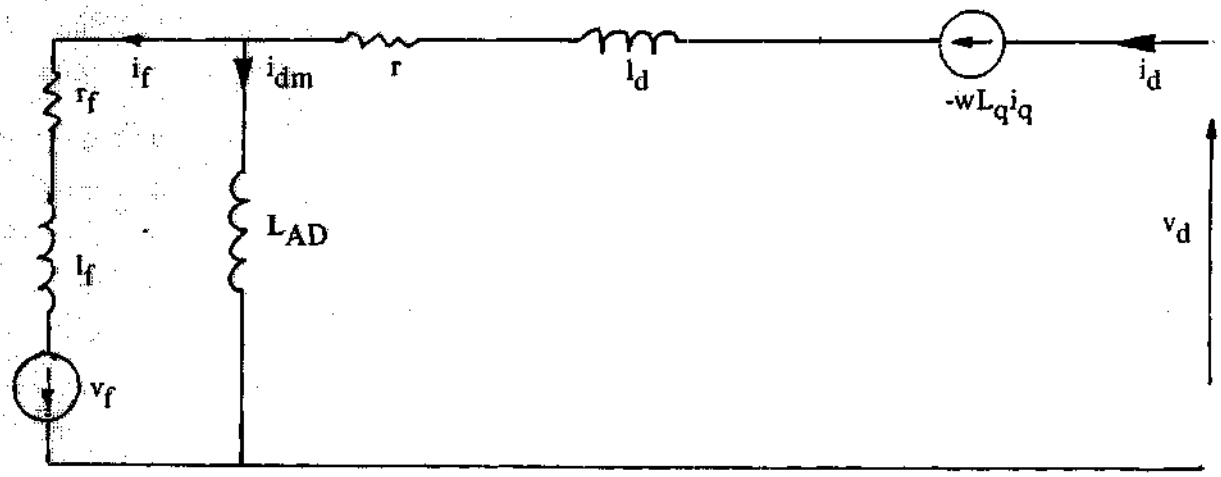

d-Axis Equivalent Circuit

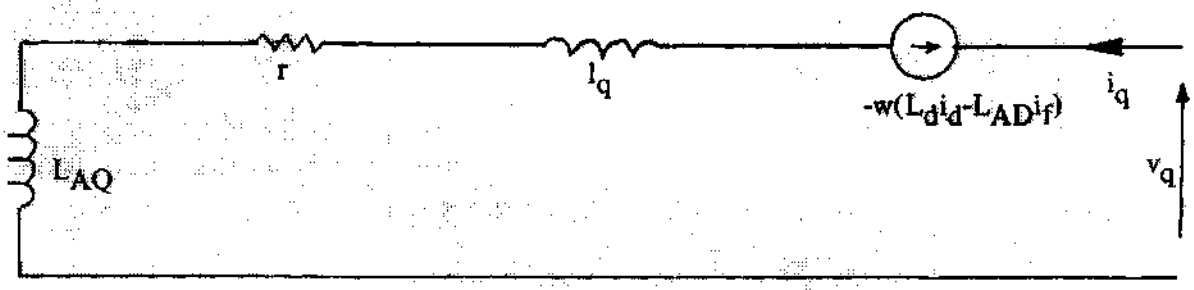

q-Axis Equivalent Circuit

Figure **12.** Generator 0-d-q Equivalent Circuits

$$c = D/3\tau$$

$$B = \begin{bmatrix} 1 & 0 & 0 \\ 0 & 1 & 0 \\ 0 & 0 & 1 \\ 0 & 0 & 0 \\ 0 & 0 & 0 \\ 0 & 0 & 0 \end{bmatrix}$$

The coordinate transformation needed to translate the above equations, Xg, to the fixed coordinate system, Xs, is given by:

$$Xs = T.Xg$$

where:

$$T = \begin{bmatrix} 1 & 0 & 0 \\ 0 & \cos\delta & \sin\delta \\ 0 & -\sin\delta & \cos\delta \end{bmatrix}$$

Once these variables are transformed, the equations are linearized around the operating point.

Let $Xs = x'$ and $Xg = x$. Then:

$$E\dot{x} = Ax + Bu$$

$$x' = Px$$

where:

$$P = \begin{bmatrix} T & 0 \\ 0 & I \end{bmatrix}$$

Also $u' = Tu$

Thus,

$$\dot{x}' = [PE^{-1}\ AP^{-1} + \dot{P}P^{-1}]x' + [PE^{-1}\ BT^{-1}]u'$$

which can be written as:

$$\dot{x}' = A'x' + B'u'$$

where: $A' = PE^{-1}\ AP^{-1} + \dot{P}P^{-1}$

$B' = PE^{-1}\ BT^{-1}$

$$P = \begin{bmatrix} T & 0 \\ 0 & I \end{bmatrix}$$

$$\dot{P} = \begin{bmatrix} \dot{T} & 0 \\ 0 & 0 \end{bmatrix}$$

Composite System Linearized Model

To obtain the composite system linearized model the structural properties of the system are exploited. As seen in the previous sections, each device in the system is considered independently. Then, for each component, a set of dynamical equations is obtained. Moreover, the state has been so selected that the equations are expressed in terms

of the natural (describing) variables: voltage at each node, current through each loop, etc. In general, each component is described with:

$$Ei.\dot{x}i = Ai.xi + Bi.ui$$

$$yi = Ci.xi$$

where the matrix Ei is a nonsingular or singular matrix. The case where Ei is invertible corresponds to the usual state space representation.

The objective of this section is to find a state space representation of the composite system given the component descriptor representations and the interconnection constraints. This objective is achieved in 4 steps:

Step 1. Express all component models in the same coordinate system

Step 2. Assemble device models

Step 3. Consider interconnection constraints

Step 4. Obtain composite system state space representation.

It is important to note that the electric power system is a regular system. This means that a state space representation always exists. As an example consider an RLC circuit for which a state vector is selected to comprise voltages across capacitors and currents through inductors.

Since a state space representation is known to exist for an electric power system the four steps mentioned above will yield such a representation.

Step 1 consists in expressing all the device models in the same coordinate system. If this is not already the case, then, as discussed earlier, a coordinate transformation is applied.

The second step consists in assembling the individual device models. Each device Sk has a descriptor form representation. The set of the descriptor variables can be partitioned into a set of interface variables, x_A, and a set of internal variables, x_B. For the composite system, the following descriptor variables are defined:

$$x \triangleq \begin{bmatrix} x_A^1 \\ x_A^2 \\ x_A^3 \\ \cdot \\ \cdot \\ x_A^p \\ x_B^1 \\ \cdot \\ \cdot \\ x_B^p \end{bmatrix} \qquad u \triangleq \begin{bmatrix} u_1 \\ u_2 \\ \cdot \\ \cdot \\ \cdot \\ u_p \end{bmatrix}$$

Then, by stacking the individual models according to the variables defined above, the composite system will have a descriptor form representation:

$$E.\dot{x} = A.x + B.u \qquad (47)$$

$$y = C.x$$

where E, A, B and C are block diagonal matrices obtained from the component descriptor form matrices Ek, Ak, Bk and Ck.

In fact, step 2 is just an orderly stacking procedure. The interconnection constraints have not been considered yet. These constraints are considered in the third step. Specifically, for the electric power system, the interconnection constraints are expressed in terms of interface voltage conservation equations and nodal equations. At each interconnection, I, of the system all the devices D(I) which are connected to this interconnection share the same interface voltage, i.e.,

$$x_A^k = x_A^I \quad \text{for all } k \varepsilon D(I)$$

in addition, the nodal equations at interconnection I yield:

$$\sum_{k \varepsilon D(I)} i_k = 0$$

or

$$i_{el} = - \sum_{k \varepsilon D(I)-I} (i_k)$$

The composite system must satisfy the interconnection constraints.

Considerations of these constraints result in elementary row and column operations on the (E, A, B, C) matrices.

An elementary row (column) operation on a matrix M, which results in a matrix M', can be expressed mathematically as a pre (post) multiplication of the matrix M by a unimodular matrix P, i.e.,

$M' = PM$: row operation

$M' = MP$: column operation.

A unimodular matrix is a matrix whose determinant is ± 1.

Then, elementary row and column operations on the system matrices (E,A,B,C) yield:

$$E' = P1.E.P2$$

$$A' = P1.A.P2$$

$$B' = P1.B.P3$$

$$C' = P4.C.P1$$

where P1, P2, P3 and P4 are unimodular matrices describing the elementary row and column operations performed to satisfy the interconnection constraints. Thus the composite system, in descriptor form, is modeled with:

$$E'.\dot{x} = A'.x + B'.u$$

$$y = C'.x$$

where the matrices E', A', B', C' are no longer block diagonal.

Dropping the (') for notational simplicity, then step 4 consists in considering a descriptor system:

$$E.\dot{x} = A.x + B.u \tag{48}$$

$$y = C.x$$

The next task is to find the usual state space representation from the above descriptor form.

Let E and A be nxn matrices, B be an nxr matrix and C be a pxn matrix. Since the electric power system is a regular system, assume then that a state space representation of order $m < n$ exists. By elementary row operation the descriptor system representation can be represented by the equivalent equation:

$$\begin{bmatrix} T \\ \\ 0 \end{bmatrix} \dot{x} = \begin{bmatrix} F \\ \\ D \end{bmatrix} x + \begin{bmatrix} G \\ \\ H \end{bmatrix} u \tag{49}$$

where T has full rank m. Luenberger [69] provides for discrete systems

a necessary and sufficient condition for a descriptor representation of the generic form (49) to have a state space representation. The result can be easily extended to the continuous time case.

Theorem: The system $E.\dot{x} = A.x + B.u$, or alternatively system (49), is regular if and only if the nxn matrix $\begin{bmatrix} T \\ D \end{bmatrix}$ is invertible.

This theorem is utilized to derive a state space representation for system (49). Since the electric power system is regular, then $\begin{bmatrix} T \\ D \end{bmatrix}$ is invertible. Let [M N] be its inverse, where M is nxm and N is nx(n-m). The expansion of the system model equation yields:

$$T.\dot{x} = F.x + G.u$$

$$0 = D.x + H.u$$

Also $[M\ N].\begin{bmatrix} T \\ D \end{bmatrix} = MT + ND = In$

Thus: $T.\dot{x} = F(MT+ND)x + G.u$

or: $T.\dot{x} = FMT.x + FND.x + G.u$

But $D.x = -H.u$

Then: $T.\dot{x} = FMT.x + (G-FNH).u$

Let $T.x \triangleq x'$

$$FM \triangleq A'$$

$$G\text{-}FNH \triangleq B'$$

With the above definitions, the system equivalent state space representation is then given by:

$$\dot{x}' = A'.x' + B'.u \tag{49}$$

The above equation represents the linearized state space representation of the composite system. It is obtained from the individual component models with a series of row operations and transformations.

Another approach to define an equivalent state space representation for the composite system is given by Rosenbrock [70]-[71]. It is based on the following theorem:

Theorem: Any polynomial matrix

$$P(s) = \begin{bmatrix} sE-A & B \\ -C & 0 \end{bmatrix}$$

with determinant of sE-A not identically zero, can be brought by strict system equivalence to the form:

$$\begin{bmatrix} I(n-m) & 0 \\ 0 & P1(s) \end{bmatrix}$$

where P1(s) is a system matrix in state space form, i.e.,

$$P1(s) = \begin{bmatrix} sIm - A1 & B1 \\ -C1 & 0 \end{bmatrix}$$

It is necessary to define the terminology of the above theorem.

1) strict system equivalent operations:

- multiply any of the first n rows (columns) by a constant
- add a multiple of any of the first n rows (columns) to any other rows (columns)
- interchange any 2 of the first n rows (columns)

2) Two systems

$$\begin{bmatrix} T1 & U1 \\ -V1 & W1 \end{bmatrix}, \quad \begin{bmatrix} T2 & U2 \\ -V2 & W2 \end{bmatrix}$$

are strict system equivalents if there exist unimodular polynomial matrices M(s), N(s) and polynomial matrices X(s), Y(s) such that:

$$\begin{bmatrix} M(s) & 0 \\ X(s) & Ip \end{bmatrix} \begin{bmatrix} T1 & U1 \\ -V1 & W1 \end{bmatrix} \begin{bmatrix} N(s) & Y(s) \\ 0 & Ir \end{bmatrix} = \begin{bmatrix} T2 & U2 \\ -V2 & W2 \end{bmatrix}$$

The electric power system, as mentioned earlier, is a regular system. Thus the condition that the determinant of sE-A is not identically zero is always satisfied. Hence the application of the above theorem is straightforward. The matrix P(s) of the theorem corresponds to the system (47). Thus the equivalent state space representation of the composite system can be obtained with strict system equivalent operations which amount to elementary row and column operations.

Sensitivity Analysis

In this section the derivation of the expressions for the sensitivities of a performance index in a small time interval h is presented. It is assumed that a control strategy is known. Then the linearization of the control problem leads to the following Linear Quadratic Regulator Problem:

$$\text{minimize } J = \tfrac{1}{2} \int_0^T x^T(s)Q'x(s)+u^T(s)Ru(s)ds \qquad (50)$$

$$\text{subject to } \dot{x}(t) = A'x(t) + B'u(t)$$

Assuming that the control law u depends on a parameter vector k, then the above problem can be cast into:

$$\text{minimize } J = \tfrac{1}{2}\int_0^T x^T(s)Qx(s)ds \tag{51}$$

$$\text{subject to } \dot{x}(t) = Ax(t) \tag{52}$$

where Q and A take into account the proposed control scheme. Actually Q and A correspond to the closed loop control system, and they are dependent on the parameter k.

Computations of the sensitivities dJ/dk are performed as follows. Consider the expansion of the function x(t) in a Taylor series:

$$x(s) = x(t-h) + [x(t)-x(t-h)][(s-t+h)/h] + \ \ldots \ + \text{h.o.t.} \tag{53}$$

Assuming a small time step h, the high order terms (h.o.t.) may be neglected to yield:

$$x(s) = x(t-h)[(t-s)/h] + x(t)[(s-t+h)/h] \tag{54}$$

Substituting (54) into (51), and assuming, without loss of generality, that the matrix Q is symmetric:

$$J = [h/6][x^T(t-h)Qx(t-h)+x^T(t)Qx(t-h)+x^T(t)Qx(t)] \tag{55}$$

Now, equation (52) can be integrated via the trapezoidal integration rule to yield:

$$x(t) = A1.A2.x(t-h) \tag{56}$$

where: $A1 = [I - Ah/2]^{-1}$

$A2 = I + h/2$

h = integration time step,

I = identity matrix.

Substituting (56) into (55):

$$J = [h/6][x^T(t-h)Px(t-h)] \tag{57}$$

where: $P = Q + Q.Ao + \overset{T}{Ao}.Q.Ao$ (58)

$Ao = A1.A2$ (59)

From (57) one obtains:

$$dJ/dk = [h/6][Iq*\overset{T}{x}(t-h)][dP/dk][x(t-h)] \tag{60}$$

where: * denotes Kronecker Product

$$dP/dk = (dQ/dk)(In+Ao) + (Iq*Q)(dAo/dk) + \\ + [(dAo/dk)Q+(Iq*Ao)(dQ/dk)]Ao + \\ + (Iq*Ao)(Iq*Q)(dAo/dk) \tag{61}$$

and

$$dAo/dk = (h/2)(Iq*A1)(dA/dk)[Ao+In] \tag{62}$$

In summary, equation (60) provides the closed form expression of the sensitivity of the objective function with respect to the parameter vector k in the interval [t-h,h]. The sensitivity of the objective

function over the interval of interest [0,T] is obtained by summing the contributions from all the intervals [ih,(i+1)h], i=0,1,2,...,n-1, nh=T.

Summary

Closed form expressions for the sensitivity matrix were derived. These expressions are based on the system linearized model matrices and utilize the theory of calculus of matrices. A general procedure to obtain the composite system linearized model from the individual system component linearized models was presented. Here the composite system linearized model is utilized for the sensitivity analysis. The results of this chapter are useful for other applications such as modal analysis, parameter identification, etc.

CHAPTER V

RESULTS

The objective of this chapter is to apply the methodologies presented in previous chapters to design optimal controllers for the attenuation of the subsynchronous resonance effects on electric power systems.

The effects of the subsynchronous resonance to the electric power system is fatigue of the turbine generator shaft system. The ultimate hazard is shaft fracture [72]. By definition, 100% fatigue life expenditure indicates surface crack initiation. Fatigue life expenditures are cumulative. Such a damage (i.e., shaft crack) requires shaft replacement and a corresponding unit outage of 90 days or more. These intolerable incidents are created by the transient torsional oscillations. Thus, it is absolutely necessary to identify, analyze and control the electric power systems that are sensitive to subsynchronous resonance effects. The transient torsional oscillations are identified and analyzed with the generalized digital power system dynamic simulation program developed in chapter II. Once dangerous torsional oscillations are detected the control design technique developed in chapter III is employed to devise optimal controllers for the specific system under consideration.

This chapter is organized as follows: section 1 presents the

modeling of the turbine generator system and the analysis technique that are used to detect the subsynchronous resonance effects. In section 2 the subsynchronous resonance control problem is formulated within the scope of the proposed techniques, and the control scheme to be employed is described. Finally the third section presents a detailed analysis of the system for five different uncontrolled and controlled cases. This section assesses the effectiveness of the controllers and the methodologies utilized and compares the proposed control scheme to an existing subsynchronous resonance countermeasure.

Modeling and Analysis

The subsynchronous resonance phenomenon is an exchange of energy between the electrical network and the turbine generator system. Thus the analysis of the subsynchronous resonance effects requires a detailed modeling of both the electrical and mechanical parts of the turbine generator system [73]-[75].

The mechanical system or the turbogenerator shaft system is composed of a number of different pressure turbines (e.g., low pressure turbine, intermediate pressure turbine, high pressure turbine, etc.), the generator and the exciter system. Figure 13 shows a typical shaft system.

The modeling of each one of these devices is presented next.

Turbine

A turbine k connected to devices i and j is shown in Figure 14.

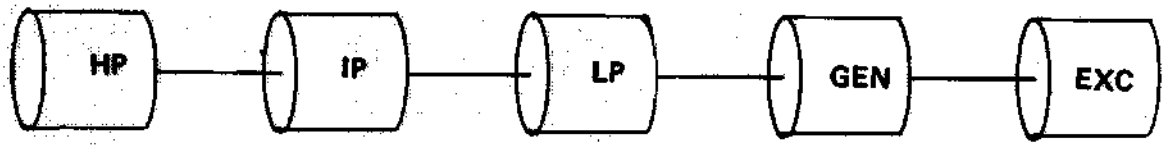

Figure 13. Typical Shaft System

HP: High Pressure Turbine
IP: Intermediate Pressure Turbine
LP: Low Pressure Turbine
GEN: Generator
EXC: Exciter

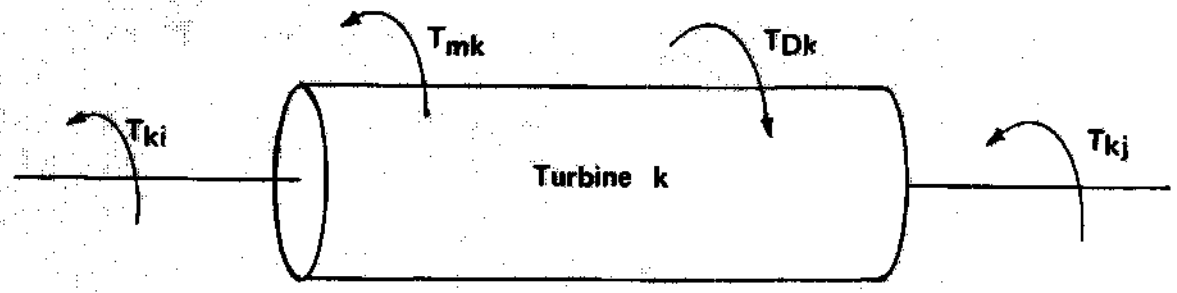

Figure 14. Turbine Shaft

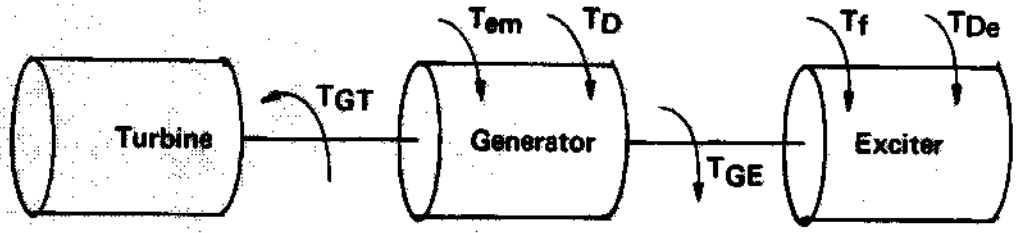

Figure 15. Generator Shaft

A set of dynamical equations that describes the turbine k is:

$$\tau \cdot \dot{\omega} = Tmk - TDk + Tki + Tkj$$

$$\dot{\delta} = \omega - 1$$

where: τ = turbine inertia

ω = speed

δ = position as measured for a predefined coordinate system

Tmk = input torque developed by the flow of steam

TDk = friction torque = Dk.ωk

Dk = friction coefficient

Tij = shaft torque = Kij.(δi - δj)

Generator

Figure 15 shows a generator connected to a turbine and an exciter system.

The generator dynamics are described with:

$$\tau_g \cdot \dot{\omega}_g = - Tem - TD + TGT + TGE$$

$$\dot{\delta}_g = \omega_g - 1$$

where Tem is the electromagnetic torque. The other quantities are as defined previously.

Exciter

The exciter dynamics are described with:

$$\tau_e \cdot \dot{\omega}_e = - TGE - Tf - TDE$$

$$\dot{\delta}_e = \omega_e - 1$$

where Tf = Vf.if is the electromagnetic torque of the exciter, and Vf is the excitation voltage.

When the shaft system is at equilibrium the following equation holds:

$$Tm = \sum_k Tmk = Tem + Tf + TD + TDE + \sum_k TDk$$

On the other hand, electrically the synchronous machine is modeled as shown in Figure 16a. The generator has 3 armature windings and an excitation system. These windings are transformed in the usual 0-d-q axes resulting in the equivalent circuits of Figure 16b. It is shown that the machine is modeled with three damper windings: one damper winding in the d-axis and two damper windings in the q-axis.

The synchronous machine dynamical model, including the turbines and the exciter, is described with a set of n dynamical equations with: $n = 20 + 2m$, where m is the number of turbines. Figure 21 illustrates the shaft system of the generator of an actual system for which results will be presented. For this case n=28. This model of the generator has

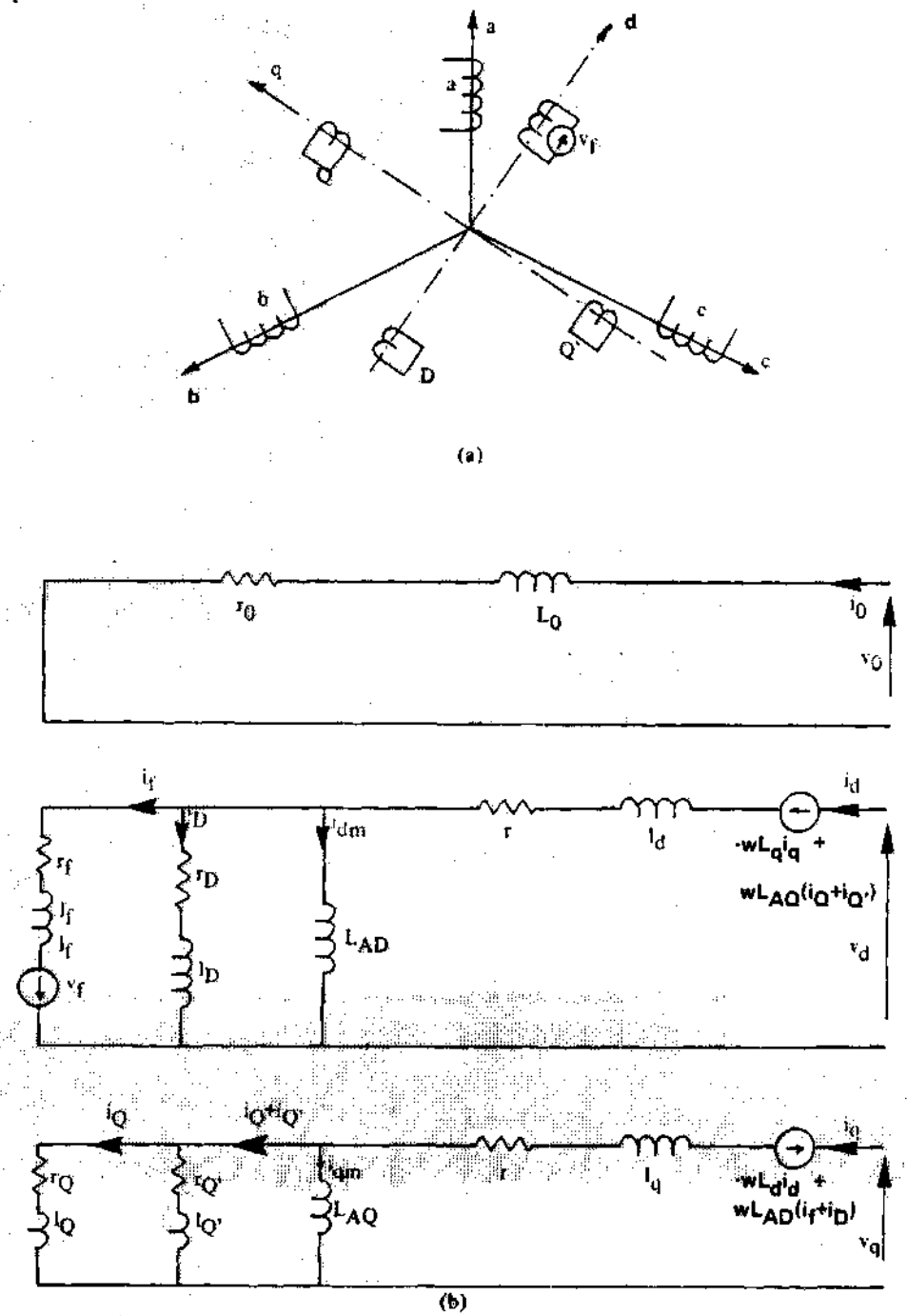

Figure 16. Electrical Representation of the Generator

a) Schematic Representation of Synchronous Machine windings
b) 0–d–q Axes Equivalent Circuits

been proven to be adequate for the analysis of subsynchronous resonance [80].

The study of the subsynchronous resonance phenomena requires the integration of these models into the digital power system dynamic simulation program. The basic information that is relevant to the subsynchronous resonance effects is contained in the behavior of the shaft torques. In fact the shaft fatigue is a function of the magnitude of the stresses [76]-[79]. These quantities are obtained as outputs of the computer program. In this program the shaft fatigue is also evaluated. It is determined as follows:

$$\text{Fatigue} = \sum_i fi(Ti/Tc)$$

where Ti is the computed transient shaft torque

Tc is a critical torque value, characteristic of the shaft design and fi is the fatigue contribution of each incident. An incident is defined as any event when the torque magnitude Ti exceeds the critical torque Tc. The critical torque Tc depends on the shaft material and design. Tc will have an expression of the form:

$$Tc = a.Tr$$

where Tr is the rated torque and a is a constant greater than one.

The function fi depends on shaft design and is determined from curves similar to that shown in Figure 17.

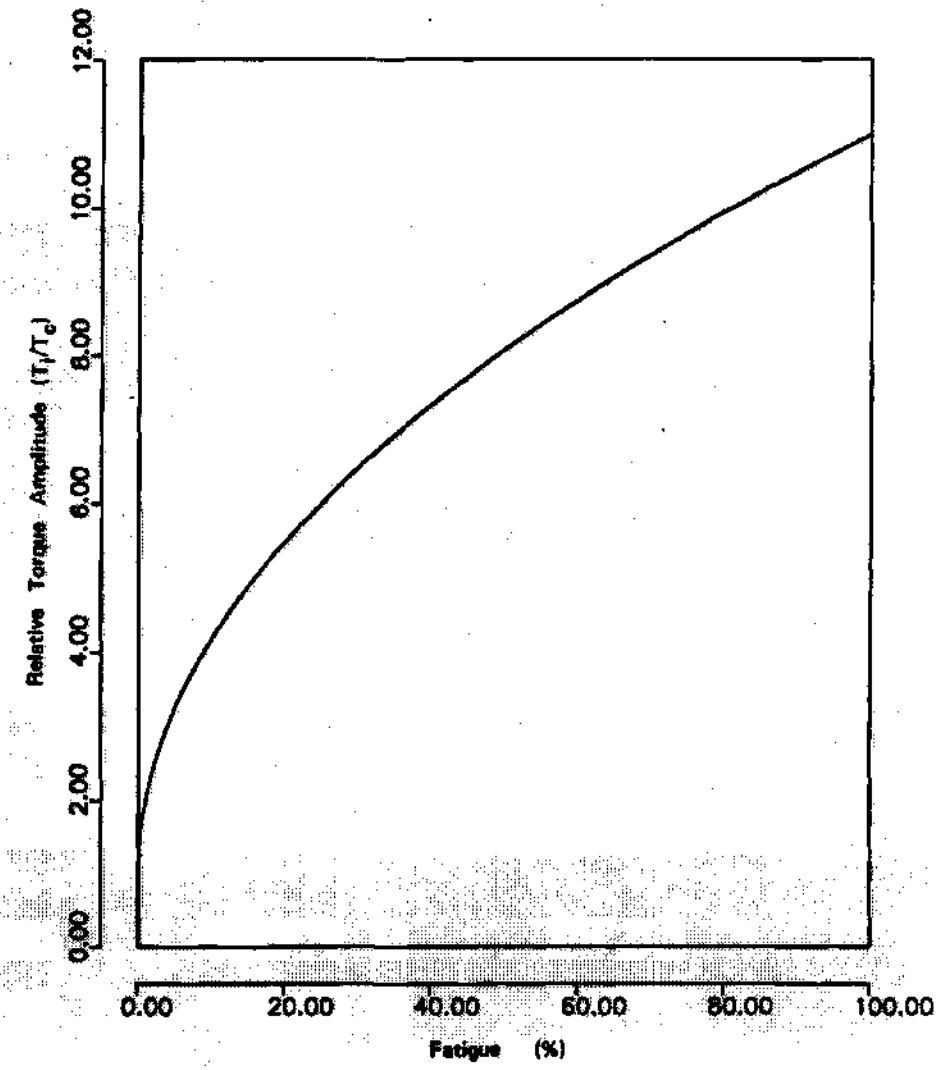

Figure 17. Typical Shaft Fatigue Curve

Subsynchronous Resonance Control Problem

The formulation of the subsynchronous resonance control problem in the framework of the proposed design methodology requires the definition or selection of a control structure and a vector performance index. Then, the control problem is formulated as follows: given a control structure, centralized or decentralized, continuous or discrete, with a number of adjustable parameters k (gains or logical variables), a vector performance index C, compute the optimal values of the control parameters k. Specifically:

$$\underset{k}{\text{minimize}}\ J = C^T W C$$

$$\text{subject to } f(\dot{x}, x, k, t) = 0$$

$$k \in K$$

where $f(\dot{x},x,k,t) = 0$ are the plant dynamical equations

$C = [J1\ J2\ J3\ \ldots\ Jp]^T$ is the vector performance index

Ji = ith component of C = a scalar performance index

x = state vector of dimension n

k = control parameter vector of dimension q

K = set of admissible control parameters

W = diagonal weight matrix of dimension pxp

As mentioned in the first chapter there is no single subsynchronous resonance countermeasure which, taken alone, solves the

problem in an economically acceptable way. However, a combination of some of those measures may provide an acceptable solution. Most of the countermeasures are decentralized control schemes applied at different locations. Also, they are either of the continuous or of the discrete type control schemes. In this study, a decentralized control structure is proposed. It consists of two localized controllers which are feasible and which are described next:

1. A continuous feedback controller applied to the generator exciter system. This controller is located at the generator site. Its feedback control law spans only the observable synchronous machine state variables. Thus, the control law is a state feedback strategy: uc = Vf + Kc.xg, where Vf is the excitation voltage at steady state, xg is the synchronous machine observable state vector and Kc are the continuous control parameters.
2. A discrete feedback controller applied to the series capacitor. This controller is located at the series capacitors site which may be many miles away from the generator. It consists in short circuiting the series capacitor with electronic switching for a short period of time. The decision to short circuit the series capacitor is based on the voltage across the capacitor and its content of subsynchronous frequency voltage. The controller structure is shown in Figure 18. It has two adjustable variables: Kd1 = triggering time and Kd2 = time interval when control scheme is on. The controller is turned

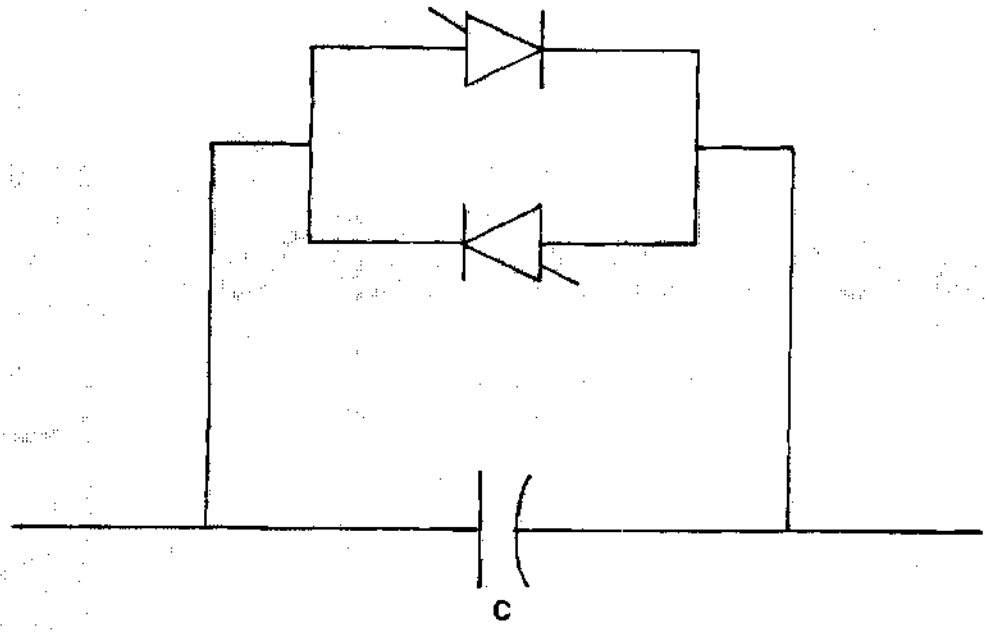

Figure 18. Series Capacitor Controller

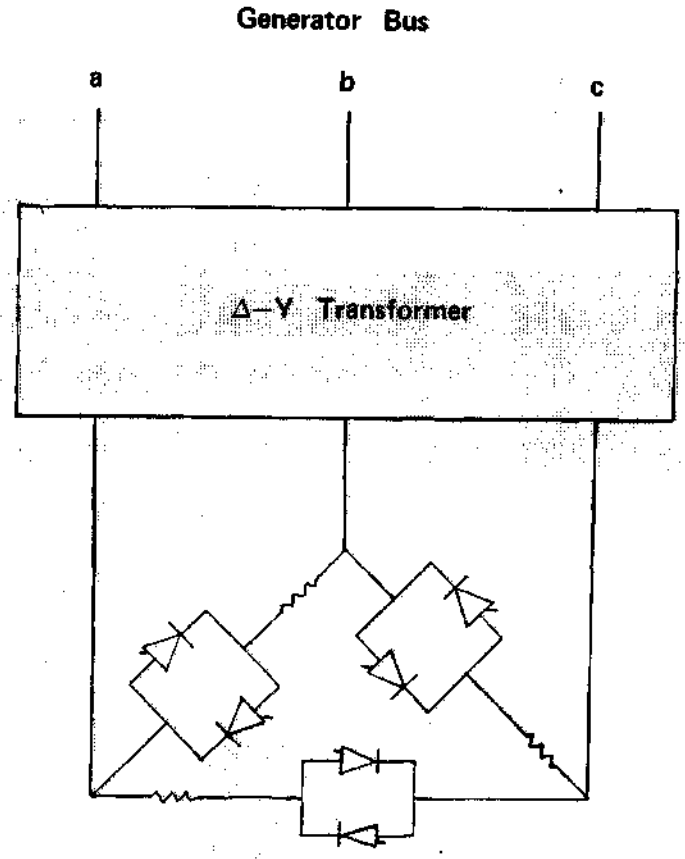

Figure 19. Dynamic Stabilizer

on whenever voltages of subsynchronous frequency are detected across the capacitor.

At this point the control structure has been selected. Next, a vector performance index must be defined. This index can include any quantity that has an effect on the cost, reliabilty or effectiveness of the control scheme. For the subsynchronous resonance control problem the quantities that need to be included in the performance index are the shaft torsional stresses. Thus, for this study the entries of the performance index are selected to be the torques at various locations of the shaft, for example torque on the shaft between generator and first turbine, etc.

In the next section specific selections will be given for an actual system.

Application to the Benchmark Test System

The test system of Figure 20 is the First Benchmark Subsynchronous Resonance Test System [80] defined by the IEEE working group on Subsynchronous Resonance. This system corresponds to an actual system. In fact it corresponds to the Navajo Project System. A 892 MVA generator delivers power to a large system via a 500 kV, 200 mile long, series capacitors compensated transmission line.

The shaft system is composed of four steam turbines: two low pressure turbines (denoted LPA and LPB), an intermediate pressure turbine (IP) and a high pressure turbine (HP) contributing respectively 22%, 22%, 26% and 30% of the torque, a generator and an exciter. Figure

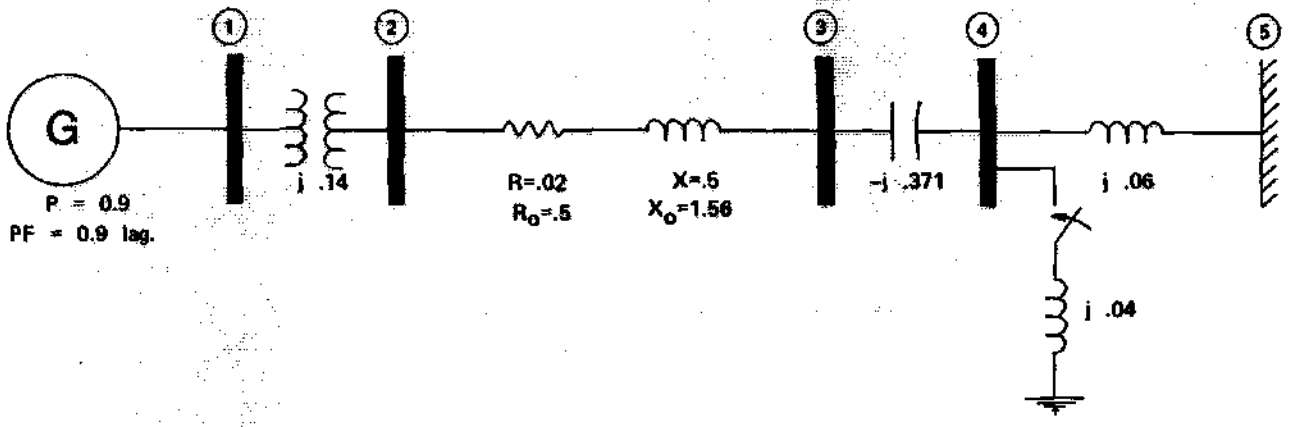

Figure 20. Single Line Diagram of the Benchmark Test System

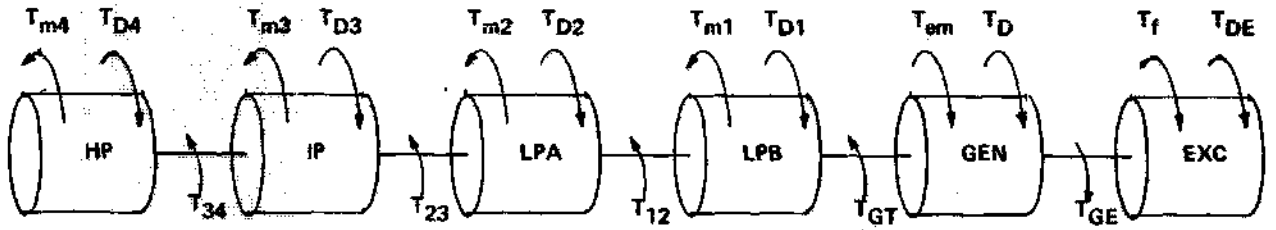

Figure 21. Spring Mass Model of the Generator Shaft System

21 shows the spring mass model of the turbogenerator.

A three phase fault is applied at bus 4 at time t=0. The fault is cleared after 0.075 seconds or 28 pu. The impedance of the fault is 0.04 pu inductive. Prior to the fault the generator delivers 0.9 pu real power at rated terminal voltage and 0.9 lagging power factor.

The control structure is as described in the previous section. The vector performance index is selected to be:

$$C = [J1\ J2\ J3\ J4\ J5]^T$$

where:

$$J1 = 0.5 \int_0^T (TGT - TGTo)^2 dt$$

$$J2 = 0.5 \int_0^T (TGE - TGEo)^2 dt$$

$$J3 = 0.5 \int_0^T (T12 - T12o)^2 dt$$

$$J4 = 0.5 \int_0^T (T23 - T23o)^2 dt$$

$$J5 = 0.5 \int_0^T (T34 - T34o)^2 dt$$

where

TGT = generator-LPA torque

TGE = generator-exciter torque

T12 = LPA-LPB torque

T23 = LPB-IP torque

T34 = IP-HP torque

T = 200 pu = 0.53 seconds = time interval under consideration

the subscript o denotes steady state.

The Benchmark Test System has been studied under five different assumptions. These studies are denoted as Cases A through E and are defined next.

Case A: No control scheme is applied. This case corresponds to the analysis of the subsynchronous resonance effects on the test system.

Case B: A centralized continuous controller is applied to the excitation system. The problem is formulated as a linear quadratic regulator. The control gains are obtained by solving an appropriate Riccati matrix equation.

Case C: A discrete controller is applied. This corresponds to the electronic switching of the series capacitors. The control parameters are adjusted utilizing the sensitivity analysis based control design technique.

Case D: A combination of the above two controllers is applied. All of the control parameters are optimized through the methodologies presented in this thesis.

Case E: This case involves excitation control and a dynamic stabilizer. The dynamic stabilizer consists of thyristor modulated shunt resistors connected through a transformer to the generator bus. It is illustrated in Figure 19. The control of subsynchronous resonance is achieved by modulation of the thyristor switch firing angles. The

power dissipated by the resistors damps the torsional oscillations. This case is included to compare the proposed control scheme with an existing subsynchronous resonance countermeasure.

The obtained results are listed in Figures 22 through 45 and summarized in Tables 1 through 4. Figures 22 through 25 illustrate the transient response of the system over the interval of interest for the study case A. Specifically the following quantities are plotted:

a) Generator Electromagnetic Torque (Tem)

b) Shaft Torque between Generator and Exciter (TGE)

c) Shaft Torque between Generator and Low Pressure Turbine A (TGT)

d) Shaft Torque between Low Pressure Turbine A and Low Pressure Turbine B (T12)

e) Shaft Torque between Low Pressure Turbine B and Intermediate Pressure Turbine (T23)

f) Shaft Torque between Intermediate Pressure Turbine and High Pressure Turbine (T34)

g) Shaft Fatigue between Generator and Low Pressure Turbine A

h) Shaft Fatigue between Low Pressure Turbine A and Low Pressure Turbine B

i) Generator Bus Terminal Voltage (Vt)

j) Generator Phase A Current (ig)

k) Voltage across series capacitor, phase A (Vc).

The same information is given for the other study cases. Moreover, the control laws are also plotted for cases B through E. Thus, the results for the controlled cases are grouped as follows:

Case B: Figures 26 through 30

Case C: Figures 32 through 36

Case D: Figures 37 through 41

Case E: Figures 41 through 45.

The results are summarized in Tables 1 through 4 for easy inspection of the effectiveness of the various control schemes. Tables 1 and 2 summarize the computed performance index for the five study cases. Table 1 simply lists the indices while Table 2 lists the percent variation from the uncontrolled case. Tables 3 and 4 summarize the maximum transient torque amplitudes recorded. Again, Table 3 simply lists the maximum transient torque while Table 4 lists the percent variation from the uncontrolled case.

Considering case A, it is seen that the shaft torques reach dangerous levels (cf. Table 3). It means that the shaft system is subjected to fatigue every time subsynchronous oscillations are triggered. This is confirmed by the fatigue curves (cf. Figure 24). It is then necessary to control the subsynchronous oscillations.

Comparing the four control schemes of cases B, C, D and E, the following conclusions are drawn:

1. The excitation control scheme is not effective to damp the relatively high amplitude torsional oscillations. Table 1 and 2 show that the reduction in torsional oscillations is not substantial. This can be explained from the fact that the time response of the excitation continuous controller is slower than the torsional oscillations that are to be damped. Moreover, the power rating of the exciter and the ceiling voltage limit

the effectiveness of this machine to induce sufficient subsynchronous currents in the generator armature.

2. Discrete controllers with fast time response result in better reduction of torsional oscillations.
3. Series capacitor control is the most effective subsynchronous resonance countermeasure. This can be explained as follows: the transient subsynchronous currents that flow into the generator to create the subsynchronous resonance problems are stored in the LC circuit. By controlling this stored energy the torsional oscillations can be effectively reduced.
4. The proposed scheme, i.e., Case D, shows the best performance as far as torsional oscillations (amplitude and oscillations) are concerned.

Tables 1 and 2 assess the reduction of the torsional oscillations for the five different cases studied. Tables 3 and 4 evaluate the impact of the different control schemes on the torques magnitudes. These tables confirm the above conclusions. The same conclusions can be deduced from the shaft fatigue curves and the transient response curves. These curves are discussed next.

First consider the uncontrolled case or case A. The analysis of this case corresponds to the analysis of the subsynchronous resonance effects on the system. From Figure 22a it is seen that the electromagnetic torsional oscillations have a subsynchronous frequency of about 24 Hz. The presence of these frequencies can also be seen from the electrical quantities response curves shown in Figures 25b and 25c

which are the generator phase A current and the phase A voltage across the capacitor oscillations. The subsynchronous resonance effects are detected from the different shaft torsional oscillations. The torsional oscillations of the generator-exciter shaft, the generator-LPA shaft, the LPA-LPB shaft, the IP-LPB shaft and the IP-HP shaft are shown in Figures 22b, 22c, 23a, 23b and 23c respectively. All the shafts experience some torsional oscillations, however some torques reach a dangerous level of magnitude. In this case Figure 24 shows that the generator-LPA shaft and the LPA-LPB shaft experience a serious problem. In fact both of these shafts will loose some life. Note that even after the fault is cleared the torques continue to oscillate and exceed the critical torque. The other shafts are not as critically affected as these two shafts. Indeed no fatigue is experienced by the other shafts.

In case B the system is modeled as a continuous time system. The subsynchronous resonance control problem is cast into an infinite time linear quadratic regulator. The solution to this control problem is obtained by solving the corresponding algebraic Riccati matrix equation. From the transient response curves of this controlled case it is seen that the solution is not satisfactory. First of all the oscillations of the electric quantities shown in Figures 26a, 29b and 29c indicate the presence of subsynchronous frequencies. Secondally Figures 26b, 26c, 27a, 27b and 27c show that the shafts are experiencing some dangerous oscillations. Figure 28 assess the fatigue of the most affected shafts. But as compared to the uncontrolled case the effect is less severe. Thus the magnitude of the torques have been reduced. However, the degree of reduction is not satisfactory. Consider Figure 30 which shows

the optimal control law applied in this case. From this figure it is seen that the Riccati gains are extremely high. Obviously the excitation system cannot provide such voltages. These high gains result in saturation of the magnetic circuits of the generator altering substantially the assumed mathematical model. The actual performance of the controller is quite different than the predicted. Figure 29a shows a drop in the magnitude of the generator terminal voltage. Notice that this control scheme has substantial effect on the generator-exciter torsional oscillations. The reason is that these oscillations are slower than the other torsional oscillations. In fact, it is not possible to solve the subsynchronous resonance control problem with this controller because the time response of the excitation system is very slow as compared to the torsional oscillations. Thus controllers with fast time responses are needed.

Such fast time response controllers can be obtained through discrete control. In case C a discrete control strategy is applied. It consists in short circuiting the series capacitors whenever subsynchronous resonance effects are detected. The control parameters are optimally selected via the design technique of this thesis. The transient response curves of the electrical quantities shown in Figures 31a, 34a, 34b and 34c show the attenuation of the subsynchronous frequencies. This discrete controller has a substantial effect in reducing the torsional oscillations as can be seen from Figures 31b, 31c, 32a, 32b and 32c. The shaft fatigue stresses are substantially reduced. Figure 33a shows that the generator-turbine shaft is no longer subjected to substantial fatigue while Figure 33b shows that the LPA-LPB

shaft does not experience any fatigue stress. The optimal discrete control law is illustrated in Figure 35. The optimal control parameters are obtained through the sensitivity based control design methodology.

In case D a better control scheme is designed. In this case a combination of the discrete controller of case C and of the continuous controller of case B is employed. However all the control parameters, discrete and continuous, are selected via the optimal control design technique developed in this thesis. In this case the excitation voltage is kept within tolerable range as can be seen from Figure 40b. Only the available generator state variables are used in a feedback law. The discrete optimal control law is shown in Figure 40a. Figures 36a, 39a, 39b and 39c show the elimination of the subsynchronous frequencies in the electrical quantities transient responses. Figures 36b, 36c, 37a, 37b and 37c show a substantial attenuation of the torsional oscillations of all the shafts. Figure 38b shows that the LPA-LPB shaft does not experience any fatigue stress. Figure 38a shows that the fatigue experienced by the generator-turbine shaft is not dangerous.

Finally, in Case E, a proposed subsynchronous resonance countermeasure is analyzed in order to compare it to the proposed scheme of Case D. In this case, the subsynchronous resonance effects are reduced but not as much as in Case D. This can be explained as follows: since the series capacitor is not controlled, transient subsynchronous currents are flowing into the generator. These currents are not adequately damped by the dynamic stabilizer.

In summary, Case D corresponds to the least shaft stress by comparison to the other four cases. Thus the control scheme utilized in

case D is the best control scheme. It is important to note that most of the attenuation of the subsynchronous resonance effects is provided by the discrete controller. As explained earlier this is due to the fact that the discrete controller has an almost instantaneous time response as compared to the continuous controller. In this case the continuous controller acts as a stabilizer of the oscillations of the generator with respect to the rest of the system.

Summary

This chapter presented the apllication of the dynamic simulation program and the control design technique to solve the subsynchronous resonance control problem for an actual electric power system. Analysis of different controlled and uncontrolled cases have been discussed. It is concluded that the optimal decentralized controllers designed in case D give the best results in attenuating the subsynchronous resonance effects.

Table 1. Performance Indices for Test System

	Case A	Case B	Case C	Case D	Case E
J1:TGT	47.630	44.311	10.044	8.771	34.199
J2:TGE	3.254	2.787	0.090	0.023	2.985
J3:T12	51.697	48.580	7.604	6.370	7.601
J4:T23	23.225	19.183	0.882	0.737	1.995
J5:T34	7.543	6.179	0.251	0.212	3.854

Table 2. Reduction in Performance Indices

	Case A	Case B	Case C	Case D	Case E
J1:TGT	0.0	6.968	78.912	81.586	28.198
J2:TGE	0.0	14.340	97.243	99.280	8.279
J3:T12	0.0	6.028	85.292	87.678	85.279
J4:T23	0.0	17.401	96.201	96.825	91.412
J5:T34	0.0	18.088	96.673	97.188	48.919

Table 3. Maximum Torque Amplitude

	Case A	Case B	Case C	Case D	Case E
TGT	2.319	2.108	1.457	1.455	1.482
TGE	0.232	0.223	0.057	0.047	0.230
T12	1.923	1.688	1.198	1.195	1.400
T23	1.323	1.282	0.681	0.680	0.933
T34	0.744	0.714	0.359	0.358	0.507

Table 4. Reduction in Maximum Torque Amplitude

	Case A	Case B	Case C	Case D	Case E
TGT	0.0	9.089	37.163	37.257	36.102
TGE	0.0	3.819	75.405	79.758	1.000
T12	0.0	12.228	37.719	37.861	27.206
T23	0.0	3.062	48.541	48.613	29.451
T34	0.0	4.016	51.767	51.815	31.818

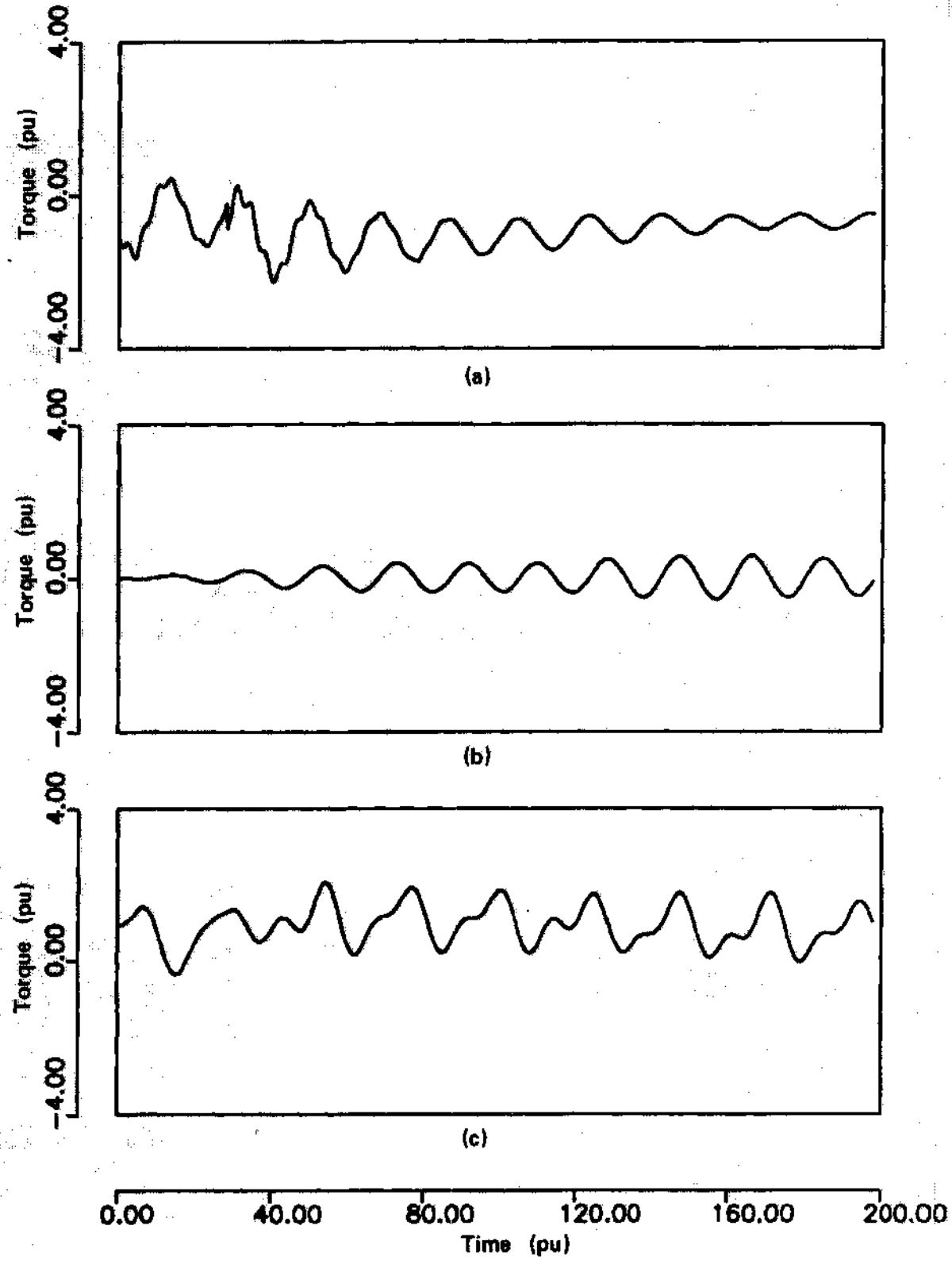

Figure 22. Torsional Oscillations for Study Case A

a) Electromagnetic
b) GEN–EXC Shaft
c) GEN–LPB Shaft

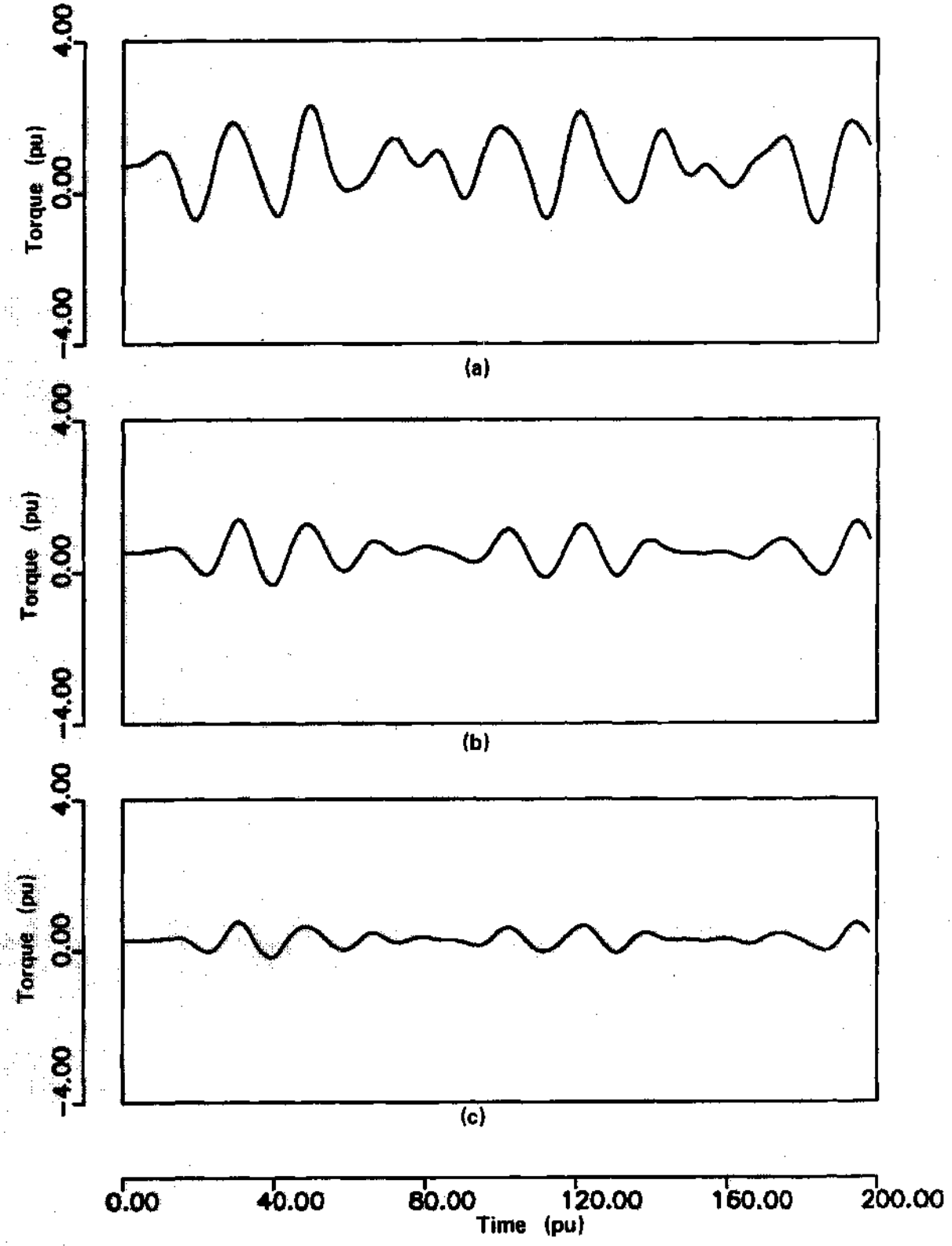

Figure 23. Torsional Oscillations for Study Case A

a) LPA–LPB Shaft
b) IP–LPA Shaft
c) HP–IP Shaft

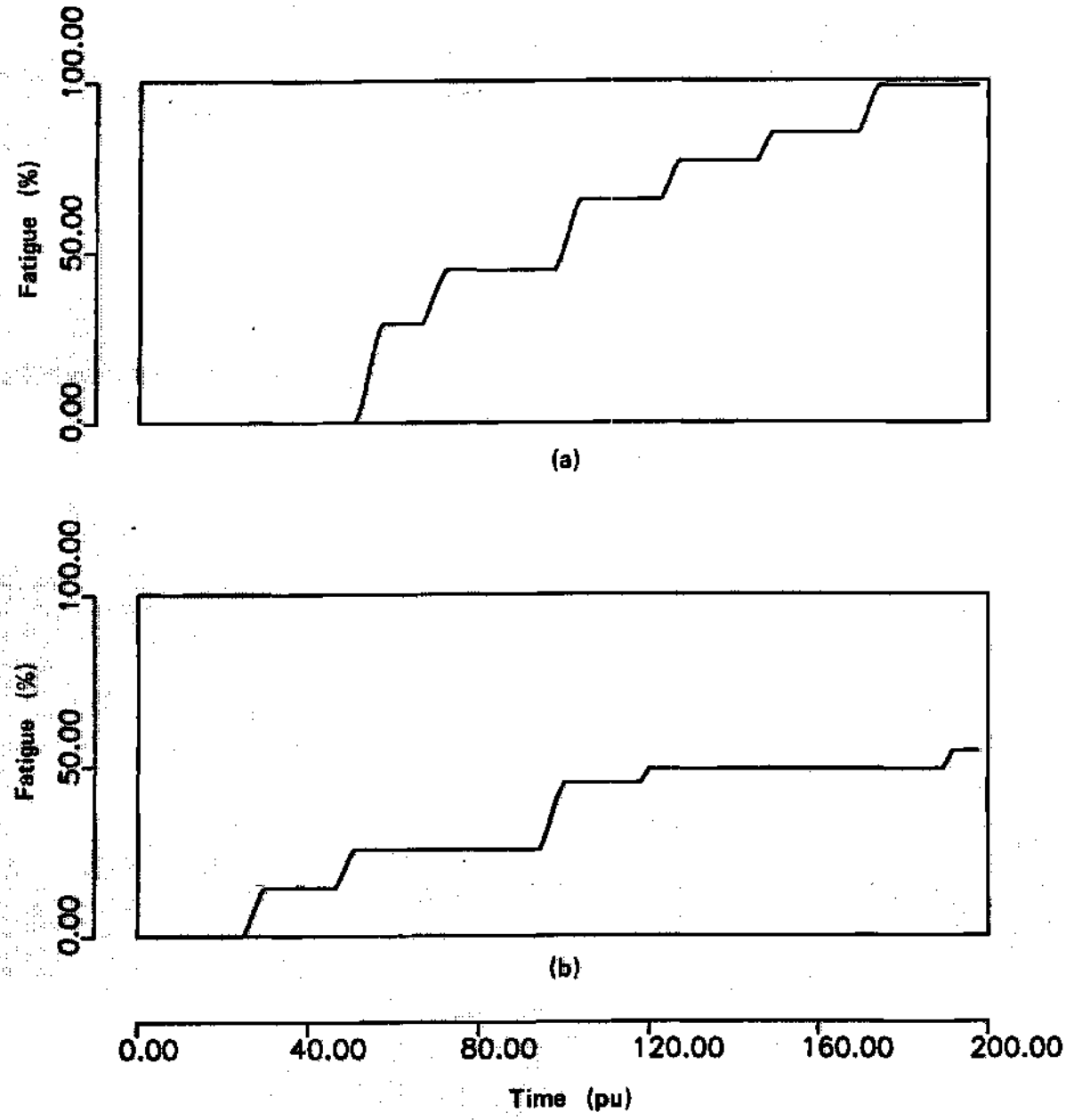

Figure 24. Shaft Fatigue for Study Case A

a) GEN - LPB Shaft
b) LPA - LPB Shaft

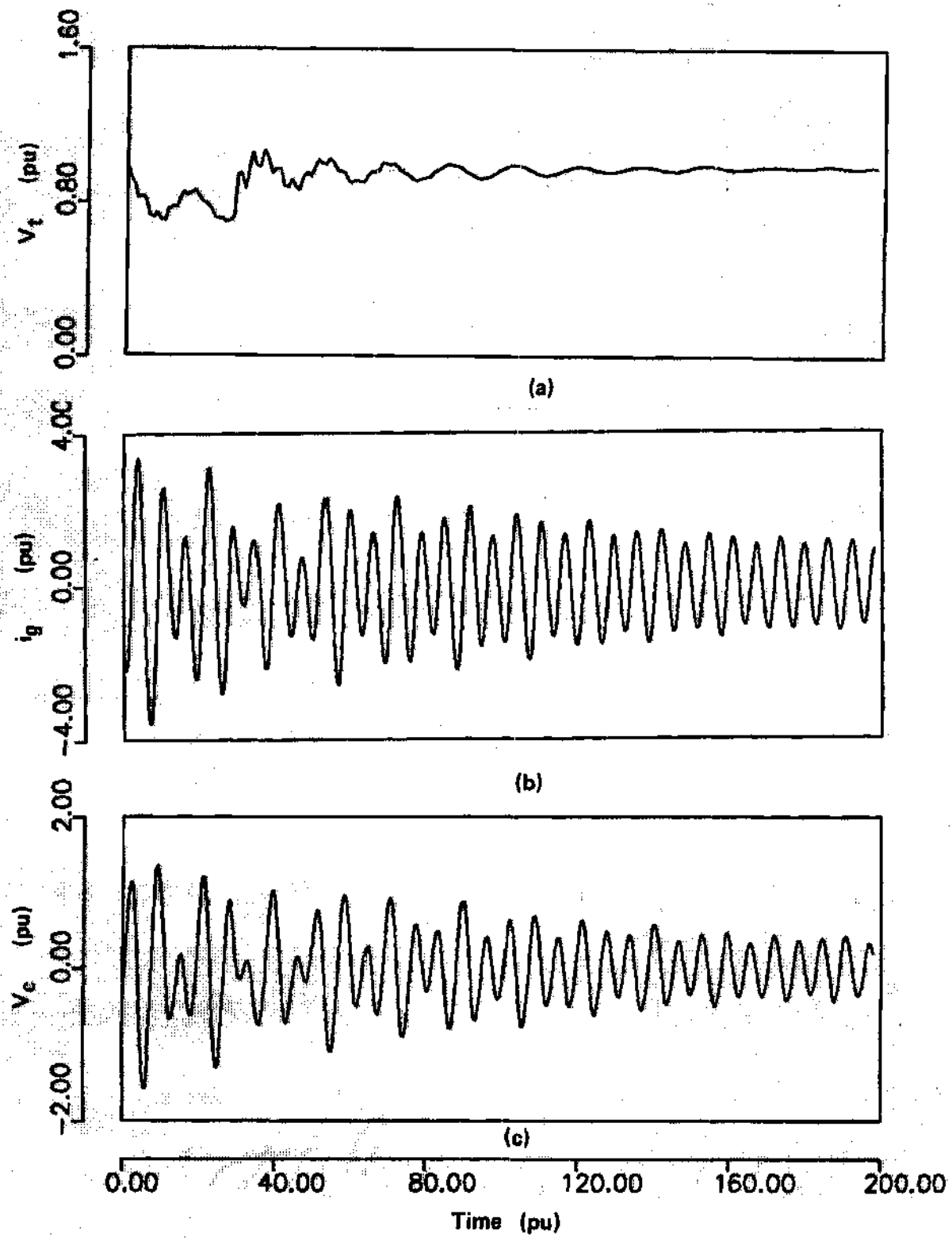

Figure 25. Electrical Oscillations for Study Case A

a) Generator Terminal Voltage
b) Generator Current
c) Voltage across Capacitor

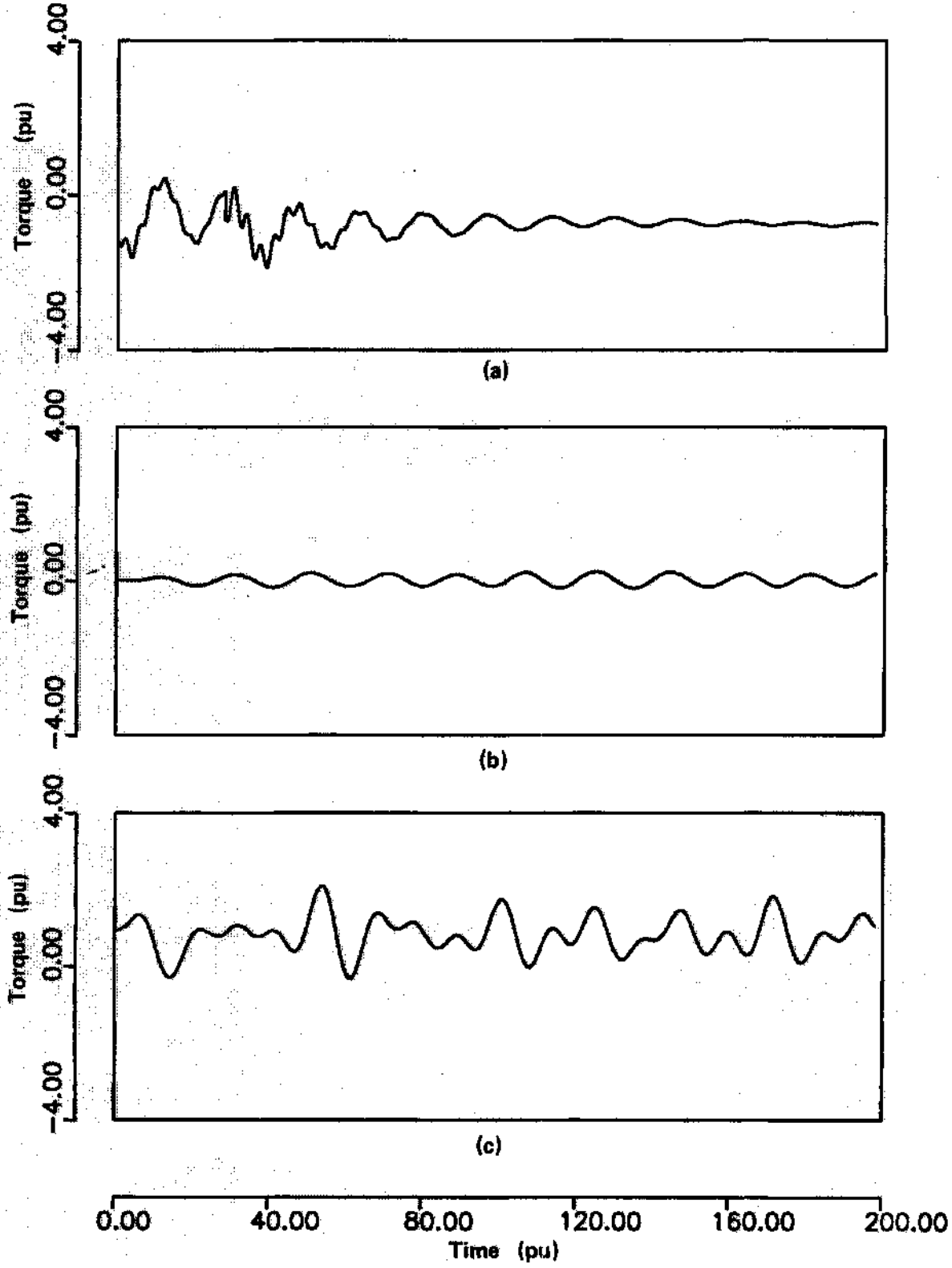

Figure 26. Torsional Oscillations for Study Case B

a) Electromagnetic
b) GEN - EXC Shaft
c) GEN - LPB Shaft

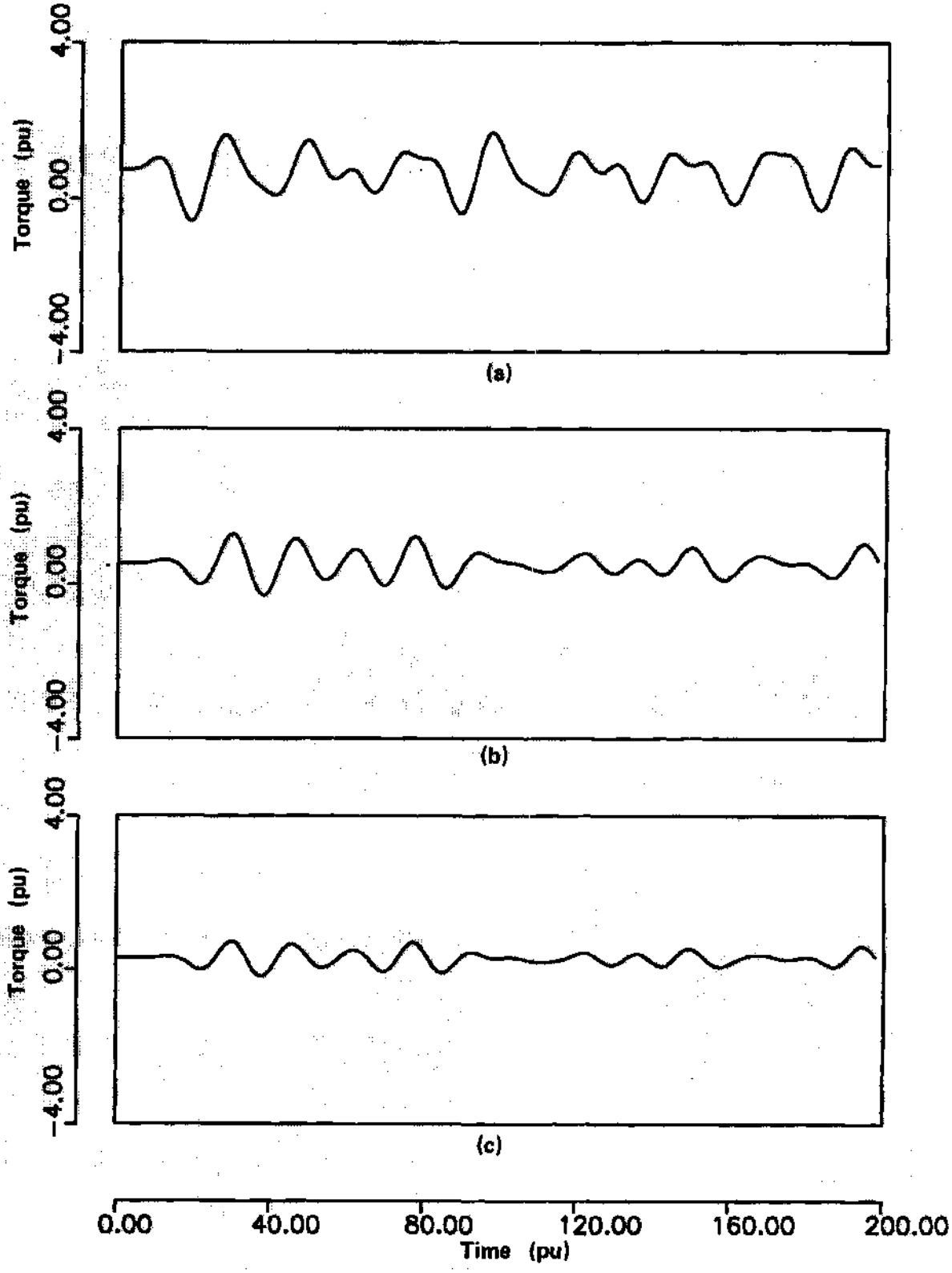

Figure 27. Torsional Oscillations for Study Case B

a) LPA - LPB Shaft
b) IP - LPA Shaft
c) HP - IP Shaft

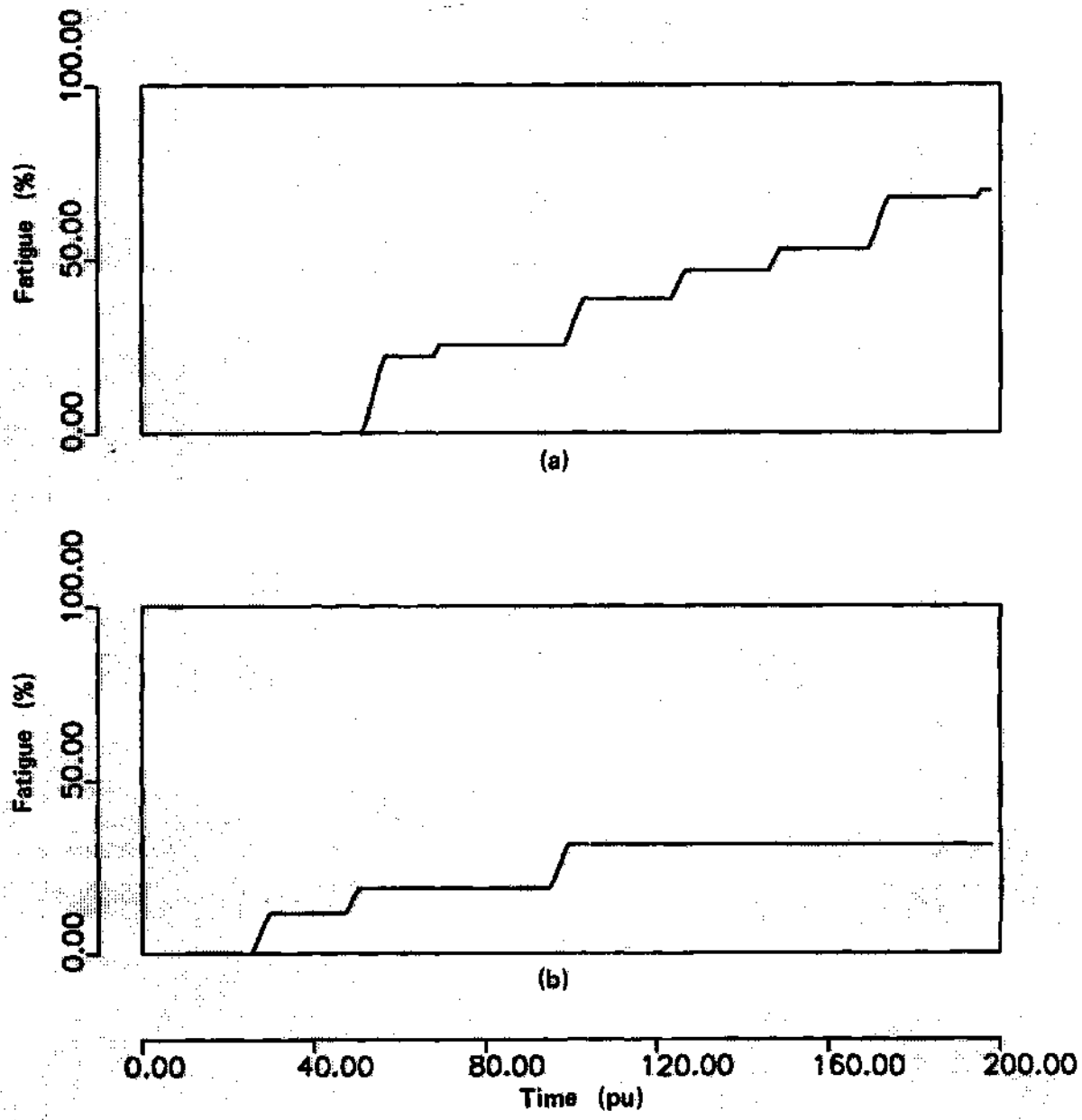

Figure 28. Shaft Fatigue for Study Case B

a) GEN - LPB Shaft
b) LPA - LPB Shaft

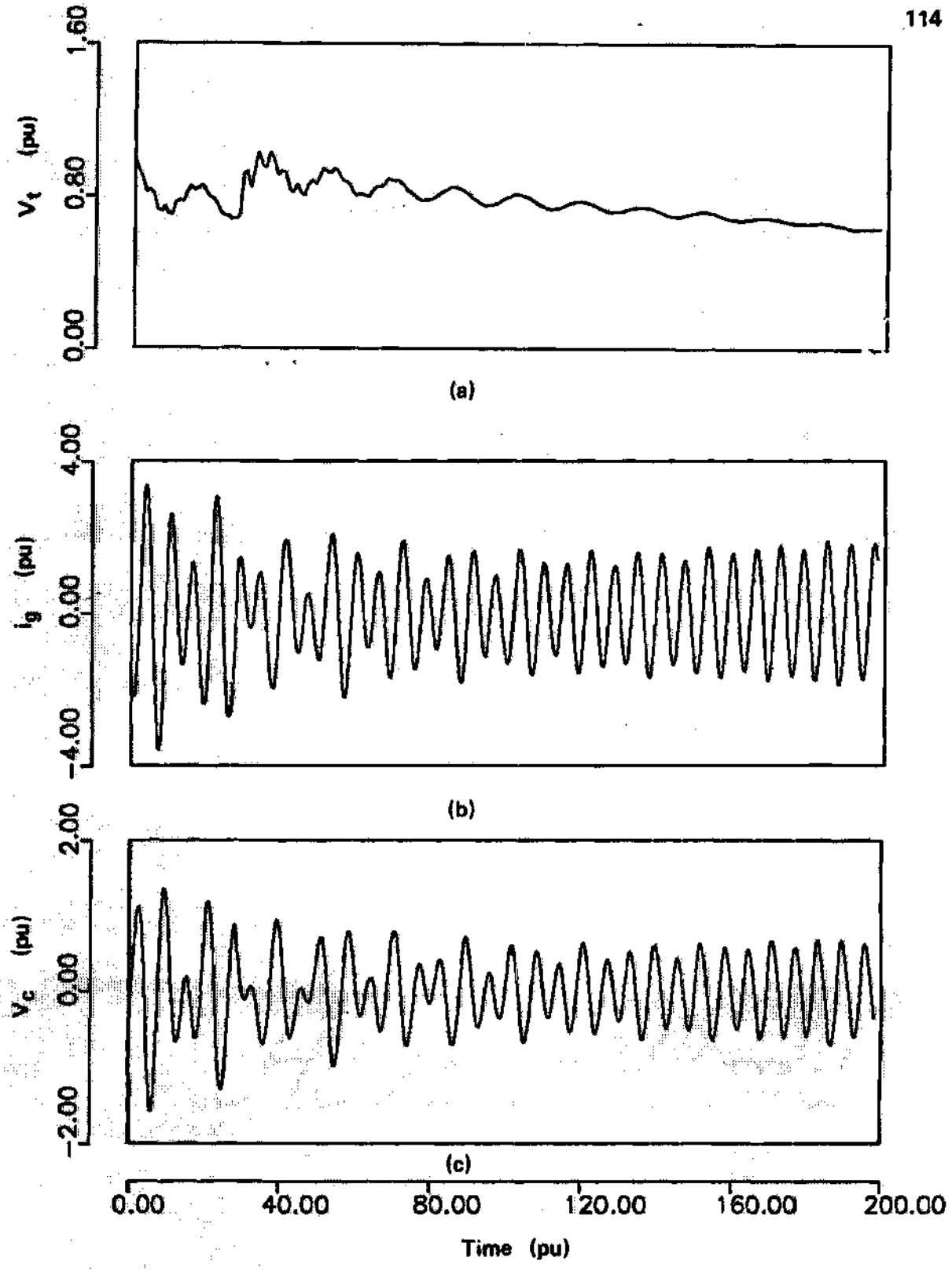

Figure 29. Electrical Oscillations for Study Case B

a) Generator Terminal Voltage
b) Generator Current
c) Voltage across Capacitor

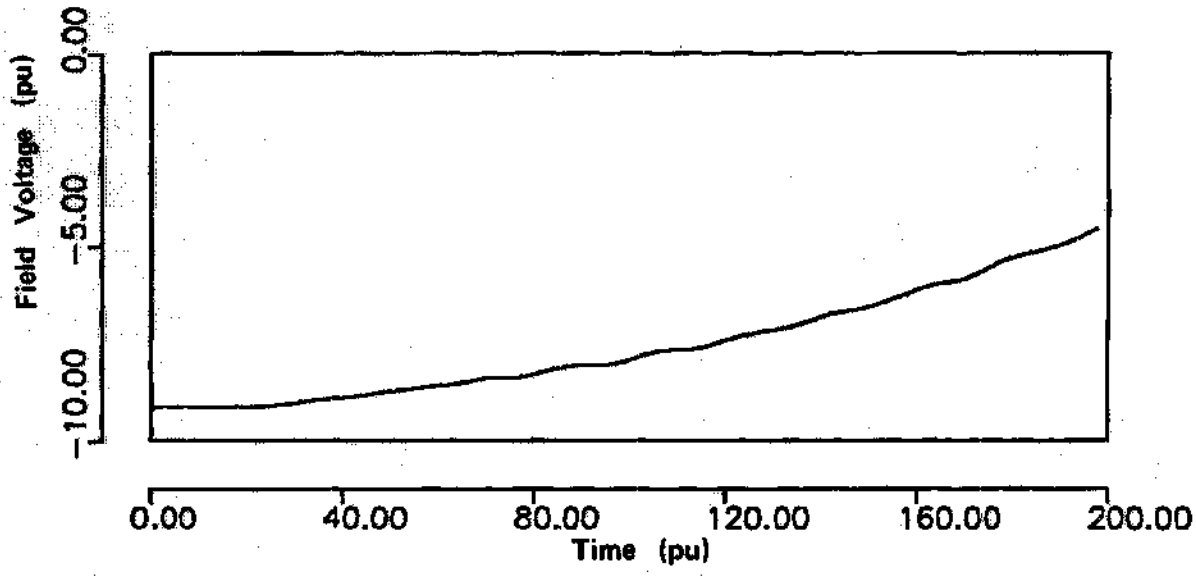

Figure 30. Control Law for Study Case B

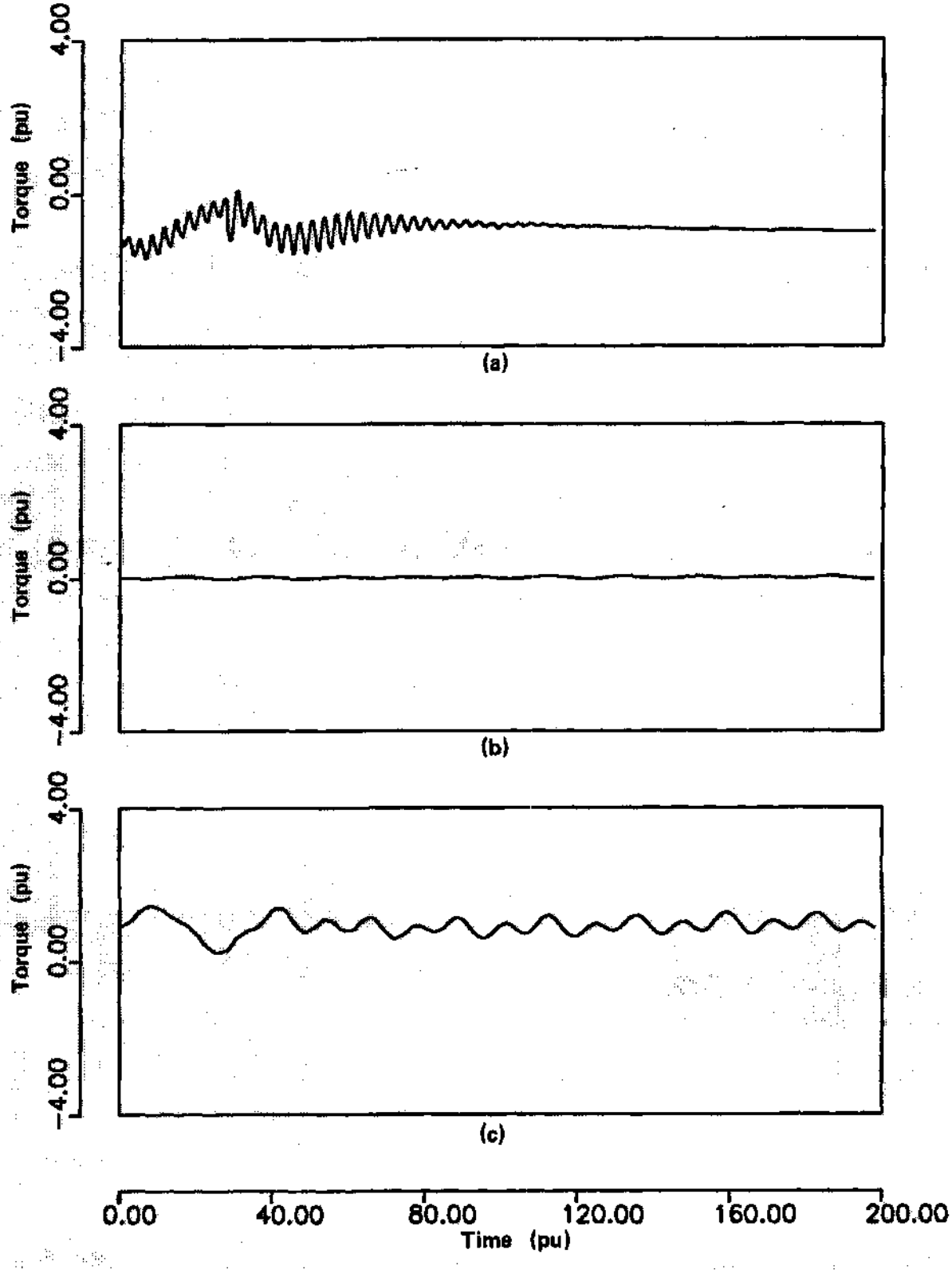

Figure 31. Torsional Oscillations for Study Case C

a) Electromagnetic
b) GEN - EXC Shaft
c) GEN - LPB Shaft

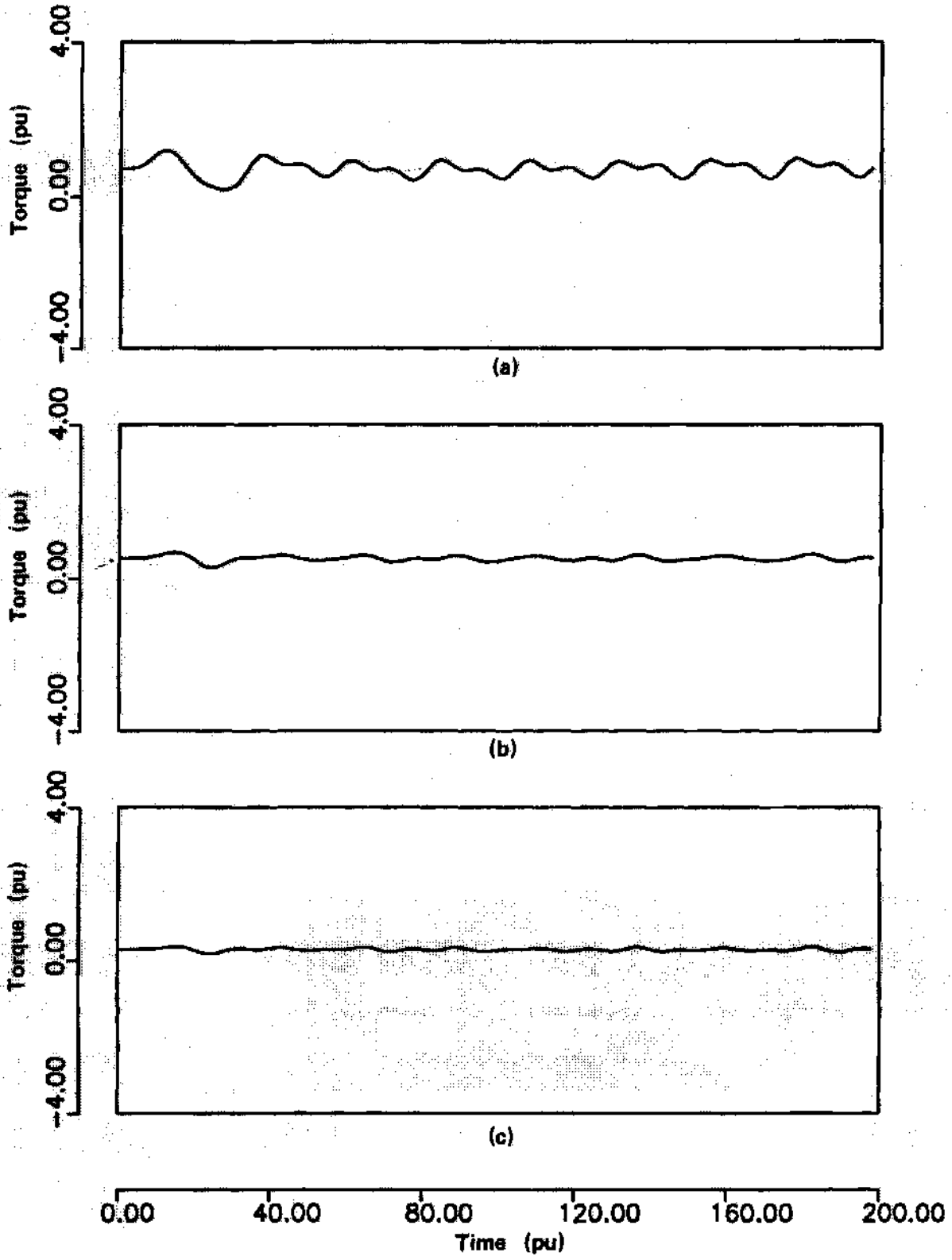

Figure 32. Torsional Oscillations for Study Case C

a) LPA - LPB Shaft
b) IP - LPA Shaft
c) HP - IP Shaft

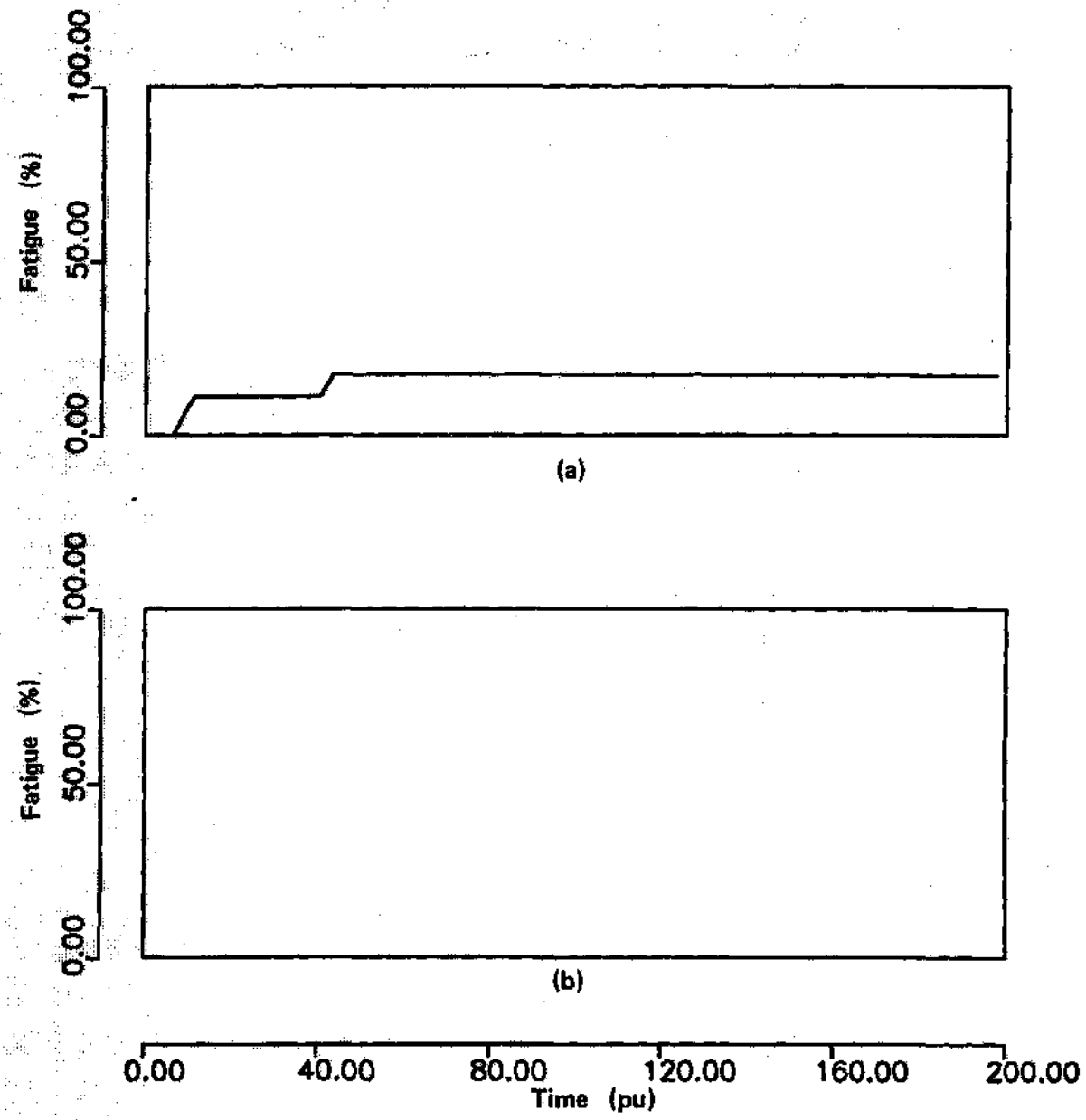

Figure 33. Shaft Fatigue for Study Case C

a) GEN - LPB Shaft
b) LPA - LPB Shaft

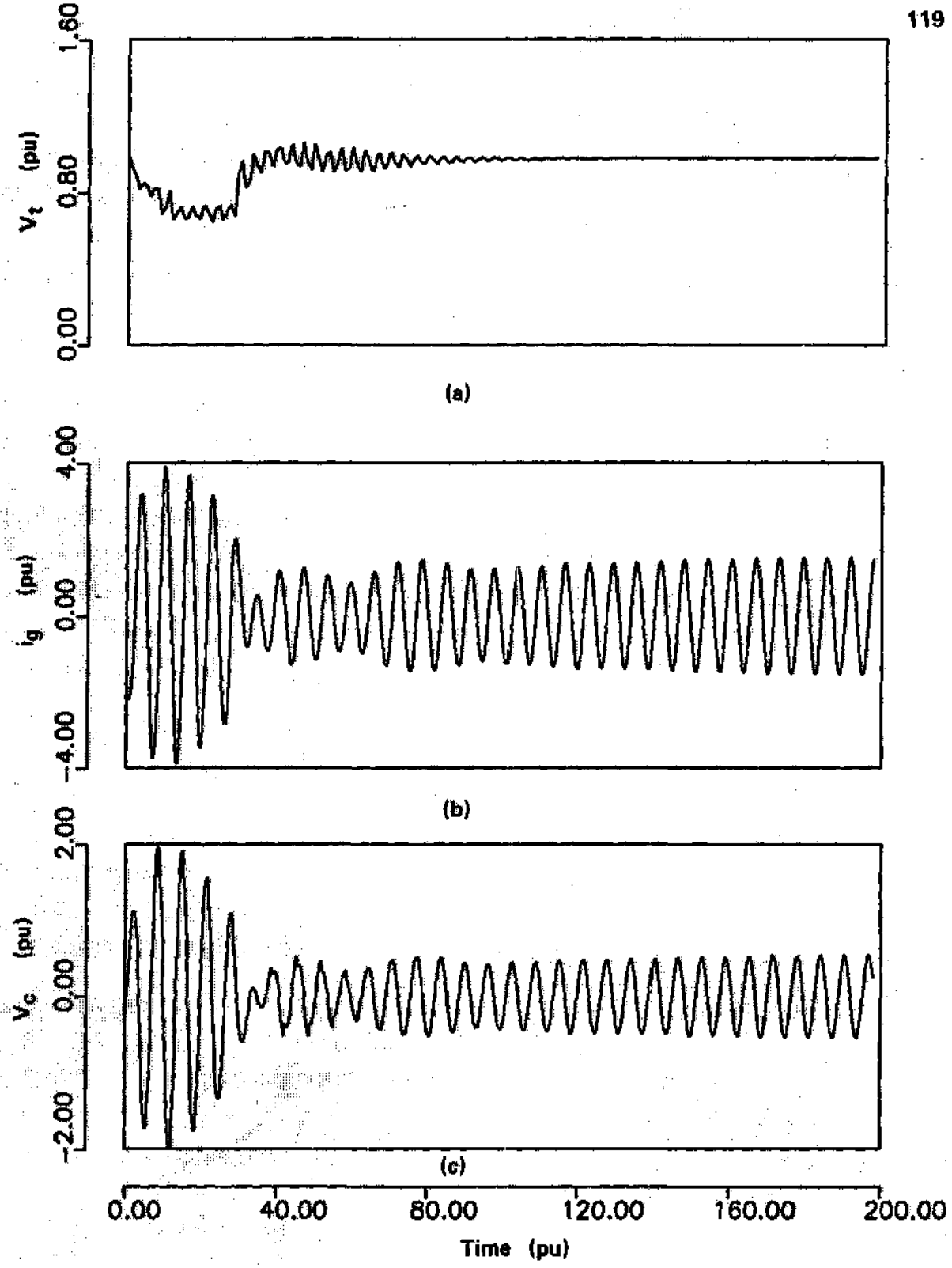

Figure 34. **Electrical Oscillations for Study Case C**

a) Generator Terminal Voltage
b) Generator Current
c) Voltage across Capacitor

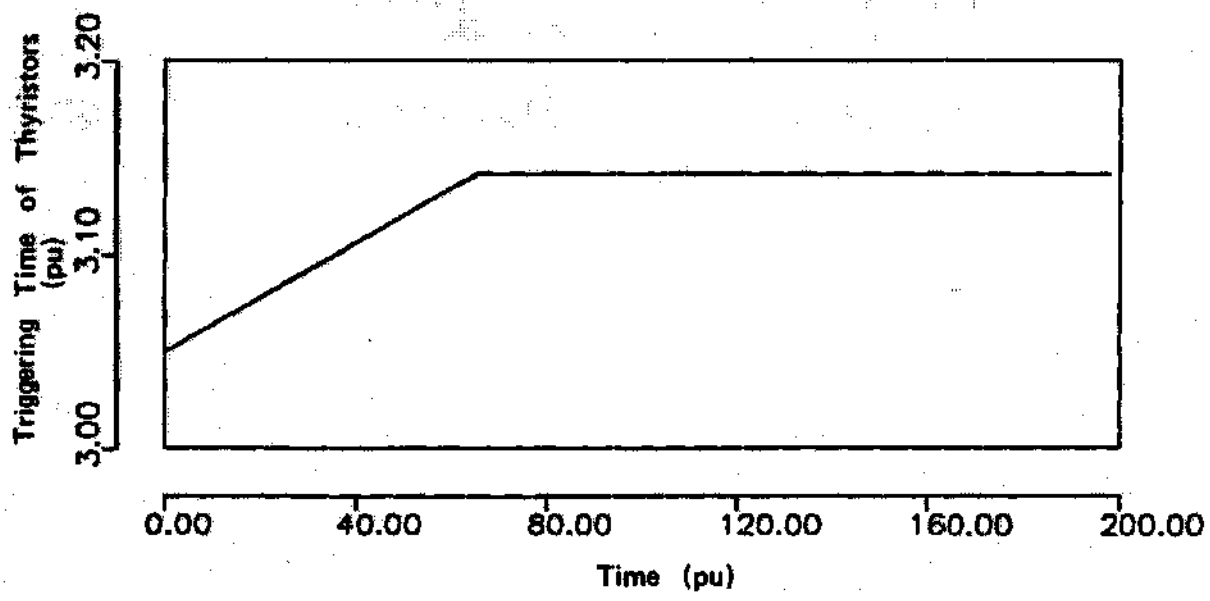

Figure 35. Control Law for Study Case C

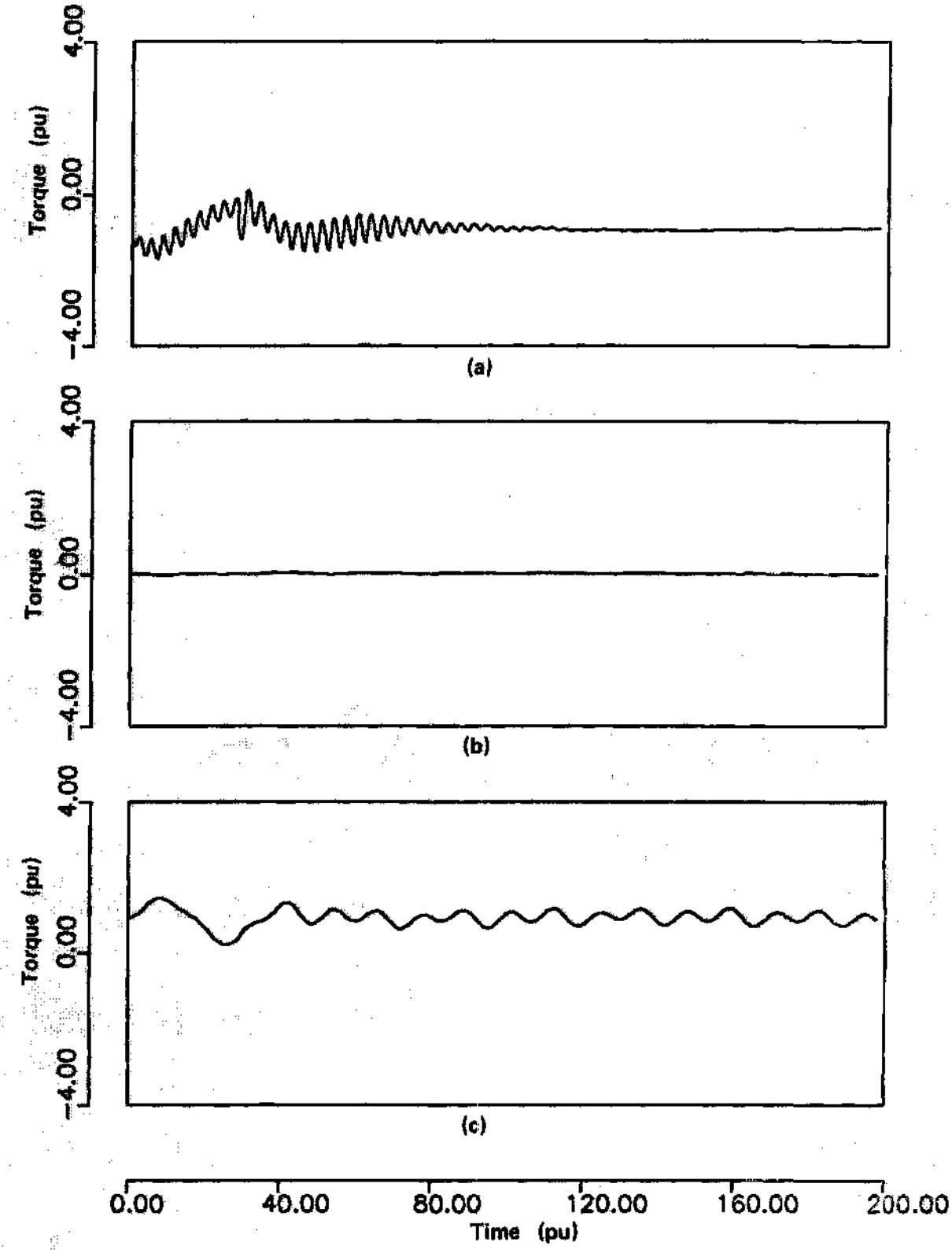

Figure 36. Torsional Oscillations for Study Case D

a) Electromagnetic
b) GEN - EXC Shaft
c) GEN - LPB Shaft

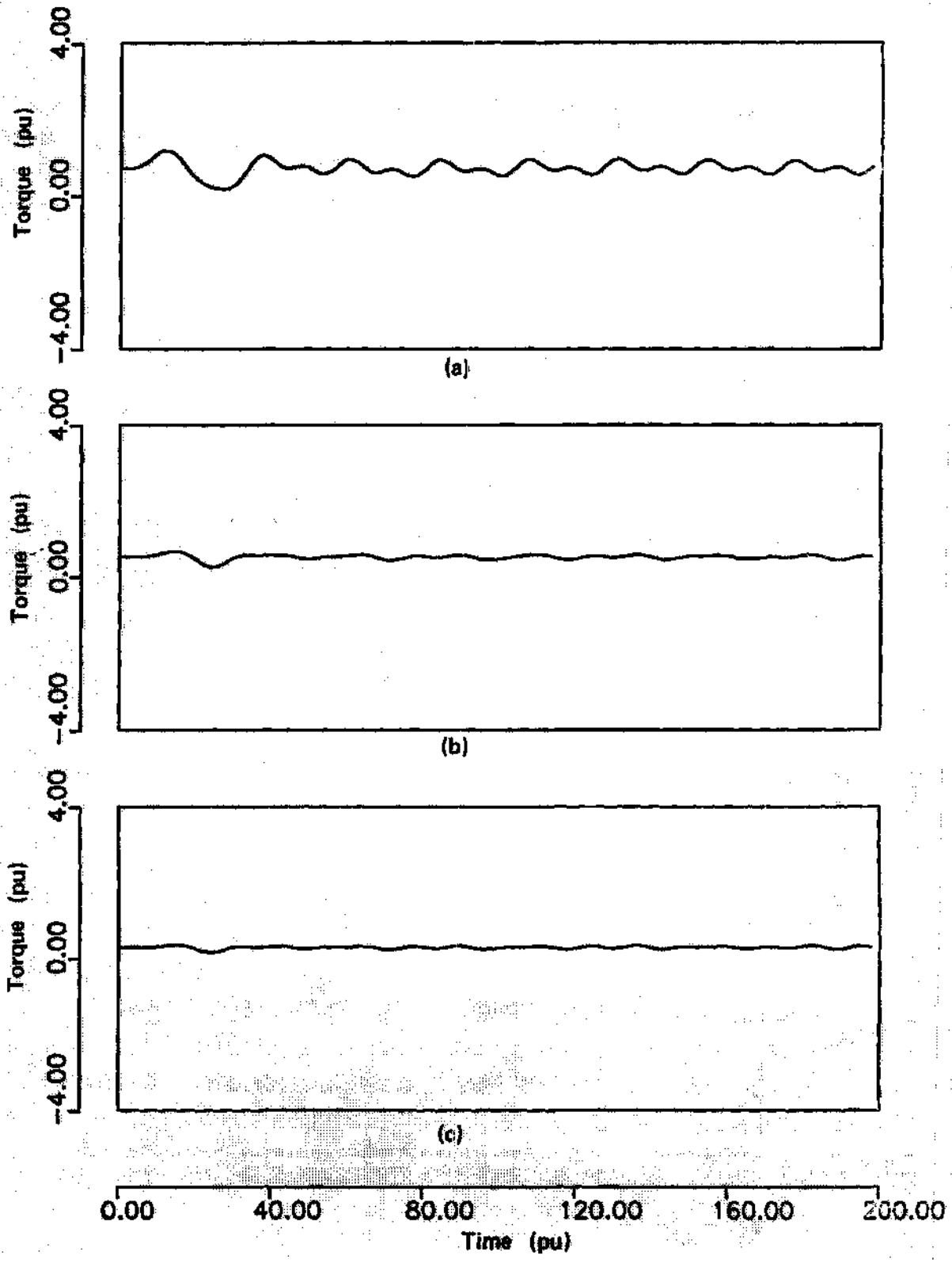

Figure 37. Torsional Oscillations for Study Case D

a) LPA - LPB Shaft
b) IP - LPA Shaft
c) HP - IP Shaft

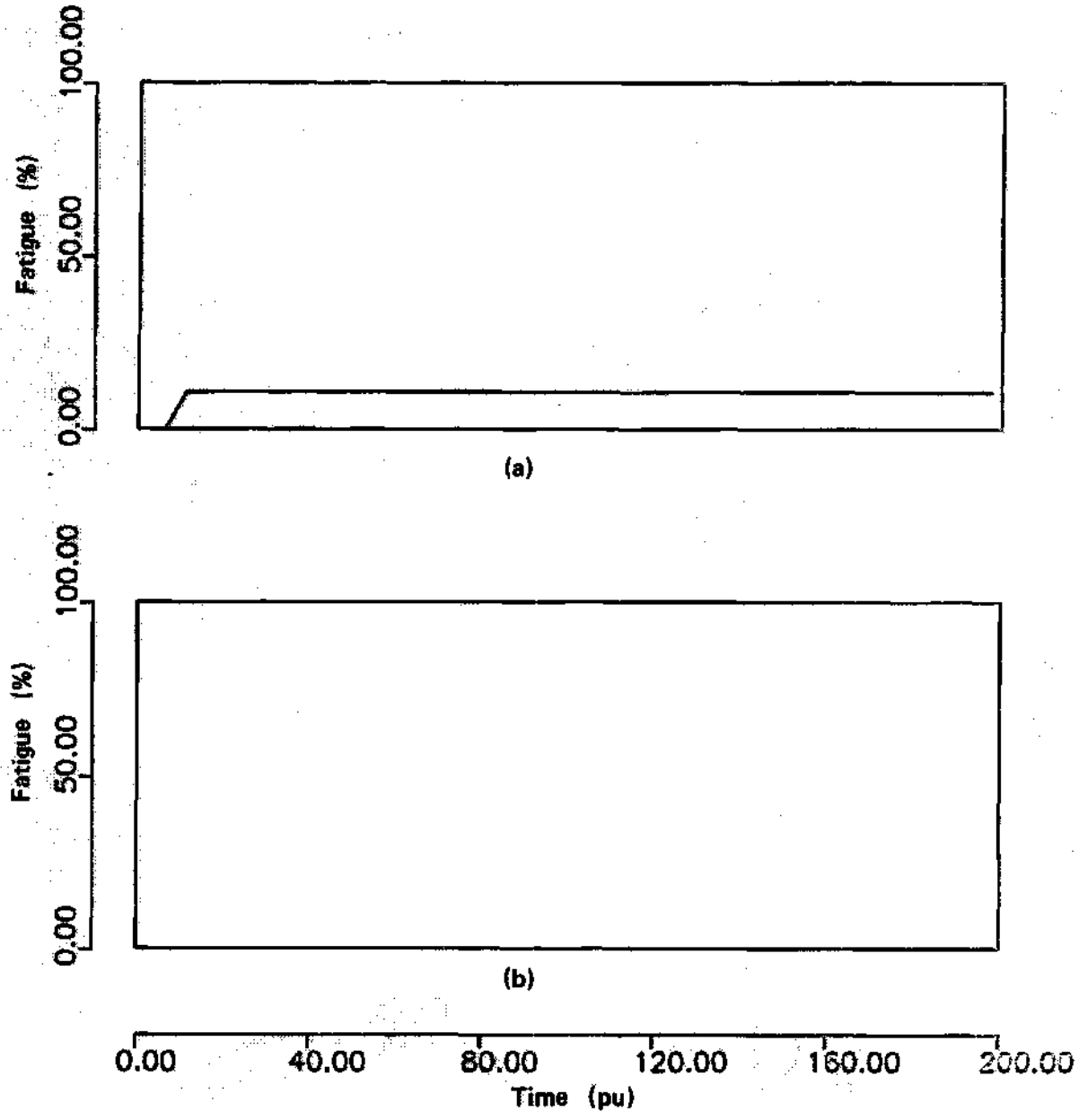

Figure 38. Shaft Fatigue for Study Case D

a) GEN - LPB Shaft
b) LPA - LPB Shaft

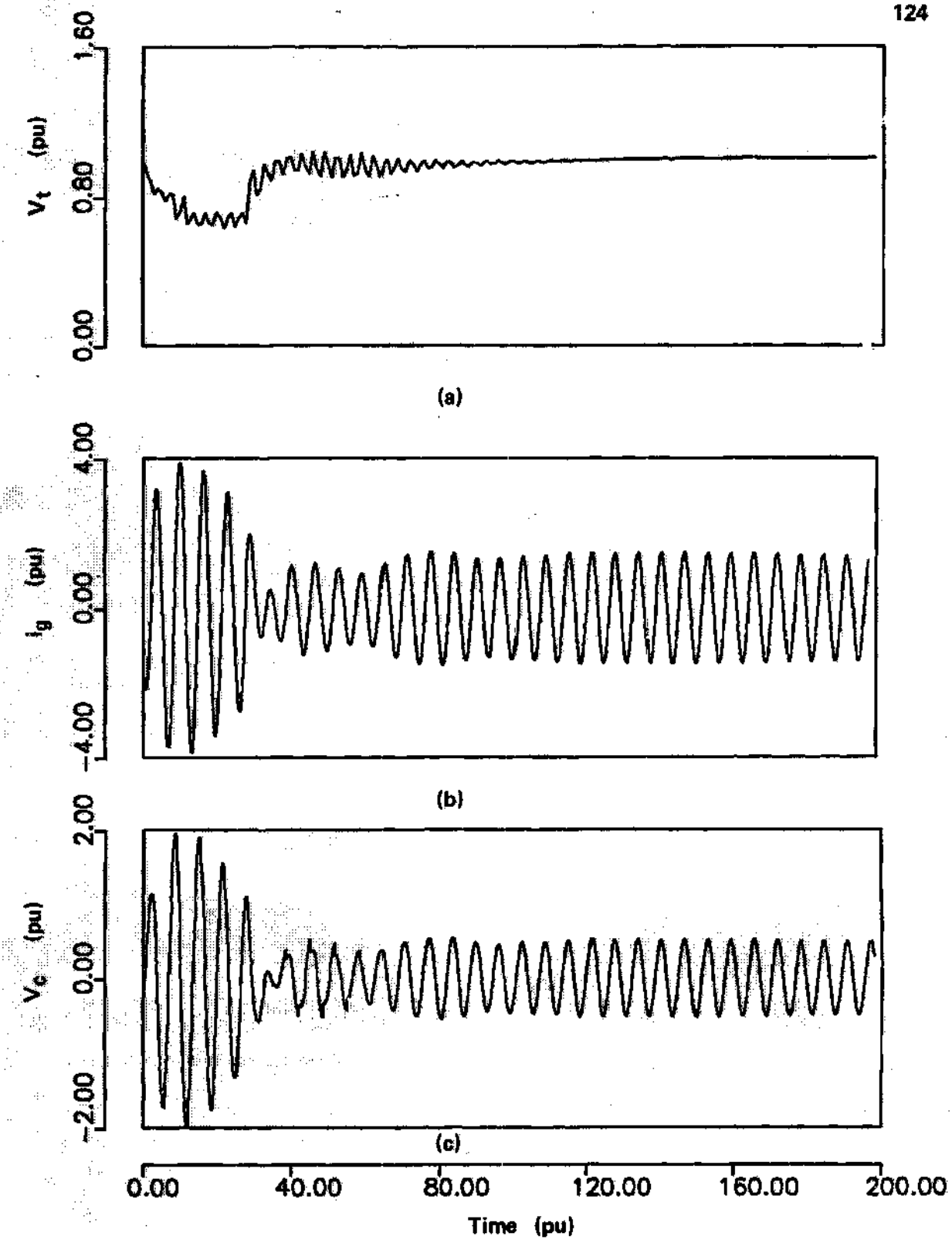

Figure 39. Electrical Oscillations for Study Case D

a) Generator Terminal Voltage
b) Generator Current
c) Voltage across Capacitor

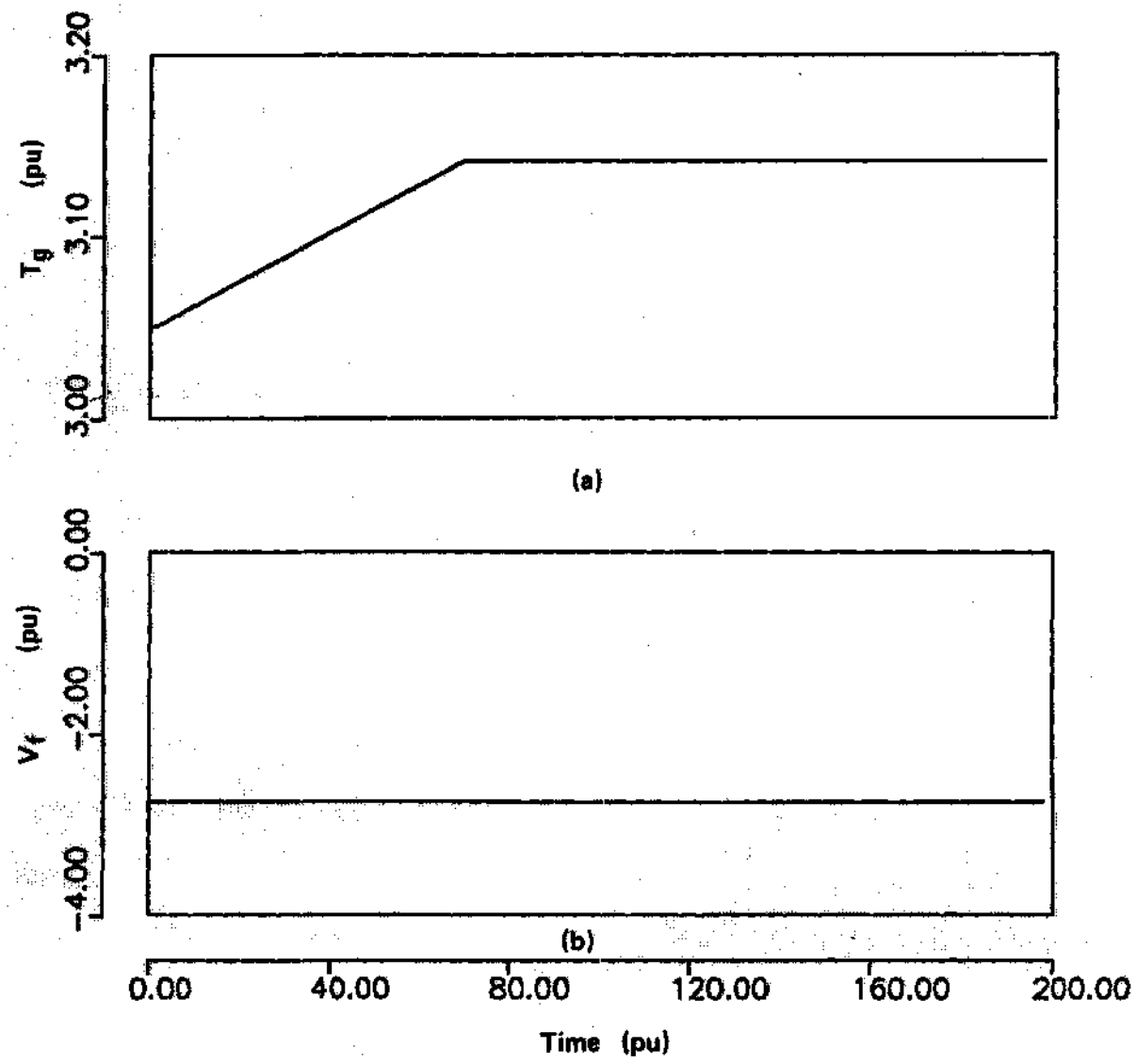

Figure 40. Control Laws for Study Case D

a) Thyristors Triggering Time
b) Excitation Voltage

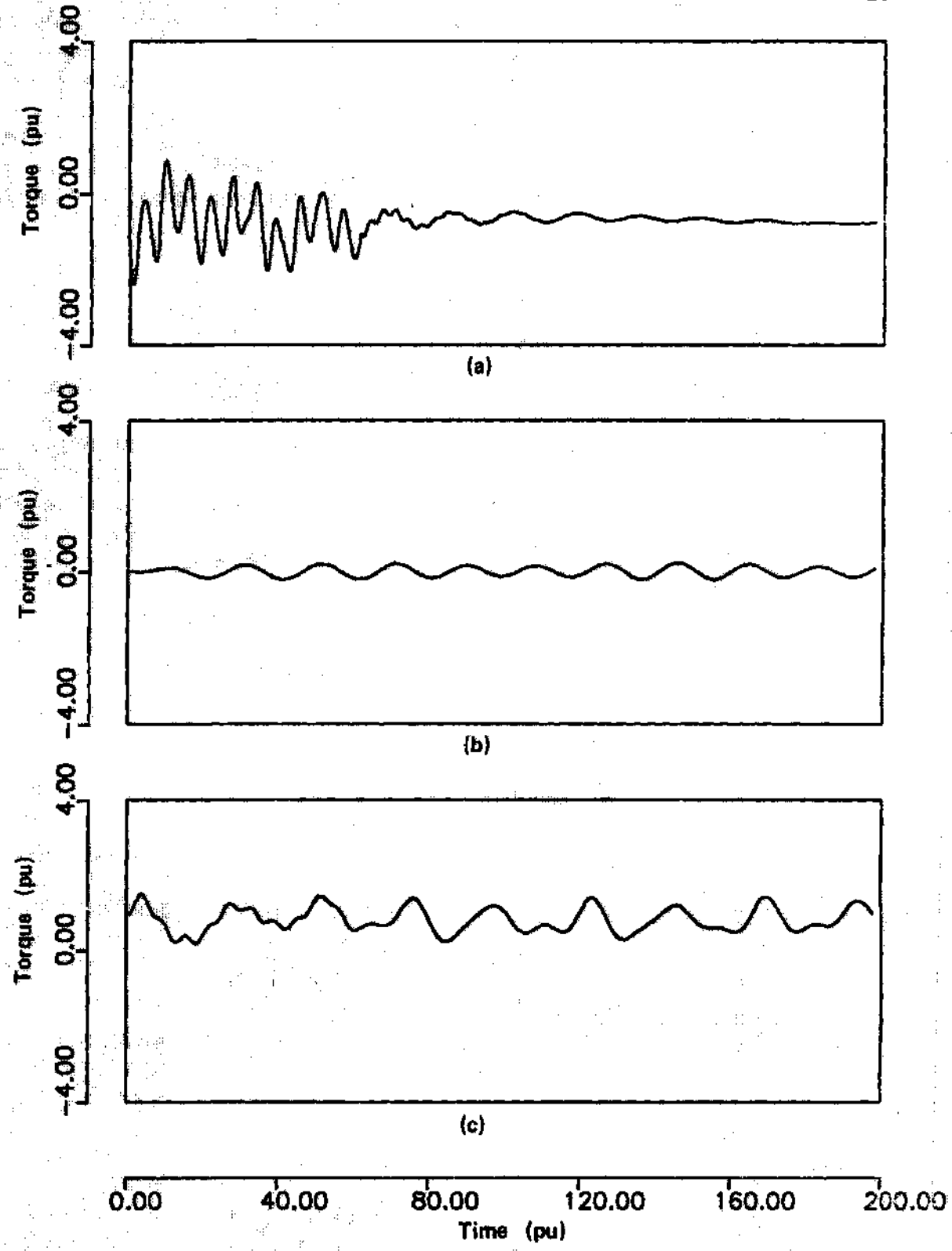

Figure 41. Torsional Oscillations for Study Case E

a) Electromagnetic
b) GEN - EXC Shaft
c) GEN - LPB Shaft

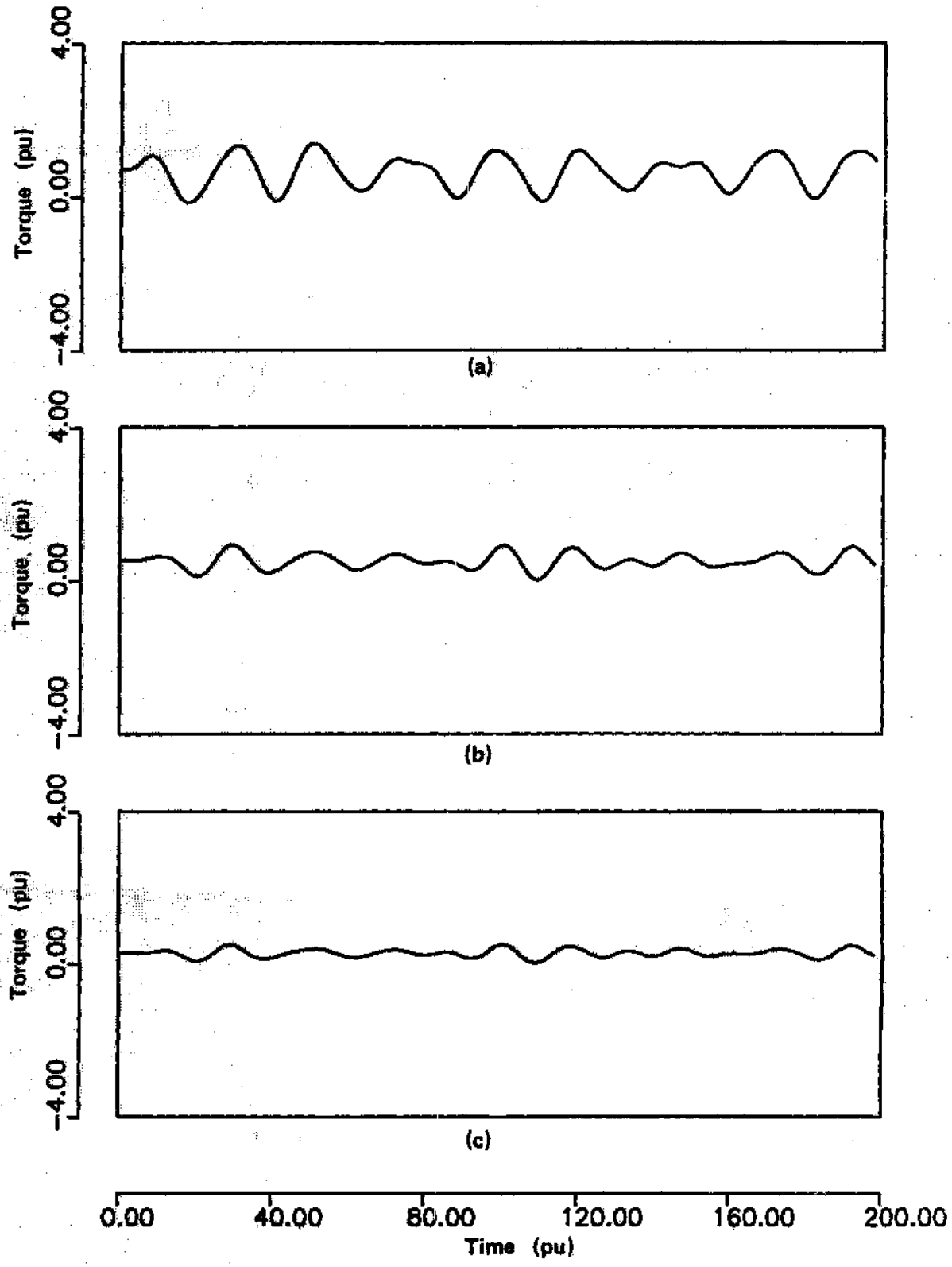

Figure 42. Torsional Oscillations for Study Case E

a) LPA - LPB Shaft
b) IP - LPA Shaft
c) HP - IP Shaft

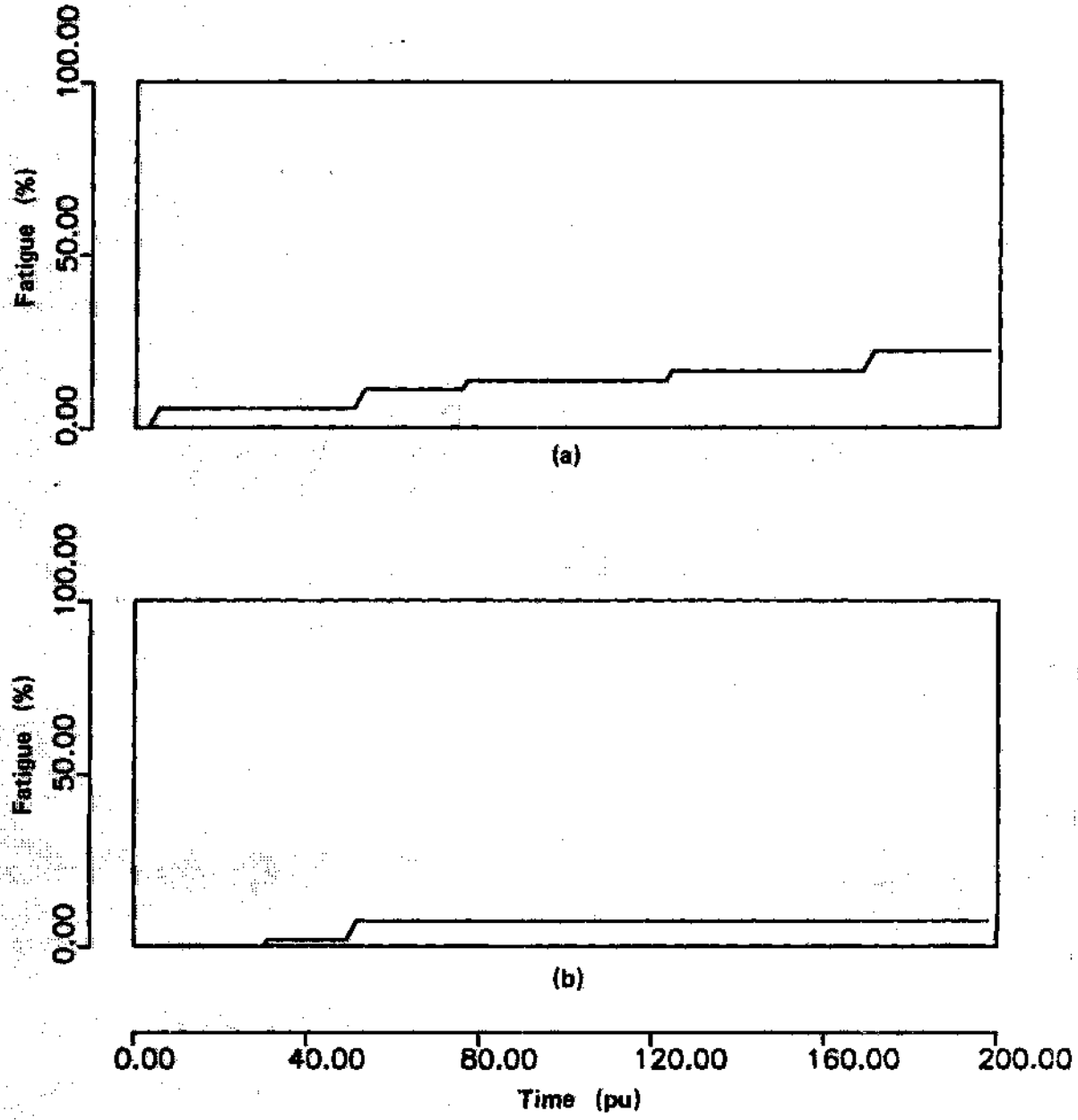

Figure 43. Shaft Fatigue for Study Case E

a) GEN - LPB Shaft
b) LPA - LPB Shaft

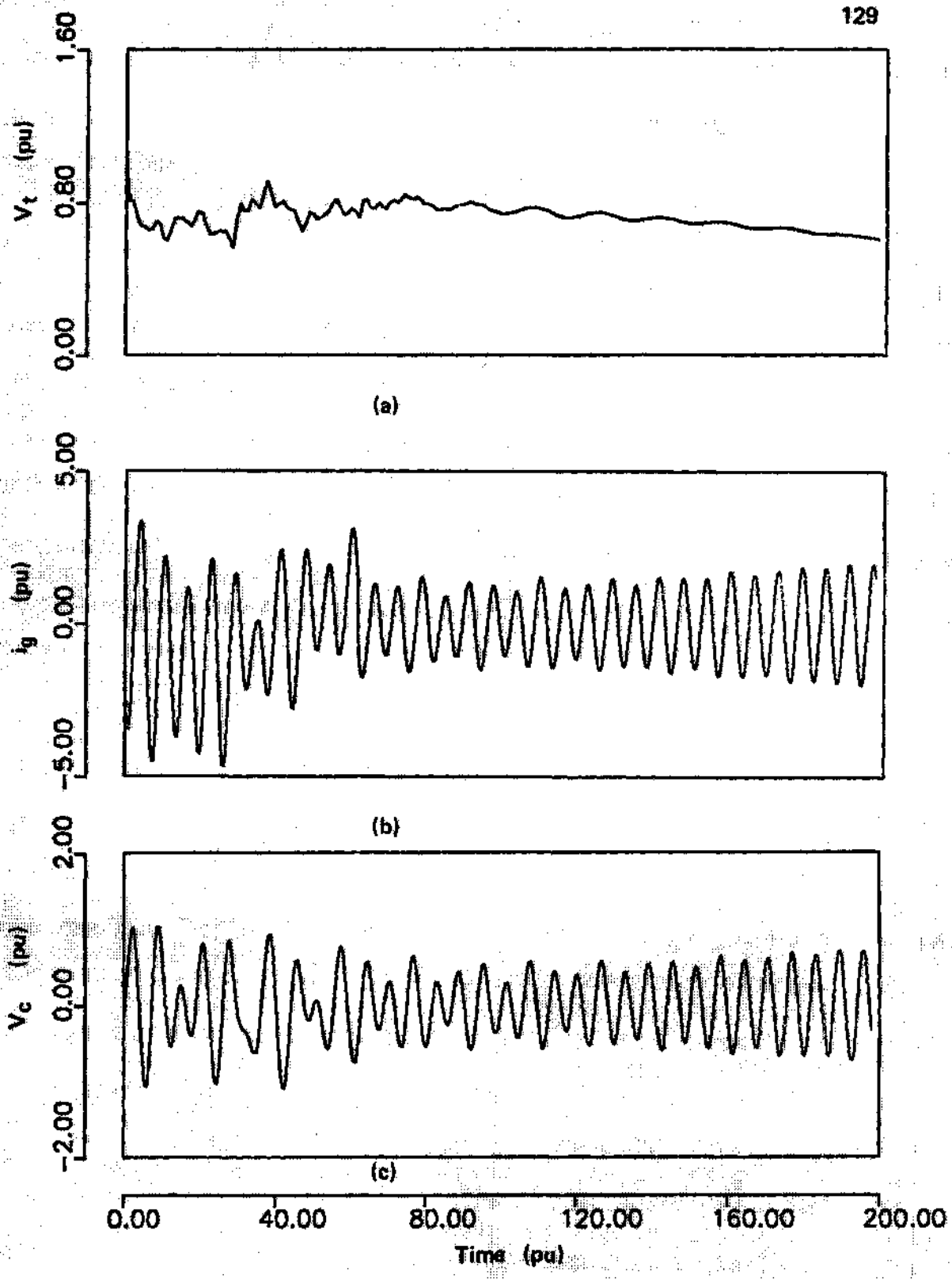

Figure 44. Electrical Oscillations for Study Case E

a) Generator Terminal Voltage
b) Generator Current
c) Voltage across Capacitor

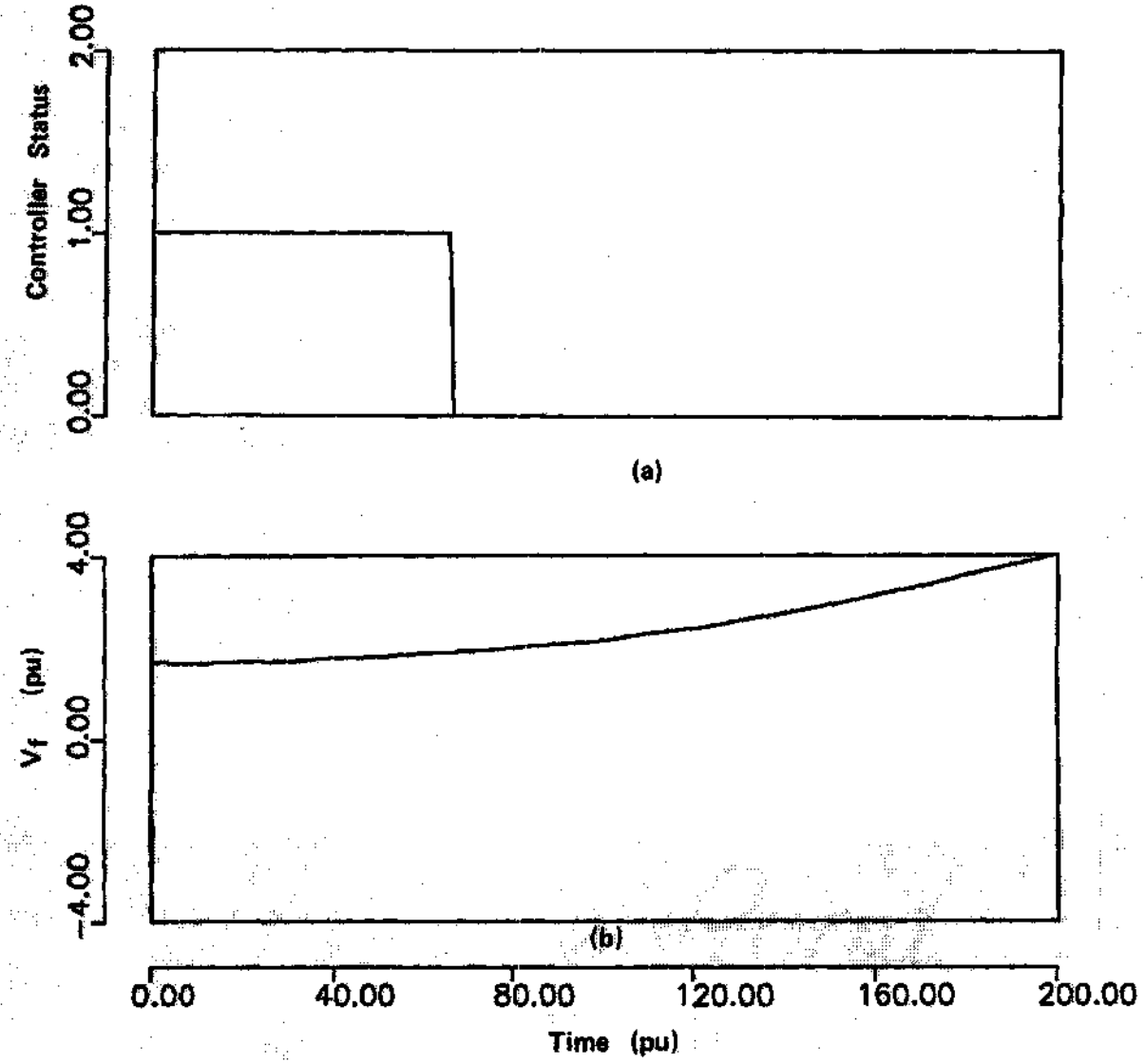

Figure 45. Control Laws for Study Case E

a) Dynamic Stabilizer (On-Off)
b) Excitation Voltage

CHAPTER VI

CONCLUSIONS AND RECOMMENDATIONS

Conclusions

The Subsynchronous Resonance phenomenon is an electric power system condition where the electric network exchanges energy with a turbine generator at one or more of the natural frequencies of the combined system below the synchronous frequency of the system. The phenomenon is responsible for shaft system fatigue resulting from excessive shaft torques and associated sheer and longitudinal stresses of shaft material. Each incident results in some loss of shaft life. These damages are cumulative and can cause shaft fracture.

In this thesis effective continuous and discrete optimal controllers have been designed to attenuate the subsynchronous resonance effects in electric power systems. The control laws have been designed utilizing a novel optimal control design methodology performed within the framework of a generalized dynamic simulation algorithm.

A general modeling procedure and a general dynamic simulation algorithm were developed by exploiting the structure of interconnected dynamic systems.

These techniques were applied to the electric power system. They resulted in a digital dynamic simulation program. The program is

modular. Each module represents a power apparatus modeled as a resistive companion network. This program has many attractive features such as expandability, model accuracy, model optimization, sparsity, suitability to parallel processing and numerical stabilty [81]-[82].

The simulation algorithm is utilized as an analysis tool and also as a control design tool. The control design methodology developed in this thesis is a gradient iterative technique performed within the framework of the dynamic simulation program. The method is based on the sensitivity analysis of some prespecified vector performance index with respect to some control parameters. At each iteration, the simulation program computes a sensitivity matrix which is used to update the control parameters. The main properties of this approach are: a) a vector performance index is optimized rather than a scalar criterion: the designer has then a clear picture of the controllers impact on different aspects of the system performance at each iteration; b) it is very simple with this approach to handle important controller structures such as decentralized laws, combination of discrete and continuous strategies. Also it is straightforward to take into consideration the physical limitations on the control gains, etc.; c) the control scheme is feasible and implementable because the control structure is user defined.

The central point of the control design technique is the computation of a sensitivity matrix. For this computation two contributions were presented: a) closed form expressions of the sensitivity matrix were derived based on the system linearized model matrices; b) a unified approach for the computation of the system

linearized model of a large scale system from the linearized models of its individual elements was developed.

The dynamic simulation and the control design methodologies are general and can be applied to general large scale interconnected dynamic systems. In this thesis they were specifically and effectively applied to analyze and control the subsynchronous resonance effects in electric power systems. For the Benchmark Test System two decentralized optimal controllers were designed. A discrete control scheme periodically short circuits the voltages which are not exactly 60 Hz and a continuous control scheme stabilizes the oscillations of the generator with respect to the rest of the system. The proposed control structure was compared to an existing subsynchronous resonance countermeasure, namely a dynamic stabilizer with excitation control. The results have shown that the proposed scheme has been more effective in reducing the subsynchronous resonance effects.

Recommendations

The modeling and control design procedures are general and can be applied to different analysis and control problems in large scale interconnected systems. The objective of the thesis was to concentrate on the subsynchronous resonance effects. However further work can be pursued to apply the procedures developed in this thesis.

First of all, the electric power system simulation program can be efficiently developed as a production grade computer program. The structure of the program also favors a hardware implementation.

Microprocessors can be allocated to different power devices. These microprocessors should work in parallel to compute the device companion resistive network parameters and then interface with a main computer. The main computer solves for the interface variables. In this fashion an expandable dynamic simulator can be constructed. The power system dynamic simulation program can also be utilized as a tool for modal analysis, stability analysis, network equivalencing, parameter identification, etc. Secondly, the control design technique can be easily implemented to other control problems such as the control of harmonics in electric power systems. Moreover it is recommended to implement the control design procedure in an interactive scheme. Thirdly, the procedure developed to determine the composite system linearized system can be utilized to study properties such as structural stability or model reduction.

APPENDIX

MATRIX CALCULUS

In this appendix results from matrix calculus are given.

Kronecker Product

Let A be an nxm matrix and B be an rxs matrix, then, the kronecker product of A and B, denoted by A*B, is the n.rxm.s matrix defined by:

$$A*B = \begin{bmatrix} a_{11}B & a_{12}B & \cdots & a_{1m}B \\ a_{21}B & a_{22}B & \cdots & a_{2m}B \\ \vdots & \vdots & & \vdots \\ a_{n1}B & a_{n2}B & \cdots & a_{nm}B \end{bmatrix}$$

Derivative

The derivative of A with respect to B, denoted by D, is the n.rxm.s matrix defined by:

$$D = \frac{dA}{dB} = \begin{bmatrix} \frac{dA}{db_{11}} & \frac{dA}{db_{12}} & \cdots & \frac{dA}{db_{1s}} \\ \frac{dA}{db_{21}} & \frac{dA}{db_{22}} & \cdots & \frac{dA}{db_{2s}} \\ \cdot & \cdot & & \cdot \\ \cdot & \cdot & & \cdot \\ \cdot & \cdot & & \cdot \\ \frac{dA}{db_{r1}} & \frac{dA}{db_{r2}} & \cdots & \frac{dA}{db_{rs}} \end{bmatrix}$$

Product Rule

If A = M.N, where M is an nxp matrix and N is a pxm matrix, then:

$$dA/dB = d(MN)/dB = (dM/dB)(Is*N) + (Ir*M)(dN/dB)$$

where Is and Ir are sxs and rxr identity matrices respectively.

Inverse

Let AI be the inverse of A, where A is an nxn matrix, then:

$$dAI/dB = - (Ir*AI)(dA/dB)(Is*AI)$$

BIBLIOGRAPHY

[1] IEEE Committee Report, "A Bibliography for the Study of Subsynchronous Resonance Between Rotating Machines and Power Systems", IEEE Transactions on Power Apparatus and Systems, Vol. PAS-95, No. 1, pp. 216-218, Jan/Feb 1976.

[2] IEEE Committee Report, "First Supplement for the Study of Subsynchronous Resonance Between Rotating Machines and Power Systems", IEEE Transactions on power Apparatus and Systems, Vol. PAS-98, No. 6, pp. 1872-1875, Nov/Dec 1979.

[3] C. Concordia, J. B. Tice, C. E. Bowler, "Subsynchronous Torques on Generating Units Feeding Series-Capacitor Compensated Lines", Proceedings of the American Power Conference, Vol. 35, pp. 1129-1136, 1973.

[4] IEEE SSR Task Force, "Proposed Terms and Definitions for Subsynchronous Oscillations", IEEE Transactions on Power Apparatus and Systems, Vol. PAS-99, No. 2, March/April 1980, pp. 506-511.

[5] IEEE Working Group Interim Report, "Effects of Switching Network Disturbances On Turbine-Generator Shaft Systems", presented at the IEEE PES 1982 Winter Meeting, New York.

[6] M. C. Hall, D. A. Hodges, "Experience with 500 kV Subsynchronous Resonance and Resulting Turbine Generator Shaft Damage at Mohave Generating Plant", IEEE Special Publication 76 ch1066-0-PWR, presented at the PES 1976 Winter Meeting and Tesla Symposium.

[7] A. J. Perez, "Mohave Project Subsynchronous Resonance Unit Tripping Scheme", Symposium on Countermeasures for Subsynchronous Resonance, The IEEE PES 1981 Summer Meeting, July 30, 1981, pp. 20-22.

[8] D. N. Walker, A. L. Schwalb, "Results of Subsynchronous Resonance Test at Navajo", Subsynchronous Symposium, the IEEE PES 1975 Summer Meeting.

[9] R. G. Farmer, E. Katz, A. L. Schwalb, "Navajo Project Report On Subsynchronous Resonance Analysis and Solutions", Subsynchronous Resonance Symposium, the IEEE PES 1975 Summer Meeting.

[10] R. G. Farmer, A. L. Schwalb, E. Katz, "Navajo Project Report

on Subsynchronous Resonance Analysis and Solutions", IEEE Transactions on Power Apparatus and Systems, Vol. PAS-96, No. 4, July/August 1977, pp.1226-1232.

[11] C. E. J. Bowler, et. al., "Operation and Test of the Navajo SSR Protective Equipment", IEEE Transactions on Power Apparatus and Systems, Vol. PAS-97, No. 4, July/August 1978, pp.1030-1035.

[12] J. F. Tang, J. A. Young, "Operation Experience of the Navajo Static Blocking Filter", Symposium on Countermeasures for Subsynchronous Resonance, the IEEE PES 1981 Summer Meeting, July 30, 1981, pp. 23-26.

[13] D. M. Triezenberg, "Characteristic Frequencies and Mode Shapes for Turbogenerator Shaft Torsional Vibrartions", IEEE Transactions on Power Apparatus and Systems, Vol. PAS-99, No.1, Jan/Feb 1980, pp. 352-357.

[14] P. J. Nolan, N. K. Sinha, R. T. H. Alden, "Eigenvalue Sensitivities of Power Systems Including Network and Shaft Dynamics", IEEE Transactions on Power Apparatus and Systems, Vol. PAS-95, No. 4, July/August 1976, pp. 1318-1324.

[15] H. M. El-Din Zein, R. Alden, "Second Order Eigenvalue Sensitivities Applied to Power System Dynamics", IEEE Transactions on Power Apparatus and Systems, Vol. PAS-96, No. 6, Nov/Dec 1977, pp. 1928-1936.

[16] B. L. Agrawal, R. G. Farmer, "Use of Frequency Scanning Techniques for Subsynchronous Resonance Analysis", IEEE Transactions on Power Apparatus and Systems, Vol. PAS-98, No. 2, March/April 1979, pp. 341-349.

[17] H. C. Hall, R. L. Daniels, D. G. Ramey, "A New Technique for Subsynchronous Resonance Analysis and an Application to the Keriparowits System", IEEE Transactions on Power Apparatus and Systems, Vol. PAS-96, No. 4, July/August 1977, pp. 1251-1255.

[18] L. A. Kilgore, D. G. Ramey, M. C. Hall, "Simplified Transmission ANd Generation System Analysis Procedures for Subsynchronous Resonance Problems", IEEE Transactions on Power Apparatus and Systems, Vol. PAS-96, No. 6, Nov/Dec 1977.

[19] R. C. Dancy, R. A. Hedin, R. N. Alford, "Hybrid Computer Simulation and Analysis of Subsynchronous Resonance", the IEEE PES 1976 Winter Meeting and Tesla Symposium, pp. 37-45.

[20] M. Enns, W. F. Tinney (Editors), Proceedings of the IEEE, Special Issue on Computers in the Power Industry, July 1974.

[21] H. H. Happ, C. Pottle, K. A. Wirgan, "Future Computer

Technology for Large Power System Simulation", Automatica, Vol. 15, pp. 621-629, 1979.

[22] "Digital Simulation of Electrical Transient Phenomena", IEEE Tutorial Course, 81 EH0173-5-PWR.

[23] H. W. Dommel, "Digital Computer Solution of Electromagnetic Transients in Single and Multiphase Networks", IEEE Transactions on Power Apparatus and Systems, Vol.PAS-88, No. 2, March/April 1969, pp. 388-399.

[24] S. N. Talukdar, "METAP-A Modular and Expandable Program for Simulating Power System Transients", IEEE Transactions on Power Apparatus and Systems, Vol. PAS-95, No. 6, Nov/Dec 1976, pp. 1882-1891.

[25] IEEE SSR Task Force, "Series Capacitor Controls and Settings as Countermeasures to Subsynchronous Resonance", IEEE Transactions on Power Apparatus and Systems, Vol. PAS-101, No. 6, June 1982, pp. 1281-1287.

[26] IEEE SSR Task Force, "Countermeasures to Subsynchronous Resonance problems", IEEE Transactions on Power Apparatus and Systems, Vol. PAS-99, No. 5, Sept/Oct 1980, pp. 1810-1818.

[27] J. B. Tice, C. E. J. Bowler, "Control of the Phenomenon of Subsynchronous Resonance", Proceedings of the American Power Conference, Vol. 37, 1975, pp. 916-922.

[28] N. G. Hingorani, "A new Scheme for Subsynchronous Resonance Damping of Torsional Oscillations and Transient Torque- Part I", IEEE Transactions on Power Apparatus and Systems, Vol. PAS-100, No. 4, April 1981, pp.1852-1855.

[29] R. A. Hedin, K. B. Stump, N. G. Hingorani, "A New Scheme for Subsynchronous Resonance Damping of Torsional Oscillations and Transient Torque -Part II, Performance", IEEE Transactions on Power Apparatus and Systems, Vol.pas-100, No.4, April 1981, pp. 1856-1860.

[30] I. M. Canay, "A Novel Approach to the Torsional Interaction and Electrical Damping of the Synchronous Machine, Part I: Theory", presented at the IEEE PES 1982 Winter Meeting, New York.

[31] L. A. Kilgore, D. G. Ramey, W. H. South, "Dynamic Filter and Other Solutions to the Subsynchronous Resonance Problem", Proceedings of the American Power Conference, Vol. 37, 1975, pp. 923-929.

[33] C. E. J. Bowler, D. H. Baker, "Concepts of Supplementary Torsional Damping by Excitation Modulation", Symposium on

Countermeasures for Subsynchronous Resonance , 81TH0086-9-PWR, 1981.

[34] N. G. Hingorani, R. A. Hedin, B. Bhargava, "Evaluation of NGH Damping Scheme Applied to Mohave Generator", Symposium on Countermeasures for Subsynchronous Resonance , 81TH0086-9-PWR, 1981.

[35] A. Yan, M. D. Wvong, Y. Yu, "Excitation Control of Torsional Oscillations", presented at the IEEE PES 1979 Summer Meeting, Vancouver, Canada.

[36] O. Wasynczuk, "Damping Shaft Torsional Oscillations Using a Dynamically Controlled Resistor Bank", IEEE Transactions on Power Apparatus and Systems, Vol. PAS-100, No. 7, July 1981, pp. 3340-3349.

[37] M. Aoki, "Control of Large Scale Dynamic Systems by Aggregation", IEEE Transactions on Automatic Control, Vol. AC-13, No. 3, 1968, pp. 246-253.

[38] E. C. Y. Tse, et. al., "Generalized Hessenberg Transformations for Reduced-Order Modelling of Large Scale Systems", International Journal of Control, Vol. 27, No. 4, 1978, pp. 493-512.

[39] B. Avramovic, et. al., "Area Decomposition for Electromechanical Modes of Power Systems", Automatica, Vol. 16, 1980, pp. 637-648.

[40] P. V. Kokotovic, "Subsystems, Time Scales and Multimodeling", Automatica, Vol. 17, 1981, p. 789.

[41] J. R. Winkelman, B. Avramovic, P. V. Kokotovic, "An Analysis of Interarea Dynamics of Multi-Machine Systems", paper 80 SM 533-0, presented at the IEEE PES 1980 Summer Meeting.

[42] P. V. Kokotovic, J. H. Chow, J. R. Winkelman, "Coherency Based Decomposition and Aggregation", Automatica, Vol. 18, No. 1, 1982, pp. 47-56.

[43] R. Podmore, "Identification of Coherent Generators for Dynamic Equivalents", IEEE Transactions on Power Apparatus and Systems, Vol. PAS-97, 1978, pp. 1344-1354.

[44] F. Saccomano, "Dynamic Modeling of Multimachine Electric Power Systems", Proceedings of the 4th PSCC, Grenoble, France, paper 2.1.22, 1972.

[45] R. L. Morris, F. C. Schweppe, "A Technique for Developing Low Order Models of Power Plants", IEEE Transactions on Power Apparatus and Systems, Vol. PS-100, No. 1, Jan 1981, pp. 264-272.

[46] W. M. Price, B. A. Roth, "Large-Scale Implementation of Modal Dynamic Equivalents", Paper 81 WM 094 2 presented at the IEEE PES 1981 Winter Meeting, Atlanta, Ga.

[47] S. T. Lee, F. Schweppe, "Distance Measures and Coherency Recognition for Transient Stability Equivalents", IEEE Transactions on Power Apparatus and Systems, Vol. PAS-92, 1973, pp. 1550-1557.

[48] J. M. Undrill, et. al., "Electromechanical Equivalents for Use in Power System Stability Studies", IEEE Transactions on Power Apparatus and Systems, Vol. PAS-90, No. 5, Sept/Oct 1971, pp. 2060-2071.

[49] J. E. Van Ness, H. Zimmer, M. Cultu, "Reduction Models of Power Systems", Proceedings of the Industrial Computer Application, 1973, pp. 105-112.

[50] J. Lawler, R. A. Schlueter, P. Rush, D. C. Hackett, "Modal Coherent Equivalents Derived from an RMS Coherency Measure", IEEE Transactions on Power Apparatus and Systems, Vol. PAS-99, No. 4, July/August 1980, pp.1415-1425.

[51] P. A. Cook, H. M. M. Hassan, "The Use of Model Following Methods to Simplify Linear Systems", Large Scale Systems, 1981, pp. 123-142.

[52] O. Wasynczuk, R. A. Decarlo, "The Component Model and Structure Preserving Model Order Reduction", Automatica, Vol. 17, No. 4, 1981, PP. 619-626.

[53] W. F. Tinney, W. S. Meyer, "Solution of Large Sparse Systems by Ordered Triangular Factorization", IEEE Transactions on Automatic Control, Vol. AC-18, No. 4, August 1973, pp. 333-346.

[54] D. E. Kirk, "Optimal Control Theory, An Introduction", New Jersey: Prentice-Hall, 1970.

[55] M. Athans, P. L. Falb, "Optimal Control: An Introduction to the Theory and its Applications", New York: McGraw-Hill, 1966.

[56] R. E. Bellman, R. E. Kalaba, "Dynamic Programming and Modern Control Theory", New York: Academic Press, 1965.

[57] L. S. Pontryagin, V. G. Boltyanskii, R. V. Gamkrelidze, E. F. Mischenko, "The Mathematical Theory of Optimal Processes", New York: Interscience, 1962.

[58] N. R. Sandell, et. al., "Survey of Decentralized Control Methods for Large Scale Systems", IEEE Transactions on Automatic Control, Vol. AC-23, No. 2, April 1978, pp. 108-127.

[59] G. Quazza, "Large Scale Control Problems in Electric Power Systems", Automatica, Vol. 13, 1977, pp. 579-593.

[60] E. J. Davison, "Decentralized Stabilization and Regulation in Large Multivariable Systems", Directions in Large Scale Systems, Ho and Mitter Editors, 1975, pp. 303-323.

[61] A. N. Michel, R. K. Miller, "Qualitative Analysis of Large Scale Dynamical Systems", New York: Academic Press, 1977.

[62] D. D. Siljak, "Large Scale Dynamical Systems - Stability and Structure", New York: North Holland, 1978.

[63] S. Barnett, "Matrices in Control Theory with Applications to Linear Programming", London: Van Nustrand Reinhold, 1971.

[64] T. N. E. Greville, "Some Applications of the Pseudoinverse of a matrix", SIAM Review, Vol. 2, 1960, pp. 15-22.

[65] F. R. Gantmakher, "Theory of Matrices", 2 Volumes, New York: Chelsea, 1959.

[66] J. W. Brewer, "Kronecker Products and Matrix Calculus in System Theory", IEEE Transactions on Circuits and Systems, Vol. CAS-25, No. 9, Sept 1978, pp. 772-781.

[67] W. J. Vetter: "Derivative Operations on Matrices", IEEE Transactions on Automatic Control, Vol. AC-15, No. 2, April 1970, pp. 241-244.

[68] P. M. Anderson, A. A. Fouad, "Power System Control and Stability", Ames: Iowa State University Press, 1977.

[69] D. G. Luenberger, "Dynamic Equations in Descriptor Form", IEEE Transactions on Automatic Control, Vol. AC-22, No. 3, June 1977, pp. 312-321.

[70] H. H. Rosenbrock, "State Space and Multivariable Theory", New York: Wiley, 1970.

[71] J. H. Wilkinson, "Linear Differential Equations and Kronecker's Canonical Form", Recent Advances in Numerical Analysis, edited by C. DeBoor and G. H. Golub, pp. 231-265, New york: Academic Press, 1978.

[72] L. A. Kilgore, "Factors to Consider when Applying Subsynchronous Resonance Countermeasures", Symposium on Countermeasures for Subsynchronous Resonance , 81TH0086-9-PWR, 1981.

[73] G. Gross, M. C. Hall, "Synchronous Machine and Torsional Dynamics Simulation in the Computation of Electromagnetic

Transients", IEEE Transactions on Power Apparatus and Systems, Vol. PAS-97, No. 4, July/August 1978, pp. 1074-1086.

[74] H. W. Dommel, "Nonlinear and Time-Varying Elements in Digital Simulation of Electromagnetic Transients, Proceedings of the 1971 Power Industry Computer Applications Conference.

[75] V. Brandwajn, H. W. Dommel, "A New Method for Interfacing Generator Models with an Electromagnetic Transient Program", Proceedings of the 1977 Power Industry Computer Applications Conference, pp. 260-265.

[76] M. C. Jackson, et. al., "Turbine Generator Shaft Torques and Fatigue: Part I -Simulation Methods and Fatigue Analysis", IEEE Transactions on Power Apparatus and Systems, Vol. PAS-98, No. 6, Nov/Dec 1979, pp 2299-2307.

[77] R. D. Dunlop, et. al., "Turbine Generator Shaft Torques and fatigue: Part II -Impact of System Disturbances and High Speed reclosures", IEEE Transactions on Power Apparatus and Systems, Vol. PAS-98, No. 6, Nov/Dec 1979, pp. 2308-2328.

[78] J. S. Toyce, T. Kulig, D. Lambrecht, "Torsional Fatigue of Turbine Generator Shafts Caused by Different Electrical System Faults and Switching Operations", IEEE Transactions on Power Apparatus and Systems, Vol. PAS-97, No. 5, Sept/Oct 1978, pp. 1965-1977.

[79] J. S. Joyce, D. Lambrecht, "Status of Evaluating the Fatigue of Large Steam Turbine Generators Caused by Electrical Disturbances", IEEE Transactions on Power Apparatus and Systems, Vol. PAS-99, No. 1, Jan/Feb 1980, pp. 111-119.

[80] IEEE SSR Task Force, "First Benchmark model for Computer Simulation of Subsynchronous Resonance", IEEE Transactions on Power Apparatus and Systems, Vol. PAS-96, No. 5, Sept/Oct 1977, pp. 1565-1572.

[81] A. Feliachi, A. Bakirtzis, A. P. Meliopoulos, "Generalized Dynamic Simulators and Applications", Proceedings of the 14th Southeastern Symposium on System Theory, Blacksburg, VA, April 15-16 1982, pp. 297-300.

[82] A. Feliachi, A. P. Meliopoulos, "Mitigation of Subsynchronous Resonant Oscillations via Optimal Control", Proceedings of the 1982 Conference on Decision and Control, Orlando, Florida, December 8-10, 1982, pp. 798-800.

VITA

Ali Feliachi was born in Biskra, Algeria, on February 2, 1953.

He attended elementary and secondary schools in Biskra and high school in Batna. After he received the degree "Baccalaureat, Serie: Mathematiques Elementaires" in June 1971, he attended the Ecole Nationale Polytechnique of Algiers and graduated with the degree "Ingenieur en Electrotechnique" in June 1976.

He entered Georgia Institute of Technology in September 1977 and received the M.S. and Ph.D. degrees in Electrical Engineering in June 1979 and March 1983 respectively. During his graduate studies at Georgia Tech he held teaching and research assistanships positions.

Dr. Feliachi is a member of the IEEE and Pi Mu Epsilon.